ASSESSING INPUT UNCERTAINTY AND SENSITIVITY OF THE PROCESS-BASED WETLAND WATER QUALITY MODEL, WETQUAL

by

Recep Tayyip Kanber

A thesis submitted to the Graduate Faculty of
Auburn University
in partial fulfillment of the
requirements for the Degree of
Master of Science

Auburn, Alabama
August 3, 2019

Keywords: Wetlands, WetQual, Bathymetry, Wetland Water Temperature, Temporal resolution of Input Forcings

Approved by

Latif Kalin, Chair, Professor of School of Forestry and Wildlife Sciences
Sanjiv Kumar, Assistant Professor of School of Forestry and Wildlife Sciences
Sabahattin Isik, Research Associate II of School of Forestry and Wildlife Sciences

ABSTRACT

Wetlands are among the most important natural ecosystems having numerous benefits to people and wildlife. One of the key functions of wetlands is water purification. Wetlands are known to improve water quality and act as natural water purifiers. They can trap sediments and other pollutants from waterbodies. However, their functioning can be impacted by various factors. Wetland hydrology and water quality models have been developed to better understand their functioning and represent wetlands in the landscape for improved terrestrial models. *WetQual* is a recently developed process-based model which simulates hydrology, sediment transport and nutrient and carbon cycles in wetlands. *WetQual* represents certain processes in detail and therefore require comprehensive input data. In other instances, it uses simpler processes and requires less data. The overarching goal of this study was to explore whether we can reduce the data needs in *WetQual* or if there is a need to improve certain processes, which may result in more data need. To achieve this goal, I studied (1) the significance of having detailed wetland bathymetry, (2) the efficacy of the water temperature calculation currently employed in *WetQual*, and (3) the consequences of using sub-daily level input forcings as opposed to the existing daily level inputs such as loading to the wetland, climatic data, etc., on nitrogen, phosphorous, and sediment simulations. A restored wetland in Maryland has been used to answer these questions.

Wetland bathymetry is needed for flow routing. It also plays important role for nutrient and sediment transport. Wetland bathymetry data can be best deduced from topographic surveys, but in a landscape abundant of wetlands this poses a daunting task, thus simplifications are needed.

Several geometric profiles were assumed, and volume-area-depth relationship were generated assuming that the only known information is maximum depth, surface area and volume. Model performances, parameter sensitivities and predictive uncertainties for each profile were compared to the results obtained with the actual bathymetry. Results from most geometric shapes were comparable to the results from the actual profile.

Temperature is known to affect the fate and transport of chemicals and biological activities. The effect of temperature on biochemical reactions rates in *WetQual* is represented through the Arrhenius equation. Temperature is also key in evapotranspiration (ET) calculation. Water temperature in *WetQual* is calculated as a simple linear function of air temperature and the coefficients are fixed. As a second experiment, the adequacy of this relationship was explored to see if a more complex model is needed. Results showed that over the whole simulation period, the simple equation is adequate for most constituents, except for nitrate which showed the highest sensitivity to temperature. Further, results revealed that the simple equation can generate some misleading results when seasonality and interannual variability are concerned.

Input forcings to *WetQual* are currently provided at daily time scale. However, since model runs at small time increments for numerical purposes, it internally disaggregates the daily data by simple linear interpolation. In a third experiment, the temporal resolution of temperature and evapotranspiration to the wetland were increased in a more realistic way, and runoff input to wetland was provided at hourly time scale to assess the temporal resolution impacts on model performance, parameter sensitivity and model uncertainty. Increasing the temporal resolution of temperature alone did not have a much impact. On the other hand, model was very sensitive to the temporal resolution of inflow data. Therefore, spending the extra time and money (if available) to obtain sub-daily inflow data is a worthy investment.

ACKNOWLEDGEMENT

I would first like to acknowledge General Directorate of State Hydraulic Works (DSI) under Republic of Turkey Ministry of Agriculture and Forestry which has provided a fellowship to me with grand number 33070922-772.02-748553 to study in the US.

I would like to thank my thesis advisor Dr. Latif Kalin of the School of Forestry and Wildlife Sciences at Auburn University. His limitless support, kindness, and patience was always helpful for my research. I will never be able to thank to him enough.

I greatly appreciate Dr. Sabahattin Isik for not only serving on my committee but also for his assistance on my research. The door to Dr. Isik's office was always open to me when I faced a problem with the model or the model code needed to be modified. I would also like to thank Dr. Sanjiv Kumar for being my committee member.

I specially thank Yasemin Eldayih for her friendship and support since we met. Without her support I would have had tough times in my life in Auburn.

I also want to thank my friends Abdullah Hanar, Sengul Kalin, Gokhan Ucar, Halil Ibrahim Kurt, Gokhan Benk, Suleyman Alparslan, Seval Celik, Junhao He, Zhuonan Wang, Henrique Haas, and Arshdeep Singh for being a family to me in Auburn.

Finally, I must express my deepest gratitude to my father Mehmet Ali Kanber, my mother Hanife Kanber, and sisters Kubra Kevser Kanber, Seyma Kanber, and Kadriye Nur Kanber for providing me continuous encouragement throughout my years of study.

TABLE OF CONTENTS

LIST OF FIGURES

LIST OF TABLES

1 INTRODUCTION

1.1 Background

Wetlands are areas where the water table is usually at or near the surface, or the land is covered by shallow water for extended periods. They are defined as transitional zones between aquatic and upland environments characterized by permanent or temporary inundation. Wetlands are amongst the most valuable and vulnerable natural ecosystems that provide various benefits to people and wildlife. They improve water quality, provide habitats to wildlife, and prevent floods. They act as natural water purifiers and remove sediments and other pollutants from waterbodies. In the ecosystem, the water purification function of wetlands plays significant roles. For instance, one study found that more than 1000 kg of nitrogen and 130 kg of phosphorous can be removed from waterbodies per hectare of wetland each year (Meng et al., 2017). Mitsch and Gosselink (2007) calls wetlands "kidneys of the Earth" because when they receive wastewater they can purify it. Wetlands cover 6% of the world's land surface and store 12% of the global carbon, playing an important role in the global carbon cycle (Erwin, 2009).

Wetland loss and degradation is an undisputed reality and the main factor is human activities. Wetlands have been drained, filled and converted to other purposes for many centuries, for example in Europe since Roman times (Davidson, 2014), in North America since European settlement (Dahl, 1990), and in China for at least the last 2000 years (An et al., 2007). The main causes of degradation and loss of wetlands are changes in land use/cover (urbanization and agriculture), water diversion (dams, canalization), and pollution (air, water and excess nutrients)

(Davidson, 2014). It has been reported that the world has lost 50% of its wetlands since 1900 (Finlayson, 2012). For instance, in the US twenty-two states have lost over 50% of their original wetlands between the years 1780's and 1980's (Dahl, 1990). Most importantly, seven states – Indiana, Illinois, Missouri, Kentucky, Iowa, California, and Ohio have lost over 80% of their original wetlands. Figure 1.1 shows the percentages of wetlands acreage lost in the US between the years 1780's and 1980's.

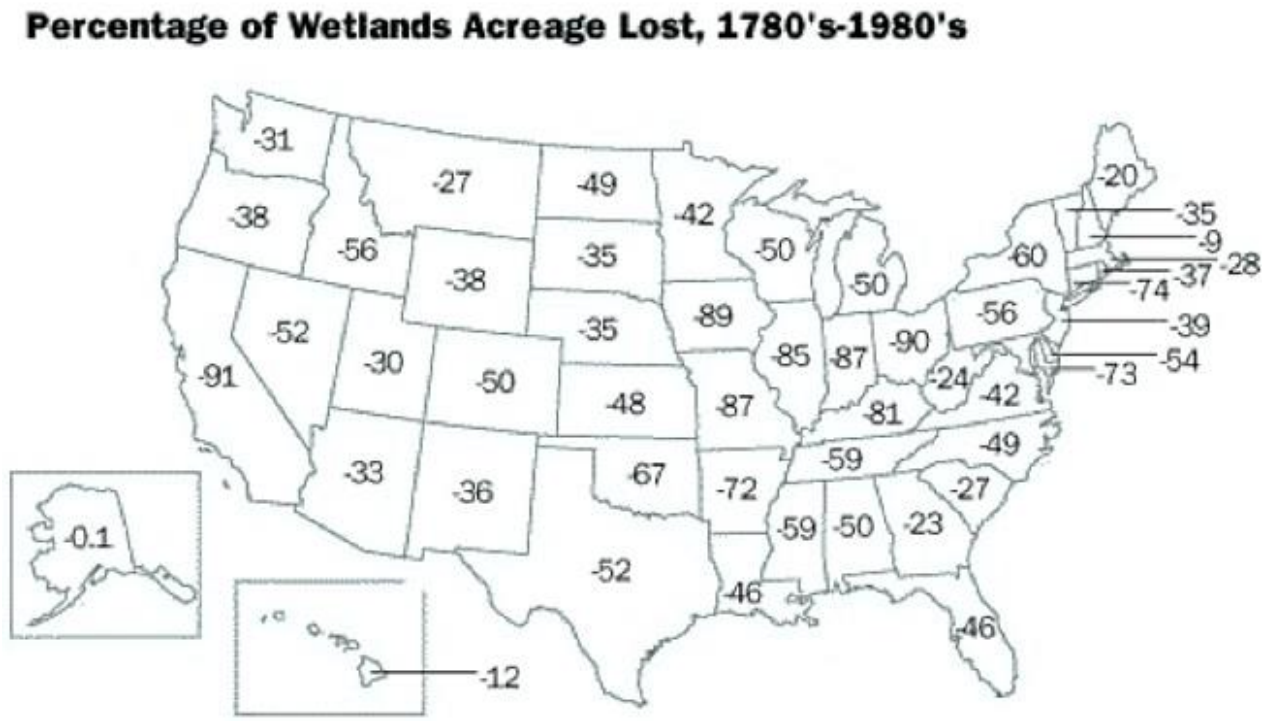

Figure 1.1. Percentage of wetland area lost between 1780's and 1980's (adapted from Mitsch and Gosselink, 1993)

Climate change is inarguably one of the greatest threats to the world's ecosystems and the living species that reside within them with potential consequences of water shortages, more frequent floods and see level rise. Similar to other systems, climate change impacts wetland ecosystems through changes in precipitation and temperature regimes worldwide. Due to this influence of climate change on the wetlands, these ecosystems need to be assessed for its possible

impacts, such as changes in hydrology, increase in temperature and flooding, and decrease in water quality.

Hydrological and temperature changes are the most important drivers impacting a wetland's water budget. Summers are predicted to get longer and warmer in the future in the Northern hemisphere (Dankers and Christensen, 2005). A change in the water balance because of enhanced evaporation will not only cause greater water loss from wetlands but will also decrease the water inputs from their catchments. For example, due to the increased temperature and longer and warmer summer seasons, snowpack will melt much earlier, and enhanced evapotranspiration (ET) will be seen. This can result in the disappearance of snowmelt-fed wetlands (Erwin, 2009). Although these effects are associated with high uncertainties, all climate scenarios show that snow-covered areas will decrease while ET will increase (Mote et al., 2003; Woo et al., 2006). Significant changes in the wetland management are required to deal with these problems.

To help in mitigating wetland losses, we need to understand how wetlands respond to various stressors. Unfortunately, experimenting with them is not a realistic option. To assess the impacts of various stressors on functioning of wetlands, either for diagnostic or prognostic purposes, wetland models can be very useful. Models are simplifications of real systems; therefore, they can only imitate a real system's behavior. Since experimenting and observing the behavior of wetland systems by conducting on the ground experiments are often not feasible, wetland models can serve as cost effective and efficient tools in this regard.

Hydrologic and water quality models have been in existence since 1950's (Padmanabhan and Bengtson, 1999), and several of these models are used to simulate hydrological and biochemical processes of wetlands, such as the wetland nutrient cycling model WetQual, the riparian ecosystem management model REMM, and WETSAND model (Hantush et al, 2013;

Kazezyılmaz-Alhan et al, 2007; Rashleigh, 2009). However, it is impossible to represent all the physical and biochemical processes accuring in wetlands in the models.

Sensitivity analysis is a field of study that studies how uncertainty in the output of a model can be attributed to different sources of uncertainties in model input (Saltelli et al, 2004). Sensitivity analysis methods can be divided in two broad groups: global and local sensitivity analysis. A global sensitivity analysis identifies the sensitivity regarding the entire distribution of parameter set while a local sensitivity analysis uses one-at-a-time techniques to address sensitivity relative to point estimates of parameters values. Performing global sensitivity analysis is much more important in complex models (Saltelli, A.,et al., 2007). Also, checking sensitivity to input forcings can reveal whether all the input forcings are needed in great accuracy and detail and whether crude estimation of some inputs would suffice. The goal of the sensitivity methods involves reducing the number of parameters that need to be estimated with great care.

Process-based wetland water quality models simulating constituents such as nutrients, sediments, and other compounds must account for many processes such as sedimentation, mineralization, diffusion, volatilization, burial, plant uptake, etc. The more processes model simulates, the more inputs model needs. This increases the complexity of the models, and therefore model predictive uncertainty. Due to the increase in the number of model inputs, sensitivity analysis becomes very critical in order to understand the dominant processes in a study wetland, as well as to calibrate the model parameters more efficiently.

In this research, input uncertainty and sensitivity of the process-based wetland water quality model, WetQual, was studied by specifically focusing on importance of accurate wetland bathymetry data, wetland water temperature predictions, and temporal resolution of hydro climatic input forcing on wetland water quality predictions. Bathymetry analysis can help us understand

the level of accuracy needed in wetland bathymetry data. Temperature analysis will be focused on the sensitivity of the temperature conversion equation (from air temperature to water temperature) and its impact on input uncertainty and sensitivity. Temporal resolution study assessed the value of having higher temporal resolution hydroclimate data. Below I provide a summary of relevant work in the literature.

1.1.1 Wetland Bathymetry Effect on Wetland Water Quality

In wetland models, accuracy in hydrological variables, such as water depth (h), volume (V), surface area (A), and outflow (Q_{out}), is a prelude to getting improved predictions in water quality constituents. Given inflow (Q_{in}), bathymetry data to get $V-A-h$ relationships, and a hydraulic relationship relating Q_{out} to h, these hydrological variables are estimated using a combination of flow routing and mass balance approaches. Wetland water depth, volume and surface area affect various hydrological and biochemical fluxes such as evapotranspiration, ammonia/methane gas release, oxygen exchange, nitrate/ammonium diffusion, etc.

Despite the clear importance of wetland bathymetry, there is inadequate information on the required level of detail in representing wetland bathymetry and its effect on the accuracy of the $h-V$ and $h-A$ relationship and eventually to the simulated hydrologic and water quality variables (Gurrieri and Furniss, 2004; Dimova and Burnett, 2011). Due to the lack of detailed bathymetry measurements, or to find a less labor-intensive way to the standard determination of $h-A$ and $h-V$ relationships from topographic data, some studies used simple mathematical equations that require limited number of measurements (C. Castaneda, 2008; Hayashi and van der Kamp, 2000). For example, Hayashi and van der Kamp, (2000) studied 27 wetlands and ephemeral

ponds in the northern prairie region of North America and developed the following $h - A$ and $h - V$ relations as power functions;

$$A = s\left(\frac{h}{h_0}\right)^{2/p} \dots\dots\dots\dots\dots\dots\dots\dots\dots\dots\dots\dots\dots (1)$$

$$V = \frac{s}{(1 + 2/p)} * \frac{h^{1+(2/p)}}{h_0^{2/p}} \dots\dots\dots\dots\dots\dots\dots\dots\dots (2)$$

where, s is a scaling constant representative of wetland size (equal to A when $h = h_0$), h is depth of water (m), h_0 is unit depth (m), and p is a dimensionless constant which depends on the shape. They found the value of p around 2 for small and convex wetlands. As the bottom of the wetland becomes flatter, p increases, and for the extreme case, $p \rightarrow \infty$, which represents a cylinder.

These simplified relationships require only two measurements of (h, A, V), and in some cases only one measurement. Often there is no measurements of $V - A - h$ at all and topographic maps are used to estimate them. This naturally introduces uncertainties in A and V predictions from h, which could contribute to the overall prediction uncertainty. There is almost no study in the literature that looked into this important problem. *Trigg et al., (2014)* found that uncertainty introduced by bathymetry on the predicted hydrologic variables is very small if the assumed bathymetry shape roughly catches the shape of the shallow wetlands.

1.1.2 Temperature Effect on Wetland Water Quality

One of the critical functions of wetlands are removal of nutrients and sediments from the system and purification of the water. Temperature is an effect of the climate that plays important roles in

the wetland systems regarding this function (El-Refaie, 2010). Kadlec, (2006) lists three factors in explaining the importance of the water temperature in wetlands;

(1) Changes in the temperature can cause changes in the biological processes in the wetlands

(2) In some cases, temperature can count as a water quality parameter

(3) Water temperature is the main determinant of evaporative water loss (water budget)

Temperature is directly related to the biological and physical processes in wetlands. The biological processes such as mineralization, nitrification and denitrification are known to be temperature dependent, and these effects are often modeled though relationships between temperature and reaction rates, such as the Arrhenius equation (Schipper et al., 2014). Studies has shown that water temperature in wetlands has direct correlations with nitrogen (N) removal and plant physiology (Hua et al., 2017). In a range around 10 ^{0}C, temperature has a powerful effect on the microbial nitrogen processing (Kadlec, 2006). El-Refaie, (2010) found a reverse relationship between temperature and wetland sediment removal efficiency, and a direct relationship between phosphorous removal efficiency and temperature.

There is scant information on modelling wetland water temperature from air temperature in the literature. However, there are many methods to model stream water temperature. Those can be mainly classified as physically-based and empirical models(Caissie, 2006). Physically-based models simulate temporal changes of water temperature based on conservation of energy and mass balance principles. These types of models, although attractive, may not always be practical. They are time consuming because they need a great amount of input parameters such as solar radiation, long-wave radiation, evaporative and convective heat fluxes (Hebert et al., 2011). Empirical models have been developed to estimate water temperature from the ambient air temperature

(Ahmadi-Nedushan et al., 2007; Mohseni et al., 1998; Morrill et al., 2005). These models are much simpler than physically-based models because they predict water temperature purely as a function of air temperature.

Empirical models of water temperature prediction consist of linear regression, logistic regression, and non-linear regression models (Caissie, 2006). Simple linear regression models use air temperature as the only input parameter to estimate water temperature by using weekly and monthly data (Smith, 1981). For daily and sub-daily calculations of water temperature from air temperature, time lag should be added into the equations (Stefan and Preud'homme, 1993). To calculate time lag, discharge is also needed along with minimum, maximum, and daily average air temperature (Jourdonnais et al., 1992). Logistic regression models assume that the relationship between air and water temperature are not necessarily linear because of the impacts of groundwater at low temperatures and evaporative cooling at high temperatures (Caissie, 2006). For example, the rise in water temperature at high air temperature can be decreased by evaporative cooling. Other regression models cannot catch this non-linearity as good as the logistic regression models (Mohseni et al., 1998). Non-linear regression models are modifications of logistic regression models to get accurate results for streams, which are not freezing while air temperature is below zero. To get nonzero water temperature, a parameter is added to the equation which is the estimation of minimum water temperature (Mohseni et al., 1998). The equations of the regression-based models can be summarized as;

Linear Regression: $$T_w(t) = A + BT_a(t) + \varepsilon(t) \dots\dots\dots\dots (3)$$

Logical Regression: $$T_w(t) = \frac{\alpha}{1+e^{\gamma(\beta - T_a(t))}} \dots\dots\dots\dots\dots\dots\dots (4)$$

Non-Linear Regression: $$T_w(t) = \mu + \frac{\alpha - \mu}{1+e^{\gamma(\beta - T_a(t))}} \dots\dots\dots\dots\dots\dots (5)$$

where $T_w(t)$ is average water temperature for a given day, $T_a(t)$ is average air temperature for the same day as water temperature, *A* and *B* are regression parameters, $\varepsilon(t)$ is an error term, α is a coefficient which estimates the highest water temperature, μ is a coefficient which estimates the minimum water temperature, β represents the air temperature at the inflexion point, γ represents the steepest slope of the logistic S-shaped function (Kothandaraman, 1971; Mohseni et al., 1998; Webb and Nobilis, 1997).

Stefan and Preud'homme (1993) analyzed the linear relationship between river temperature and air temperature on eleven rivers in the Mississippi River basin. They conducted their study for two time resolutions, daily and weekly. They found the following relationships;

Daily Linear Regression: $T_w = 5 + 0.75T_a$ ... ... (6)

Daily Linear Regression with Time Lag: $T_w(t) = 5 + 0.75T_a(t - \delta)$ ... . (7)

Weekly Linear Regression: $T_w = 2.9 + 0.86T_a$ ... ... (8)

WetQual uses equation (6) to estimate daily average water temperature from average daily air temperature.

1.1.3 Effects of Temporal Resolution of Input Forcings (Temperature and Inflow) on the Wetland Water Quality

Precipitation, inflow/outflow, and ET have important places in the hydrological balance of wetlands. Each of these could be very important depending on the wetland type and the season. For instance, pothole wetlands with no significant watershed area may have precipitation and ET as the main hydrologic sources and sinks. A wetland constructed for wastewater treatment, however, receives majority of water as inflow. On the other hand, a headwater wetland may be sustained by groundwater. The relationship between various hydrologic pathways plays an

important role in functioning of wetlands. By controlling inflow and outflow rates, the treatment performance of treatment wetlands for improving water quality can be controlled. Retention time of water in wetlands directly affects the ability of a wetland's nutrient transformation processes. Retention time of water in a wetland can exhibit seasonality, which may reduce the efficiency of the wetlands (Jordan et al., 2003).

Although the importance of inflow/outflow rates are known, there is no information in the literature on how time resolution of the inflow provided to a wetland model influences the wetland water quality. According to Kadlec and Wallace, (2009), inflow should be measured or estimated daily to quantify mass balance of constituents. However, I hypothesize that different temporal resolutions of inflow hydrograph can affect the accuracy of predicted water quality constituents.

One of the most important question in watershed hydrology is how the spatial and temporal resolutions of rainfall impact the movement of the surface and groundwater (Paschalis et al., 2013). In the literature there are numerous studies that assessed the effects of precipitation variability on the hydrology. While most of these studies are mainly based on the impact of the spatial resolution, only a few studies evaluated the impact of the rainfall temporal resolution (Yang et al., 2015). These studies have generally been conducted in small watersheds, many of them used Soil & Water Assessment Tool (SWAT), and the results have been conflicting. While *Kannan et al., (2007)* found that the results of using daily rainfall data were better than using sub-daily rainfall data, *Maharjan et al., (2013)* concluded that models that used higher temporal resolutions had better performance. According to *Yang et al., (2015)*, the SWAT model with sub-daily rainfall data performed better than the model with daily rainfall data in daily streamflow simulations.

Evapotranspiration (ET) is a process that vaporize the liquid water from surface to atmosphere. ET is also a significant water loss pathway from wetlands (Gentine et al., 2007).

Generally, it is calculated at daily time scale. However, it is known that ET has a diurnal pattern: it reaches maximum values in the afternoon (White, 1932), whereas, at night it reaches a minimum value roughly just before sunrise. Due to the sub-daily variation of ET, it is important to use sub-daily ET values to get more accurate model results and reduce model uncertainty.

1.2 Objectives and Outcomes

The overarching goal of this research is to explore how wetland geometry, water temperature, and the temporal resolution of hydro-climatic input forcings affect simulated water quality constituents with WetQual. The study site selected for this purpose is a restored wetland in Kent Island, MD. More specifically, I will try to find answers to the following questions:

1. Do we always need the most accurate bathymetric information, or can we use simple mathematical relationships between h, A, and V to generate bathymetry data?
2. Do we need to introduce a physically based water temperature prediction component, or can we use much simpler regression-based equations?
3. How sensitive is WetQual to the temporal resolution of hydro-climatic input forcings?

2 METHODOLOGY

2.1 Wetland Nutrient Cycling Model (WetQual)

WetQual is a process-based model for sediment, nitrogen, phosphorus, and carbon retention, cycling, and removal in flooded wetlands (Hantush et al., 2013; Kalin et al., 2013; Sharifi et al., 2013). The model simulates oxygen dynamics and the impact of oxidizing and reducing conditions on nitrogen and carbon transformation and removal as well as phosphorus retention and release. WetQual explicitly accounts for the nitrogen loss pathways of volatilization and denitrification and considers various biogeochemical interactions affecting carbon cycling, methane emissions, and organic carbon export and retention **(**Figure 2.1**)**. These transformations are calculated in mass balance equations. Below, summary of equations describing only the main components of WetQual are provided.

Wetland water mass balance:

$$\phi_w \frac{dV_w}{dt} = Q_{in} + Q_g - Q_{out} - AET + Ai \dots\dots\dots\dots\dots\dots\dots\dots\dots\dots (9)$$

where, ϕ_w is effective wetland surface water porosity, $V_w$is wetland water volume $[L^3]$, Q_{in} is inflow $[L^3/T]$, Q_g is groundwater discharge $[L^3/T]$, Q_{out} is outflow $[L^3/T]$, A is wetland surface area $[L^2]$, ET is evapotranspiration $[L/T]$ and i is precipitation $[L/T]$.

Nitrogen compounds in water column (ON_w, N_w, NO_{3w})*;*

$$\phi_w \frac{d(V_w ON_w)}{dt} = Q_{in} ON_{w,in} + a_{na} k_{da} a + a_{na} k_{db} f_{bw} b - \phi_w V_w k_{mw} ON_w - v_s \phi_w A ON_w$$

$$+ \ v_r \phi_w A(ON_r + ON_s) - Q_{out} ON_w + A f_{Sw} S \ldots\ldots\ldots\ldots\ldots\ldots\ldots (10)$$

$$\phi_w \frac{d(V_w N_w)}{dt} = Q_{in} N_{w,in} + iAN_P - \phi_w V_w f_N k_{nw} N_w + \beta_{a1} A(N_1 + N_w) + F_{Ng}^w$$

$$- k_v \phi_w A(1 - f_N) N_w + \phi_w V_w k_{mw} ON_w - Q_{out} N_w - f_N a_{na} k_{ga} a$$

$$+ Aq_N \ldots\ldots\ldots\ldots\ldots\ldots\ldots\ldots\ldots (11)$$

$$\phi_w \frac{d(V_w NO_{3w})}{dt}$$

$$= Q_{in} NO_{3w,in} + iANO_{3p} + \phi_w V_w f_N k_{nw} N_w + \beta_{n1} A(N_1 + NO_{3w}) + F_{NO3g}^w$$

$$- f_{NO3w} a_{na} k_{ga} a - Q_{out} NO_{3w}$$

$$+ Aq_{NO3} \ldots\ldots\ldots\ldots\ldots\ldots\ldots\ldots\ldots\ldots\ldots\ldots\ldots\ldots\ldots\ldots (12)$$

where ON_w is particulate organic nitrogen concentration in free water $[M/L^3]$, N_w is total ammonia (NH_3+NH_4) -nitrogen concentration in free water $[M/L^3]$, NO_{3w} is nitrate-nitrogen concentration in free water $[M/L^3]$, a is mass of free floating plant $[M\ Chl\ a]$, b is mass of rooted plants $[M\ Chl\ a]$, N_1 and N_{n1} are pore-water concentration of total ammonia and nitrate nitrogen in anaerobic layer, respectively $[M/L^3]$, ON_r is concentration of rapidly mineralizing organic nitrogen in wetland soil $[M/L^3]$, ON_s is the concentration of slowly mineralizing organic nitrogen in wetland soil $[M/L^3]$, and f_N is the fraction of total ammonia in ionized form. Other related parameters are defined in the parameter list (Table 2.1).

Inorganic phosphorous (P_w) in the water column:

$$\phi_w \frac{d(V_w P_w)}{dt} = Q_{in} P_{w,in} - v_s F_{sw} m_w \phi_w A P_w + f_1 v_r \phi_w A F_{ss} m_s P_1 + f_2 v_r \phi_w A f_{ss} m_s P_2 - a_{na} k_{ga} a$$

$$+ V_w a_{pn} k_{mw} ON_w + \beta_{p1} A(F_{ds} P_1 - F_{dw} P_w) + F_{Pg}^w - Q_{out} P_w \ldots\ldots\ldots\ldots (13)$$

where P_w is the total inorganic phosphorus concentration in free water $[M/L^3]$, P_1 is the total phosphorus concentration in the aerobic layer $[M/L^3]$, P_2 is the total phosphorus concentration in the anaerobic layer $[M/L^3]$, and $F_{Pg}^{w}$is the net advective groundwater contribution $[M/T]$.

Sediment in the water column:

$$\phi_w \frac{d(V_w m_w)}{dt} = Q_{in} m_{w,in} - v_s m_w \phi_w A + v_r \phi_w A m_s - Q_{out} m_w \ldots\ldots\ldots\ldots\ldots\ldots\ldots\ldots\ldots (14)$$

where m_w is the sediment concentration in free water $[M/L^3]$, and m_s is the wetland soil bulk density $[M/L^3]$.

WetQual separates free-floating plant biomass (e.g., phytoplankton) from rooted aquatic plants and uses a simple model for plant productivity, where the daily growth rate is related to daily solar radiation and annual growth rates of plants. In the vertical domain, WetQual partitions a wetland into three basic compartments consisting of water columns (free water) and two wetland soil layers. The vertical soil layer is partitioned into aerobic and anaerobic zones, where the boundary between the two zones fluctuates up or down based on the competing oxygen supply and removal rates. Readers can refer to the works of Hantush et al., (2013) Kalin et al., (2013), and Sharifi et al., (2013) for more detailed information regarding model structure, governing equations, and case study applications of WetQual.

Table 2.1. WetQual model parameters and their symbols

Model parameter symbols	**Parameter definition and units**
L2	Thickness of anaerobic soil layer (cm)
theta	Temperature coefficient in Arhenious equation
Is	Optimal light level (ly/day), range from about 100 to 400 ly/d (Chapra, 1997, p 611)
fNup	Fraction of total ammonia nitrogen in ionized form
Kd	Ammonium ion distribution coefficient (mL/g)
kep	Parameter required as input but not used in the model (1/m)
kga0	Growth rate of free-floating plant (1/day)
kgb0	Growth rate of benthic and rooted plant (1/day)
kmin1s	First-order rapid mineralization rate in wetland soil (1/day)
knw	First-order nitrification rate in wetland free water (1/day)
kminw	First-order mineralization rate in wetland free water (1/day)
kns	First-order nitrification rate in aerobic soil layer (1/day)
kden	Denitrification rate in anaerobic soil layer (1/day)
rows	Wetland soil particle density
vels_o	Effective settling velocity (cm/day) for organic material
vels_s	Effective settling velocity (cm/day) for sediment
velb	Effective burial velocity (cm/day)
ana	Gram of nitrogen per gram of chlorophyll-a in plant/algae (gN/gChl)
rChl	Ratio of carbon mass to chlorophyll a mass in algae (gC/gChl)
Ss	Oxygen removal rate per unit volume of aerobic layer by other processes (g/L/day)
Sw	Volumetric oxygen consumption rate in water by other processes ($gr/cm^3/day$)
c_uw	Empirical parameter used for calculating volatilization mass transfer velocity kv
frap	Fraction of rapidly mineralizing particulate organic matter
c1	Used for calculating pK (Keq, equilibrium coefficient)
c2	Used for calculating pK (Keq, equilibrium coefficient)
PH	pH
S	Rate of nitrogen fixation by microorganisms (mg-N/m3/hr)
Kw	Phosphorus sorption coefficient in water (cm^3/g)
apa	Ratio of phosphorus to Chlorophyll-a in algae (grP/grChl)
Dpw	Inorganic phosphorus free-water diffusion coefficient (cm^2/day)
Ksa	Accounts for partitioning to phosphorus sorption site (cm^3/g)
Ksb	Accounts for association with iron hydroxide precipitate (cm3/g)
Ran1	Random number used for calculating soil porosity (φ) and free-water oxygen diffusion coefficient
fW	Fraction of nitrogen fixation in water
fact	Vertical diffusion magnification factor
alfa_velr_o	Coefficient for resuspension/recycling of organic material
alfa_velr_s	Coefficient for resuspension/recycling of sediment
porw	Effective porosity of wetland surface water

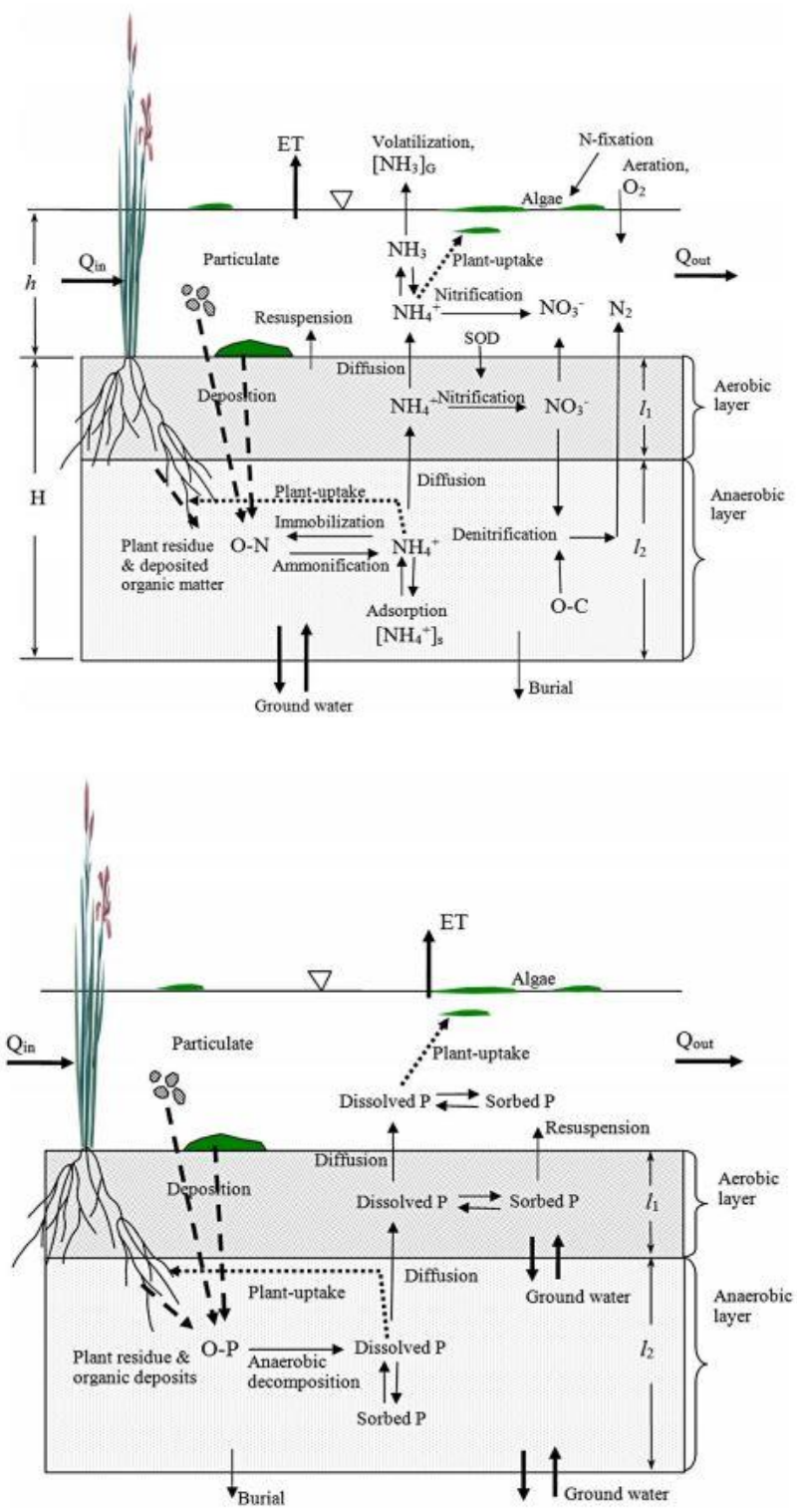

Figure 2.1. Nitrogen (top) and Phosphorous (bottom) cycle in WetQual (Hantush et al., 2013)

2.2 Sensitivity Analysis

In this study, combination of Generalized Likelihood Uncertainty Estimation (GLUE) (Beven and Freer, 2001) and General Sensitivity Analysis (GSA) (Spear and Hornberger, 1980) method was utilized to analyze sensitivity of WetQual to various input forcings and model input parameters. GLUE is based on the equality of different model parameter sets and structures because there is no perfect model structure and parameter set to be used as a true parameter set (Beven and Binley, 1992). The GSA method has several steps, starting with model parameter sampling. A matrix (***A***) is created with 100,000 randomly generated model parameters (see Table 2.1 and Table 2.2 for model parameters and their distributions). Each row of ***A*** represents a model parameter set. Then, a Monte Carlo (MC) simulation is performed with these parameter sets. WetQual will basically be run for each row created in ***A*** to generate ensemble of model output time series for each component of the model. Each MC simulation corresponds to a parameter set. Nash-Sutcliffe coefficient (E_{NS}) (Nash and Sutcliffe, 1970) was used in this study to evaluate the model performance of each MC simulation for each model output.

$$E_{NS} = 1 - \left[\frac{\sum_{i=1}^{n}\left(A_i^{obs} - A_i^{sim}\right)^2}{\sum_{i=1}^{n}\left(A_i^{obs} - A^{mean}\right)^2}\right] \dots\dots\dots\dots\dots\dots\dots\dots\dots\dots\dots (15)$$

where A_i^{obs} is the i^{th} observation value, A_i^{sim} is the i^{th} simulation value, and A^{mean} is the average of observed data.

Table 2.2. Model parameters' distributions and their minimum and maximum values

Parameters	Distribution	Min	Max
L2 (cm)	Uniform	5	50
theta	Uniform	1.15	1.35
Is (ly/day)	Uniform	100	400
fNup	Uniform	0.29	0.38
kd (mL/g)	Log-N (min max)	0.032	80
kep (1/m)	Uniform	0.15	0.45
kga0 (1/day)	Log-N (min max)	0.0009	0.002
kgb0 (1/day)	Log-N (min max)	0.0009	0.002
kmin1s (1/day)	Log-N (min max)	0.000001	0.0031
knw (1/day)	Log-N (min max)	0.0001	0.35
kminw (1/day)	Log-N (min max)	0.000001	0.001
kns (1/day)	Log-N (min max)	0.01	42
kden (1/day)	Uniform	0.004	0.15
rowp (gr/cm^3)	Uniform	1.5	2.2
vels_o (cm/day)	Log-N (min max)	0.025	138
vels_s (cm/day)	Log-N (min max)	8	6750
velb (cm/day)	Uniform	0.000274	0.006575
ana (gN/gChl)	Uniform	3.5	17.6
rChl (gC/gChl)	Uniform	20	100
Ss (g/L/day)	Uniform	0.022	0.065
Sw (g/cm^3/day)	Uniform	0	0
c_Uw	Uniform	0.0864	0.3456
frap	Uniform	0.5	1
c1	Uniform	0.04	0.14
c2	Uniform	1228	3686
PH	Uniform	4.5	8.2
S (mg-N/m^3/hr)	Log-N (min max)	0.0004	3.5
Kw (cm^3/g)	Log-N (min max)	1024	1193731
apa (gP/gChl)	Uniform	0.4	2
Dnp (cm^2/day)	Uniform	0.66	0.83
Ksa (cm^3/g)	Log-N (min max)	1024	1193731
Ksb (cm^3/g)	Log-N (min max)	8780	18549874
RanN1	Uniform	0	1
fW	Uniform	0.5	1
fact	Log-N (min max)	9.3	2021
a_vr_o	Log-N (min max)	0.00001	61
a_vr_s	Log-N (min max)	0.00001	0.46121
porw (mL/g)	Uniform	0.65	0.95

A threshold value (E_{NS}') is determined to divide the matrix ***A*** into behavioral (***B***) and non-behavioral (***B'***) matrices. If an E_{NS}' value is thought to be effective enough to represent the real system (for my study top 1% (=1000) is selected), the parameter sets with $E_{NS} > E_{NS}'$ will then belong to ***B*** matrix. After the separation of ***A*** matrix into ***B*** and ***B'*** matrices, Kolmogorov-Smirnov (K-S) Test is applied. This test constructs two cumulative distribution functions, one from ***B*** and one from ***B'***, known as CDF_B and $CDF_{B'}$ and calculates the maximum deviation (D_{max}) between the two CDFs. For a predetermined significance level of α, if D_{max} is smaller than the K-S statistic, D_α, or the *p*-value that corresponds to D_{max} is larger than α, then the separation is not achieved, and the two distributions are statistically similar; consequently, the model is not sensitive to that parameter. Lastly, D_{max} values are ranked from highest to smallest to develop parameter sensitivity rankings. Higher D_{max} values are related to higher sensitivities and vice versa (Kalin et al., 2013)

2.3 Study Site

The study site is the Barnstable Wetland on Kent Island, Maryland (Figure 2.2). Hydrologic and water quality data have been collected during a two-year study in this wetland as described in detail by Jordan et al., (2003) and Whigham et al., (2002). The wetland is on Kent Island, Maryland, which is a part of the Delmarva Peninsula on the eastern shore of the Chesapeake Bay. Much of the surrounding land is comprised of farmlands, cultivated primarily for corn and soybean production. The 14-ha watershed draining to the wetland was 18% forest and 82% cropland with an average slope of 1%. It was planted for corn in 1995 and 1997 and for soybean in 1996. Soils of the area have a silt loam texture with a moderate or moderately slow permeability. Due to the low permeability of the soils and the low topographic relief, most croplands in the study area are drained by ditches or plowed channels that discharge water into wetlands, streams, riparian forests,

or directly into the Chesapeake Bay. Artificial drainage has converted some wetlands to croplands (Jordan et al., 2003). Before being restored to the wetland in 1986 by the Chesapeake Wildlife Heritage as a part of their program to provide wildlife habitat and improve the quality of runoff from agricultural fields, the studied wetland was an artificially drained cropland. During the restoration, a 1 m deep depression was created by removing a layer of soil, some of which was later used to create a low dike to retain water. Topsoil was returned to the surface after excavation, and wetland vegetation was established by natural succession. Drainage leads carrying surface runoff from the surrounding watershed and precipitation falling directly on the wetland surface were the only sources of the water entering the wetland. Loss of water from the wetland was via standpipe drain installed in the dike and evapotranspiration. When the water was deep enough to flow out the drain, the entire 1.3-ha area of the wetland was submerged; it lacked well-defined flow channels. Jordan et al., (2003) reported negligible groundwater exchanges due to the impermeable layer of clay within 0.5 m of the soil surface. Clay samples from beneath inundated areas were found to be dry (Jordan et al., 2003). Removal of nutrients and suspended solids from this restored wetland, which received unregulated inflows from the 14-ha agricultural watershed, were monitored using the automated flow-proportional sampling. Water entered the wetland mainly in brief pulses of runoff, which sometimes exceeded the 2500-m^3 water holding capacity of the wetland.

Figure 2.2. Study area, Barnstable 1 Kent Island, Maryland

2.4 Summary of Barnstable Wetland Data

The input data related to the study wetland comes from Jordan et al., (2003). They measured particulate organic nitrogen, total ammonia, nitrate, inorganic phosphorous, sediment and total

organic carbon in inflow and outflow from 5/8/1995 to 5/12/1997. Jordan et al. (2003) provides detailed information about data collection. Table 1 provides a summary of the data.

Table 2.3. Summary of Data Source

Precipitation	• Rain gauges at the wetland • Wye Research Center (WRC)
Outflow	• 120° V-notch weir (every 15 min)
ET	• Smithsonian Environmental Research Center (SERC)
Temperature	• Annapolis Police Bar, MD US (ID: 00180193) NCDC Station
Wind Speed	• Baltimore Washington International Airport, MD US (ID: 00093721) NCDC Station
Atmospheric Deposition	• National Oceanic and Atmospheric Administration Station (NOAA) (Lewes DE 02)

Total water input was calculated by adding the rate of outflow and increase in wetland volume. Figure 2.3 and Figure 2.4 show the observed water input and averaged dept and constituent concentrations

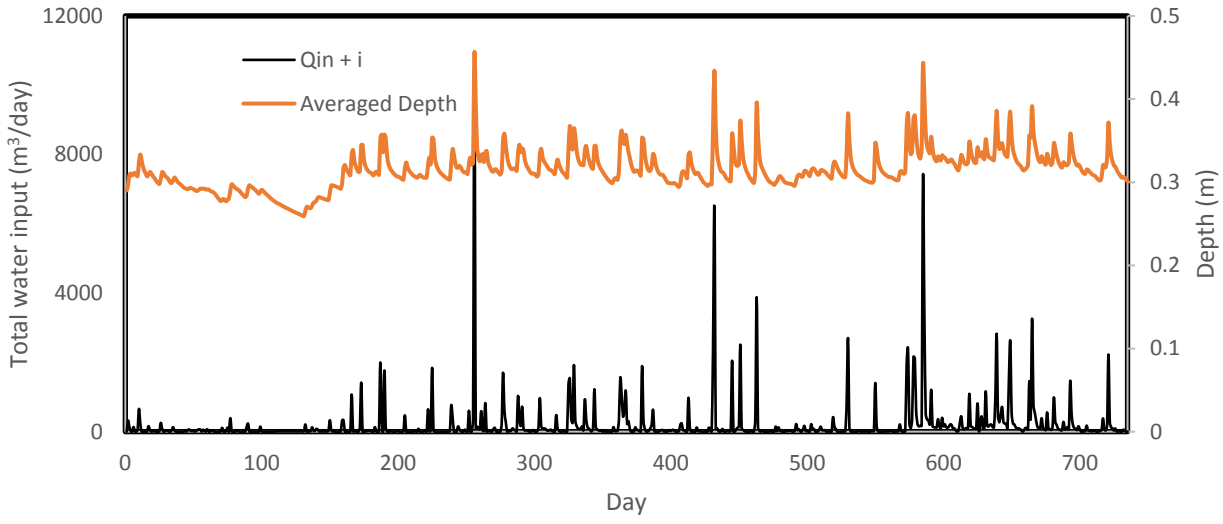

Figure 2.3. Total water input (inflow (Q_{in}) + precipitation (i)) and averaged depth

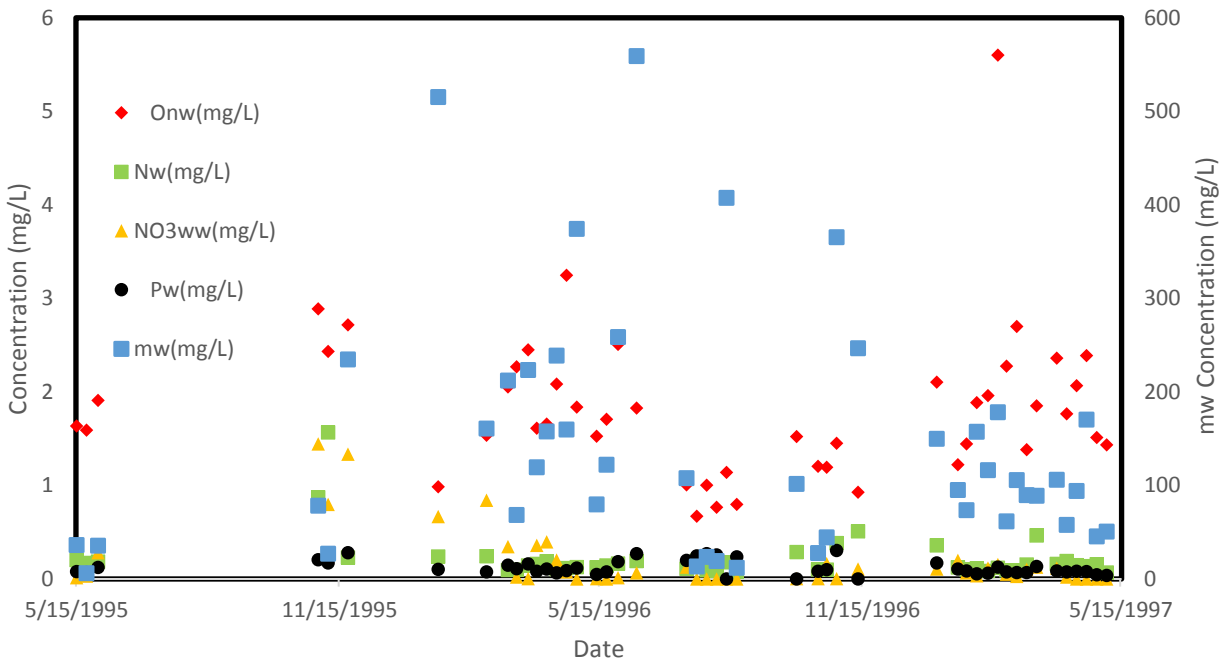

Figure 2.4. Observed nutrients and sediment concentrations for particulate organic nitrogen (ON_w), total ammonia-nitrogen (N_w), nitrate-nitrogen (NO_{3w}), total inorganic phosphorous (P_w), and sediment (m_w)

WetQual requires all the input data daily because it runs simulations on daily time scale. For numerical purposes, WetQual divides the daily data into smaller time intervals (e.g. 1/100 day or smaller) by interpolating daily data to generate values at the smaller time intervals. WetQual also requires initial concentrations. The initial concentrations were taken from the first day of input data. Due to this requirement, simulations started on 5/9/1995 and ended on 5/12/1997. Nutrient and sediment concentrations were measured weekly flow averaged generally every 5-8 days, but there were missing data periods. In these periods, averages of last measurements before the data gaps and the first measurements at the end of the gap period were used to fill missing data. There were 47 observed data for organic nitrogen (ON_w), total ammonia (N_w), and sediment (m_w) while 44 for inorganic phosphorus (P_w), and 39 for nitrate (NO_{3w}) showed in Figure 2.4. The subscript

"w" indicates that measurements are from the water column (WetQual also produces estimates of almost the same constituents in the soil layer and they have subscript "s").

2.5 Modeling Experiments

2.5.1 Bathymetry Application

Due to the difficulty in measuring bathymetry of natural wetlands and to reduce time and labor costs, coarse data or approximations are often used to determine the Depth-Area-Volume relationships ($V - A - h$), such as using digital elevation model (DEM) data, or certain geometric shapes are assumed. These simple methods can be expected to increase the predictive uncertainty of wetland models.

In this part of the research, I estimate $V - A - h$ relationships assuming that I only have maximum depth and maximum surface area data. In this respect, I considered four different shapes in the model and compared the hydrology and water quality results with the one generated using the actual bathymetry. The geometric profiles considered are as follows;

$$W_{0.5}: \quad h(x) = h_0 + a\sqrt{|x|} \quad \ldots\ldots\ldots\ldots\ldots\ldots\ldots\ldots (16)$$

$$W_1: \quad h(x) = h_0 + a|x - x_0| \quad \ldots\ldots\ldots\ldots\ldots\ldots\ldots (17)$$

$$W_2: \quad h(x) = h_0 + a(x)^2 \quad \ldots\ldots\ldots\ldots\ldots\ldots\ldots\ldots (18)$$

$$W_4: \quad h(x) = h_0 + a(x)^4 \quad \ldots\ldots\ldots\ldots\ldots\ldots\ldots\ldots (19)$$

where, h is water depth, x is radius and a is shape factor (Figure 2.5). To create the bathymetries from these equations, I assumed that wetland surface areas are is in circular shape. All the synthetic bathymetries and their $V - A - h$ relationships were calculated by integrating above equations. Example calculation for $W_{0.5}$ wetland is shown in Appendix 1. For W_1 wetland, I needed to provide

very low h_0, A_0, and V_0 values to create a bathymetry because of mathematical problems. The final equations for the synthetic wetlands are as follows;

$W_{0.5}$;

$$A(h) = \frac{A_{max} * h^4}{h_{max}^4} \dots\dots\dots\dots\dots\dots\dots\dots\dots\dots\dots\dots\dots\dots\dots\dots\dots (20)$$

$$V(h) = V_{max} - \left(\frac{A_{max}}{5 * h_{max}^4} * (h_{max}^5 - h^5)\right) \dots\dots\dots\dots\dots\dots (21)$$

W_1;

$$A(h) = A_0 * \left(\frac{1 + \left(1 - \frac{\sqrt{A_0}}{\sqrt{A_{max}}}\right) * (h - h_0)}{\frac{\sqrt{A_0}}{\sqrt{A_{max}}} * (h_{max} - h_0)}\right)^2 \dots\dots\dots\dots (22)$$

$$V(h) = V_0 * \left(\frac{1 + \left(1 - \frac{\sqrt[3]{V_0}}{\sqrt[3]{V_{max}}}\right) * (h - h_0)}{\frac{\sqrt[3]{V_0}}{\sqrt[3]{V_{max}}} * (h_{max} - h_0)}\right)^3 \dots\dots\dots\dots (23)$$

W_2;

$$A(h) = \frac{A_{max} * h}{h_{max}} \dots\dots\dots\dots\dots\dots\dots\dots\dots\dots\dots\dots\dots\dots\dots\dots\dots (24)$$

$$V(h) = V_{max} - \left(\frac{A_{max}}{2}\right) * \left(h_{max} - \frac{h^2}{h_{max}}\right) \dots\dots\dots\dots\dots\dots (25)$$

W_4;

$$A(h) = \frac{A_{max} * \sqrt{h}}{\sqrt{h_{max}}} \dots\dots\dots\dots\dots\dots\dots\dots\dots\dots\dots\dots\dots\dots\dots\dots\dots (26)$$

$$V(h) = V_{max} - \left(\frac{2}{3} * \frac{A_{max}}{\sqrt{h_{max}}}\right) * \left(\sqrt{h_{max}^3} - \sqrt{h^3}\right) \dots\dots\dots (27)$$

where h is depth, A is surface area, V is volume, $h_{max}, A_{max},\ and\ V_{max}$ are maximum depth (1.14 m), surface area (11616 m^2), and volume (8477 m^3), respectively and h_0, A_0 and V_0 are initial water depth (0.007 m), surface area (158.15 m^2), and volume (1.58 m^3), respectively. From this point,

wetlands which are related to synthetic bathymetries are called $W_{0.5}$, W_1, W_2, and W_4 (equations 20 to 27). Also, actual wetland is called W_A. Figure 2.5 shows the simplified vertical profiles along with the actual surveyed profile for the study wetland.

As clearly seen from figure 4, the profile W_4 wetland has the highest similarity to the W_A wetland profile. This means that we can expect the model results from these two profiles to be closer than others. On the other hand, the results coming from the $W_{0.5}$ can be expected to be much different than others, but the question is whether this difference will be significant. The model results to be scrutinized will be based on particulate organic nitrogen (ON_w), total ammonia-nitrogen (N_w), nitrate-nitrogen (NO_{3w}), total inorganic phosphorus (P_w) and total suspended sediment (m_w) loads in free water. At the end of the study, I will have an answer to the question whether the most accurate bathymetry information is needed, or whether I can assume a simple geometry and create my own bathymetry data using easily accessible data. However, I need to mention that although results will shed light into the importance of accuracy needed in bathymetry, results will still be specific to the study wetland and therefore caution is needed before generalization of the results.

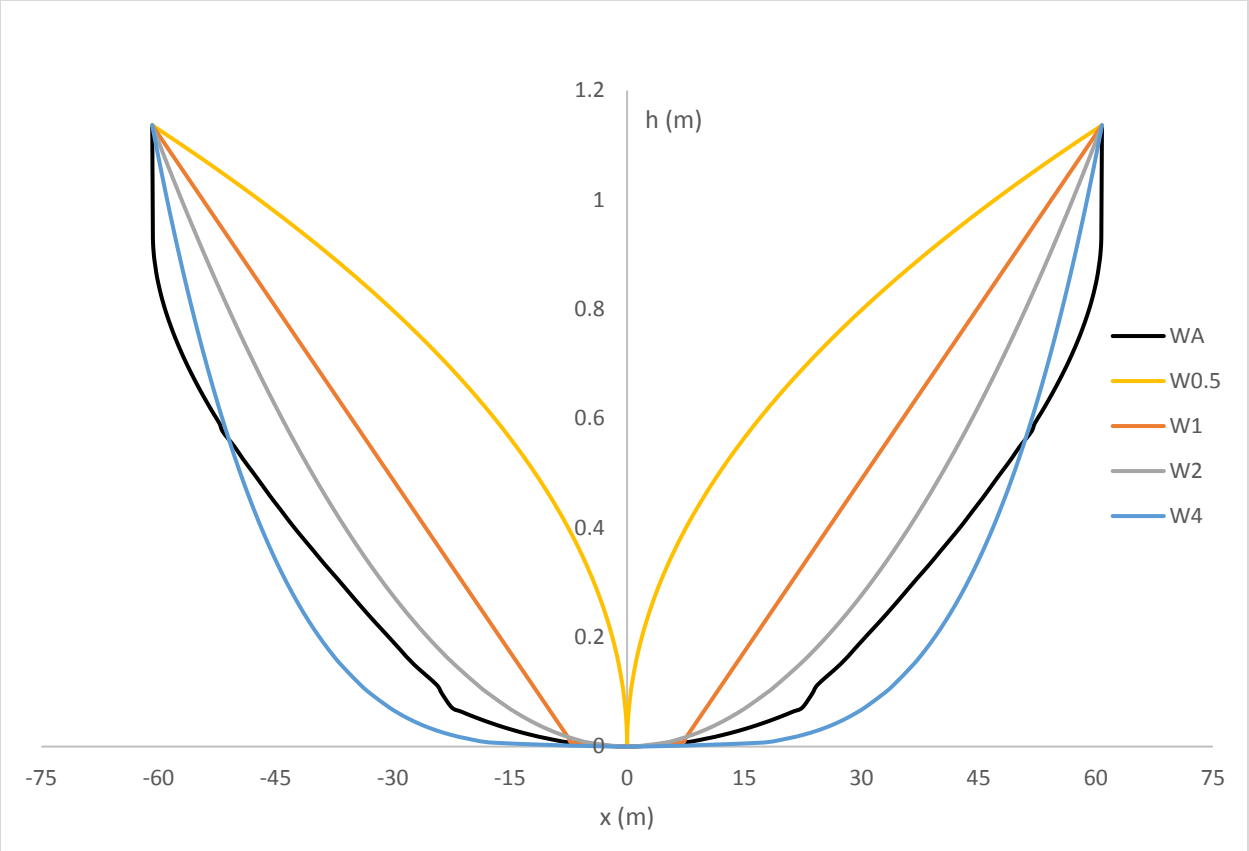

Figure 2.5. Geometric profiles of the actual and synthetic wetlands

2.5.2 Temperature Application

Water temperature is needed in WetQual in order to update biochemical reaction rates. Reaction rates in WetQual are updated for temperature changes based on the Arrhenius equation (Schnoor, 1996);

$$k_T = k_{20}\theta^{T_w-20} \ldots\ldots\ldots\ldots\ldots\ldots\ldots\ldots (28)$$

where T_w is water temperature (^{0}C), θ is constant (temperature coefficient), k_{20} is rate constant at 20 ^{0}C.

WetQual uses the following equation to calculate water temperature (T_w) from air temperature (T_{air});

$$T_w = 5.0 + 0.75\, T_{air} \ldots\ldots\ldots\ldots\ldots (29)$$

This equation was originally developed for streams and was adopted in WetQual (Hantush et al., 2013). In reality, water temperature in wetlands can be affected by vegetation cover, groundwater discharge and depth of water. Without making this relationship more complicated, it is reasonable to expect the two constants in above equation vary from wetland to wetland. By taking this idea in this application, I replaced the two constants with unknown coefficients in order to determine the models' sensitivity to these parameters and their impacts on model uncertainty. Therefore, the new equation becomes;

$$T_w = a_T + b_T\, T_{air} \ldots\ldots\ldots\ldots\ldots\ldots\ldots\ldots (30)$$

The coefficients a_T and b_T were generated within a range between 1 and 10 and between 0.1 and 0.9, respectively. The sensitivity of the coefficients and their optimal range were assessed to explore whether the equation currently adopted in WetQual is adequate. At the end of this experiment, I look for an answer to the question whether we need to introduce a more complex, or a physically-based water temperature prediction component, or if we can continue using the existing simple equation.

2.5.3 Effects of Temporal Resolution of Hydroclimatic data

The current version of WetQual requires daily temperature and inflow as inputs. However, since the model actually runs at sub-daily time scale for numerical purposes, it needs sub-daily values. For this WetQual disaggregates the daily data into sub-daily data by assuming constant rates. Nowadays, precipitation and temperature data can be often found at hourly or even smaller time scales. Also, inflow data could be available at smaller time intervals too (e.g. 15 min). According

to the literature, the use of sub-daily input forcing data provides more accurate results than the use of daily data (Yang et al., 2015).

In this study, I have increased the temporal resolution of temperature and temporal resolution of temperature and inflow together to identify the impacts that are caused by temporal resolution of inputs on parameter sensitivity and model uncertainty. The sub-daily time interval used was 0.01 days. The application of increasing time resolution of temperature is called T_{sub} and increasing time resolution of inflow is called QT_{sub} in this application. The results from these two applications were compared with T_{new} application because I would like to see the importance of temperature conversion equation.

Observed data was available for inflow at sub-daily level. For temperature, we had daily maximums and minimums. To increase temporal resolution of temperature I used the following sinusoidal function (Campbell, 1985):

$$T_h = \left(\frac{T_{max} + T_{min}}{2}\right) + \left(\frac{T_{max} - T_{min}}{2}\right)\cos(0.2618(h - 15) \dots\dots\dots\dots\dots (31)$$

where, T_h is air temperature at time h (hour of day), and T_{max} and T_{min} are maximum and minimum daily air temperatures, respectively.

Due to the changes in time resolution of temperature data, the temporal resolution of ET was also changed into sub-daily format using the approach proposed by Fayer (2000);

$$ET_P(t) = 0.24T_p^* \qquad \frac{t}{d} < 0.264, \frac{t}{d} > 0.736\text{d} \dots\dots\dots\dots\dots\dots\dots\dots\dots\dots\dots (32)$$

$$ET_P(t) = 2.75T_p^* \sin\left(\frac{2\pi t}{d} - \frac{\pi}{2}\right) \qquad 0.264 < \frac{t}{d} < 0.736 \dots\dots\dots\dots\dots\dots (33)$$

where, ET_p^* is the daily potential evapotranspiration (PET), $\frac{t}{d}$ is fraction of a day. These equations assume that hourly ET values between 0-6 a.m. and 18-24 p.m. are equal to the 1% of the total daily value of ET. ET in rest of the day is represented with a sinusoidal function.

Next chapter presents the results from these experiments. Rresults are divided in two groups, which are model performances and uncertainty and sensitivity for each study. A brief information of methodology is presented in Figure 2.6.

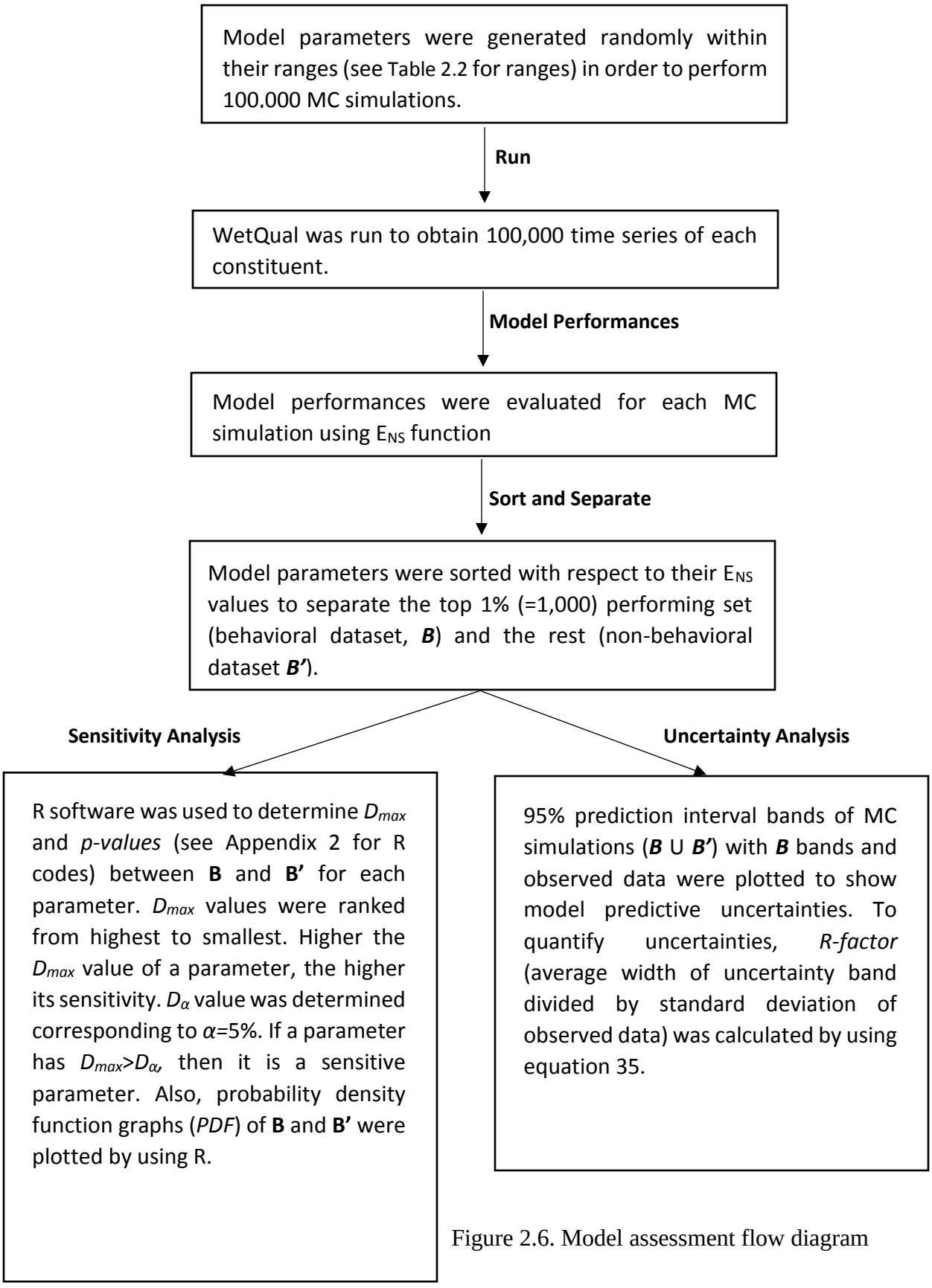

Figure 2.6. Model assessment flow diagram

In this research, 100,000 independent parameter sets were generated to perform MC simulations with WetQual. WetQual was run 100,000 times with each parameter set, and after each run model generated time series for each constituent. To evaluate model performances, E_{NS} values were calculated to quantify the goodness of fit between model outputs and observed data. Parameter sets were sorted from highest to smallest with respect to E_{NS} values and top 1% (1000) datasets were separated as behavioral dataset (***B***) because this limit was recognized effective for all 5 constituents. Rest of the parameter sets were deemed as non-behavioral dataset (***B'***). Kolmogorov-Smirnov test (K-S test) was then applied to ***B*** and ***B'*** datasets using R software to calculate D_{max} and *p-values*. An example R-script for K-S test is available in Appendix 2. The D_{max} values of parameters were sorted from largest to smallest for each constituent. The order of D_{max} values was also the order of sensitivity. Most sensitive parameter had the highest D_{max} value. Each D_{max} values is associated with a *p*-value. Parameters having *p*-values>α were assumed to be non-sensitive. For this study, confidence level was set at 95% (i.e., α=0.05). Further, probability density functions (PDF) were plotted using R software to visually see the difference between ***B*** and ***B'*** sets of each parameter. An example R-script for PDF plots is also available in Appendix 2.

To assess model predictive uncertainty, time series of outputs generated from ***B***, 95% prediction interval of (***B*** U ***B'***) and observed time series were plotted. *r-factor values* were calculated for each constituent to compare the efficiency of the applications on the model predictive uncertainties. *r-factor* is a dimensionless performance metric calculated by dividing the average width of the uncertainty band by the standard deviation of observed data (eq. 35).

In the next chapter, comparison of results from the synthetic wetlands ($W_{0.5}$, W_1, W_2, and W_4) to the actual wetland (W_A) results will be presented and discussed in order to assess the uncertainty introduced by different shapes created using the basic equations presented earlier. In

temperature analysis part, temperature conversion equation coefficients were varied to see if any improvement in model performances can be achieved compared to the results obtained with the default temperature conversion equation. To have a deeper understanding, assessment was carried out for year 1 and year 2 separately too, as these two years had hydrological dissimilarities. Lastly, results are also presented comparing model sensitivities and uncertainties under daily time scale and sub-daily inputs.

3 RESULTS

3.1 Bathymetry Analysis Results

3.1.1 Hydrology Results

The actual and approximated wetland profiles were shown in Figure 2.5. Due to the similarity of the profiles, model results based on W_2 and W_4 are expected to be comparable to results of W_A. To test this inference, simulated flow depths were examined carefully. Figure 3.1 and Table 3.1 compare the water depths from all these created wetlands. Figure 3.1 shows the probability of exceedance of depths for these wetlands.

A quick glance at the graphs reveals some striking similarities between the W_A and W_4 results. On the other hand, by far the most significant difference is between W_A and $W_{0.5}$ when the probability of exceedance graphs of water depths are compared. The depth-duration-curves for wetlands W_1 and W_2 are not as close to that of W_A compared to W_4. However, they are much closer than the depth-duration-curves of $W_{0.5}$.

Table 3.1 shows a number of differences and similarities between the wetlands in terms of maximum, minimum and average water depth and volume. One interesting fact is that the average depths are very similar showing a very small variation (59.9-60.2 cm). $W_{0.5}$ has the highest maximum (85.5 cm) and minimum water depth (54.3 cm) values while W_A has the lowest maximum water depth (83.6 cm) and W_4 has the lowest minimum water depth (47.4 cm). It can be seen from Table 3.1 that W_A and W_4 have very close values compared to other wetlands. The

minimum and maximum depths for $W_{0.5}$ shows the greatest deviation compared to values of W_A, which supports our observations in Figure 2.5.

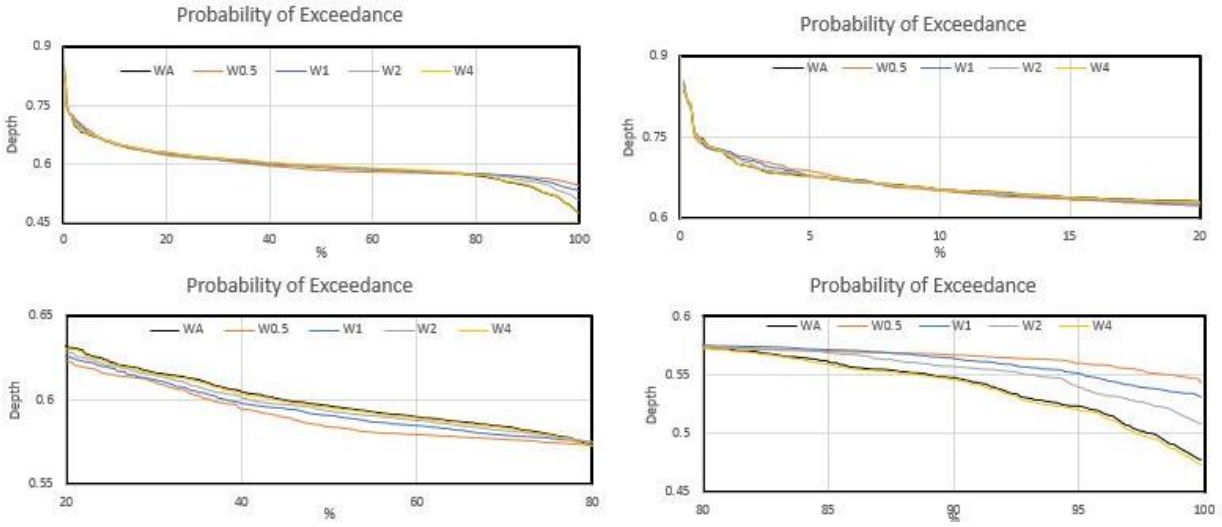

Figure 3.1. Water depth probability of exceedance curves for each wetland

Table 3.1. Maximum, minimum, and average water depth (*H*) and volume (*V*) in the actual and hypothetical wetlands.

Wetland	H_{max} (cm)	H_{min} (cm)	H_{avg} (cm)	V_{max} (m^3)	V_{min} (m^3)	V_{avg} (m^3)
W_A	83.6	47.7	60.0	5120	1773	2745
$W_{0.5}$	85.5	54.3	60.0	636	66	114
W_1	84.9	53.2	60.2	3725	1029	1454
W_2	84.5	50.9	60.1	3650	1323	1858
W_4	84.0	47.4	59.9	5595	2370	3379

Wetland volume plays an important role in wetland water quality. Table 3.1 and Figure 3.2 summarize the water volumes in the wetlands. Flow routing revealed that W_4 always holds more water than the other geometries, including the actual profile. On the other hand, it is still closer to

the actual wetland than the others. $W_{0.5}$ wetland always has the lowest volumes and the values are significantly lower than the volumes of the other wetlands.

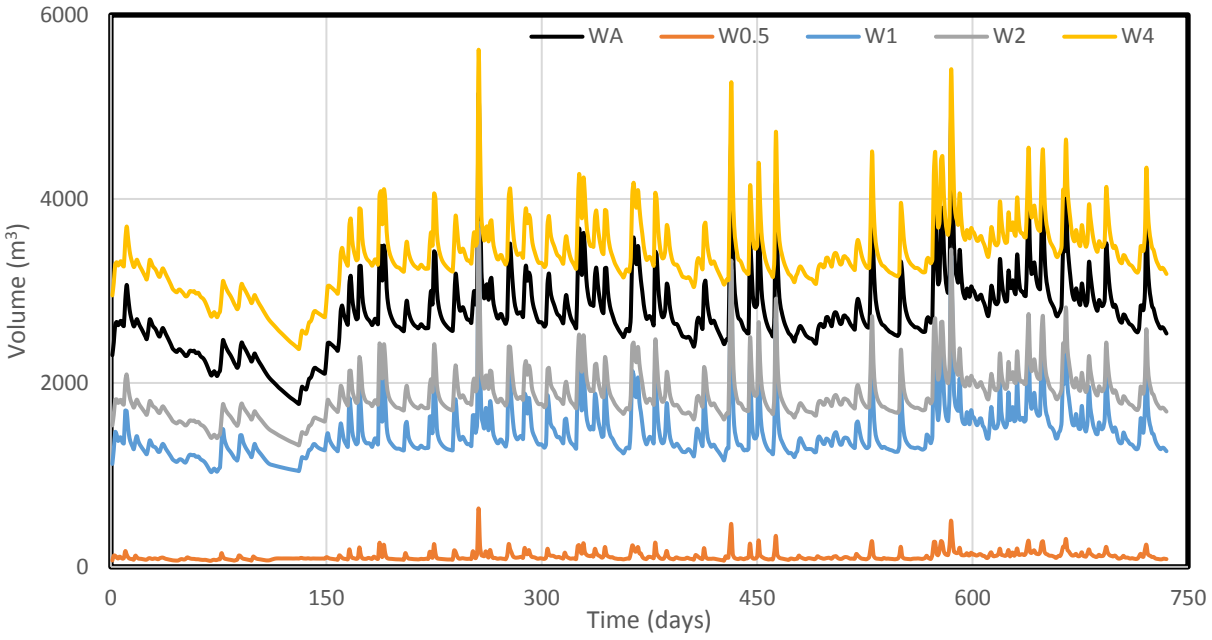

Figure 3.2. Daily water volumes in the wetlands

When the outflows of the created wetlands are compared to the actual wetland outflow, a similar picture shows up as can be seen in

Table 3.2. Again, Outflow of W_4 is the closest outflow with the actual wetland. In addition to this, $W_{0.5}$ has the highest maximum outflow and W_A has the lowest maximum outflows. Flashiness indexes (FI) were calculated for outflows using the formula below to assess their flashiness behavior.

$$FI = \frac{\sum_{i=1}^{735} Q_{i+1} - Q_i}{\sum_{i=1}^{735} Q_i} \dots\dots\dots\dots\dots\dots\dots\dots\dots\dots (34)$$

where, Q_i is outflow at i^{th} day.

As other bathymetry parameters, W_4 has the closest *FI* with W_A and $W_{0.5}$ has the farthest *FI* (

Table 3.2).

Table 3.2. Minimum and maximum outflow (Q_{out}) and number of days with no outflow and flashiness index (*FI*) in the actual and hypothetical wetlands.

	W_A	$W_{0.5}$	W_1	W_2	W_4
Min Q_{out} (m^3/day)	0	0	0	0	0
Max Q_{out} (m^3/day)	7696	9101	8668	8350	7993
Number of days with no outflow	78	6	32	46	78
FI	0.83	1.12	1.00	0.92	0.85

To sum up, aside from the physical similarities, W_4 is also highly similar to the actual wetland. The level of similarity to the actual wetland decreases in this order: W_4, W_2, W_1, and $W_{0.5}$.

3.1.2 Model Performance and Uncertainties

The focus of this study is on pollutant loads. Although results will be presented for concentrations too in several occasions, selection of behaviors sets (***B***) are based on loads. The WetQual model does a decent job in predicting nutrients and sediment loads. Table 3.3 shows the minimum, maximum and average loading-based E_{NS} values of the behavioral set (***B***) simulations for all constituents in 5 wetlands. The average E_{NS} values for ON_w, N_w, NO_{3w}, P_w and m_w are 0.48, 0.84, 0.97, 0.61, and 0.81, respectively, for the actual wetland. Comparing these model performances with those of the synthetic wetlands, performance of NO_{3w} and m_w are more or less the same for all wetlands. For ON_w, the performances of the model simulations for W_4 and W_1 are slightly higher than the actual wetland while the performance for $W_{0.5}$ is relatively lower than the actual wetland. The performances of the model simulations for total ammonia for $W_{0.5}$ and W_4 wetlands are better than the other three wetlands. The most surprising results are with inorganic phosphorus, where

$W_{0.5}$ performed better than all others, including W_A. As a matter of fact, W_A and W_4 have the lowest performances. One conclusion that can be drawn from this is that by model calibration good model performance can achieved even with a totally irrelevant shape. This can possibly lead to model parameters (thus processes) not representative of the real system. This issue will be scrutinized in detail later.

Table 3.3. Minimum, maximum and average E_{NS} values of behavioral (***B***) part for all constituents for all wetlands.

	ON_w			N_w			$NO3_w$			P_w			m_w		
Wetland	**Min**	**Max**	**Avg**	**Min**	**Max**	**Avg**	**Min**	**Max**	**Avg**	**Min**	**Max**	**Avg**	**Min**	**Max**	**Avg**
W_A	0.47	0.50	0.48	0.84	0.86	0.84	0.96	0.97	0.97	0.56	0.79	0.61	0.76	0.90	0.81
$W_{0.5}$	0.45	0.47	0.45	0.87	0.94	0.88	0.95	0.98	0.96	0.77	0.81	0.77	0.77	0.92	0.81
W_1	0.49	0.51	0.50	0.86	0.88	0.87	0.97	0.98	0.97	0.65	0.77	0.68	0.76	0.90	0.81
W_2	0.48	0.50	0.48	0.86	0.90	0.86	0.97	0.98	0.97	0.62	0.76	0.65	0.76	0.90	0.81
W_4	0.49	0.52	0.50	0.84	0.86	0.85	0.96	0.97	0.96	0.57	0.74	0.62	0.75	0.90	0.80

Figures 3.3 to 3.12 show the 95% prediction interval bands of MC simulations (***BU B'***) for loads and concentrations, the behavioral (***B***) bands and the observed data. There are 47 observed data points for ON_w, N_w, and m_w, 44 data points for P_w, and 39 data points for NO_{3w}. Note that the graphs are not continuous time series. Only the periods (typically 5 to 8 days) with a flow weighted average concentrations/loads are shown. Although one can visually see some differences in the width of the prediction bands corresponding to the behavioral sets, it is hard to do any detailed assessment based on the look. Therefore, $r-factor$, which symbolizes the relative width of the uncertainty band with respect to the standard deviation of observed data, were calculated for each wetland and constituent to compare the model uncertainties.

$$r-factor=\frac{1}{n\sigma_{obs}}\sum_{1}^{n}\left(Q_{i,max}-Q_{i,min}\right) \dots\dots\dots\dots\dots\dots\dots (35)$$

where, Q_i is the model output at i^{th}day, n is number of observed data and σ_{obs} is standard deviation of observed data. The subscripts max and min indicate the upper and lower bound of Q_i, respectively. High $r-factor$ values indicate high uncertainty, and vice versa. Typically, we want $r-factor \leq 1$. Table 3.4 shows the concentration and loading based $r-factor$ values for all wetlands and constituents.

Table 3.4. Concentration and load based $r-factor$s for all wetlands and constituents

Wetland	**ON_w**		**N_w**		**NO_{3w}**		**P_w**		**m_w**	
	Conc	**Load**	**Conc**	**Load**	**Conc**	**Load**	**Conc**	**Load**	**Conc**	**Load**
W_A	0.67	0.22	0.41	0.10	0.52	0.13	2.13	0.93	1.55	0.63
$W_{0.5}$	0.58	0.08	1.27	0.11	1.20	0.25	1.92	0.51	1.18	0.34
W_1	0.68	0.18	0.39	0.07	0.74	0.12	2.06	0.83	1.70	0.56
W_2	0.66	0.18	0.38	0.08	0.65	0.13	2.13	0.79	1.59	0.60
W_4	0.65	0.22	0.37	0.09	0.54	0.12	2.20	0.82	1.69	0.65

As can be seen in the table, load-based $r-factors$ are always smaller than the concentration-based $r-factors$. This is because loads were calculated by multiplying concentrations with flows and flow was considered deterministic in this study. Regarding ON_w loads, the $r-factors$ for W_A and W_4 wetlands are the same, 0.22, which is not surprising considering how similar their geometries are. Other wetlands have smaller $r-factors$ with $W_{0.5}$ having the lowest value at 0.08. Although $W_{0.5}$ has a very different $r-factor$ value, it is important to note that using this bathymetry reduces model uncertainty for ON_w with almost as good performance with others (Table 3.4). The trends with P_w and m_w are somewhat similar, where $W_{0.5}$ clearly has the smallest $r-factor$. This similarity can be related to the fact that ON_w and m_w are both particulate matters, and P_w is highly correlated with m_w. P_w has higher uncertainties than other constituents.

The $r-factor$s of N_w for all wetlands are about the same and the uncertainties are small. Results for NO_{3w} show that the uncertainties for created wetlands are at comparable level with the actual wetland, except for $W_{0.5}$ which has higher uncertainty (almost double of others). This is almost the opposite of the behavior observed with ON_w, P_w and m_w. NO_{3w} is dissolved and is highly reactive. Therefore, it is not surprising to see a different behavior with it. Using the bathymetry of $W_{0.5}$ instead of actual bathymetry increases the model predicted uncertainty for NO_{3w} while other bathymetries do not have significant impact on model predicted uncertainty.

To sum up, based on model performances, similar level of performances can be achieved even if the assumed bathymetries are highly different. Model calibration seems to find suitable parameter sets to produce equally good results. Based on output uncertainties W_4 wetland has the closest behavior to the actual wetland and $W_{0.5}$ wetland was the most different one. Uncertainties in outputs stemming from other geometries were not too far off compared to the actual wetland results. Hence, even from the model predictive uncertainty perspective, as long as the assumed bathymetric profile is not highly different from the actual bathymetry, one can safely approximate the bathymetry with simple geometries.

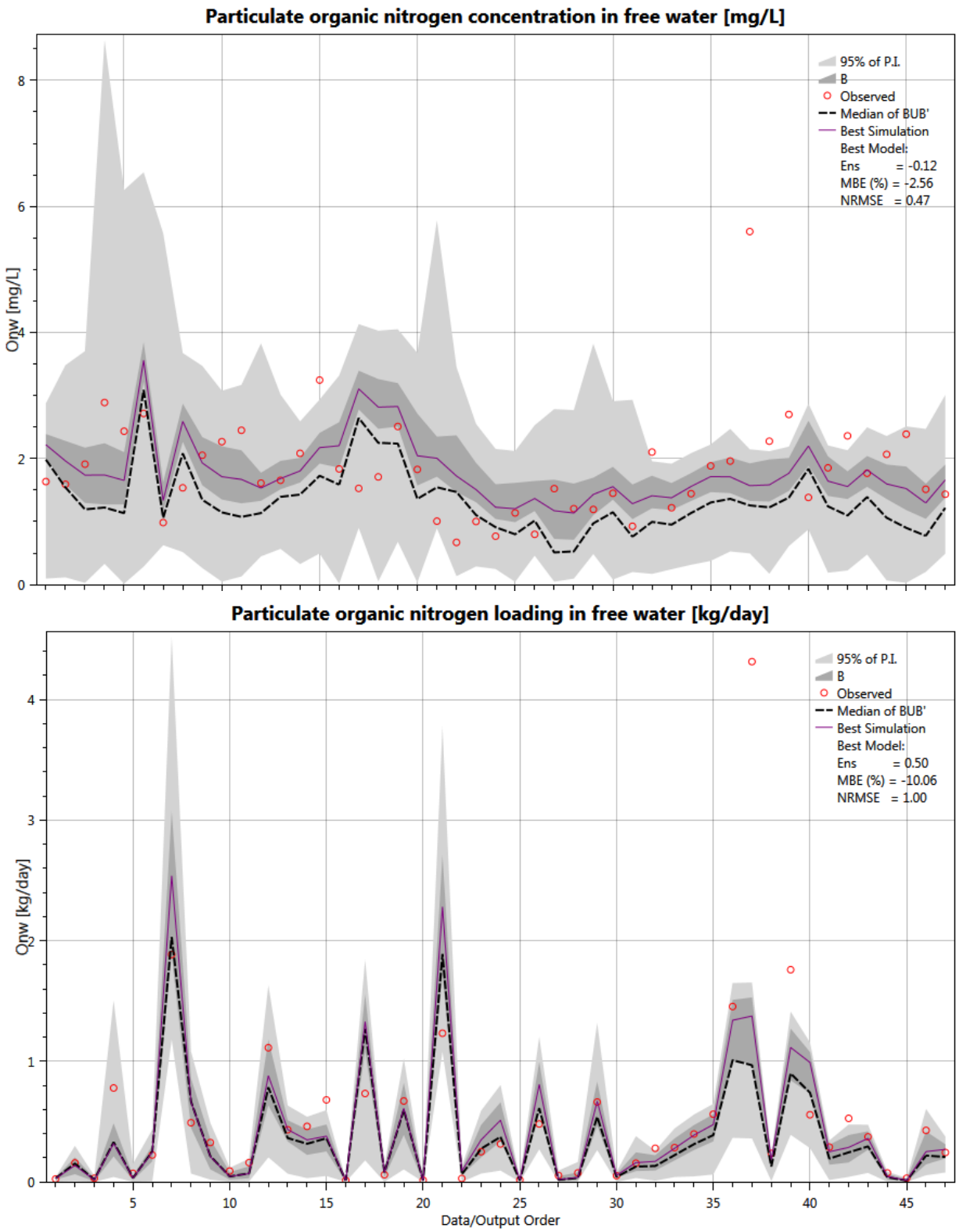

Figure 3.3. 95% prediction intervals (95% PI) of full MC simulations, behavioral simulations (B) and observed concentration and loading of organic particulate nitrogen for W_A

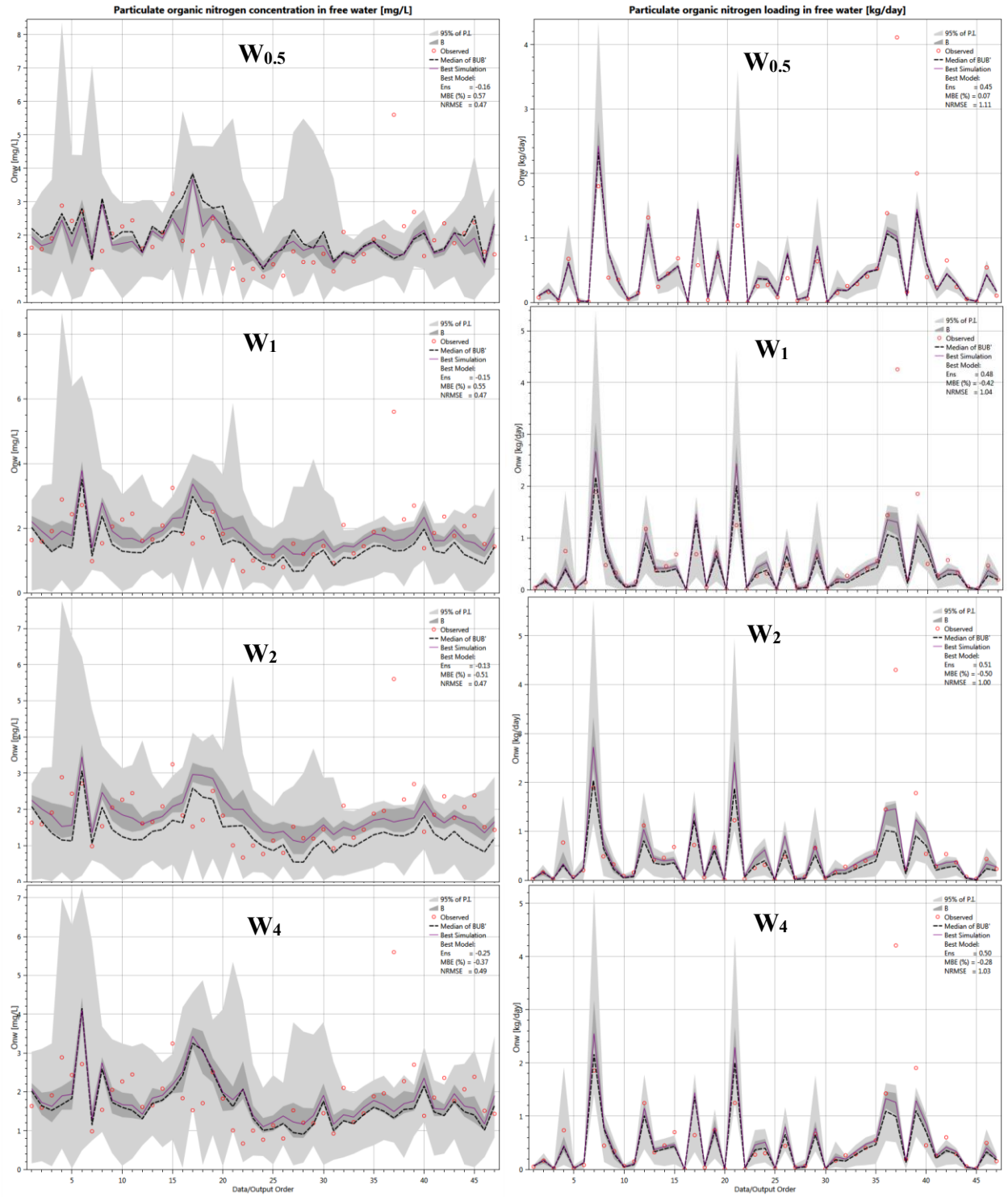

Figure 3.4. 95% prediction intervals (95% PI) of full MC simulations, behavioral simulations (B) and observed concentration and loading of organic particulate nitrogen for synthetic wetlands.

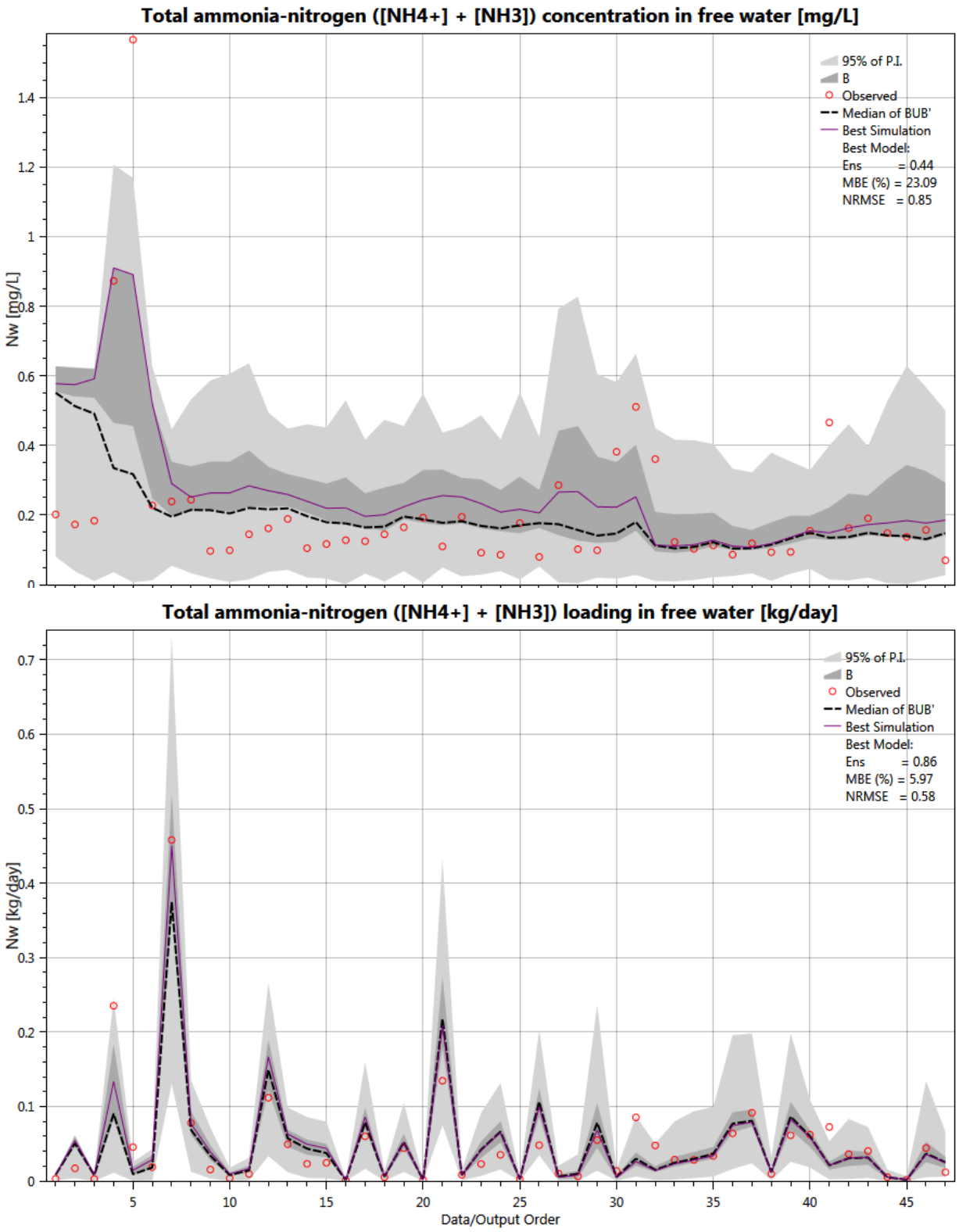

Figure 3.5. 95% prediction intervals (95% PI) of full MC simulations, behavioral simulations (B) and observed concentration and loading of total ammonia-nitrogen for W_A.

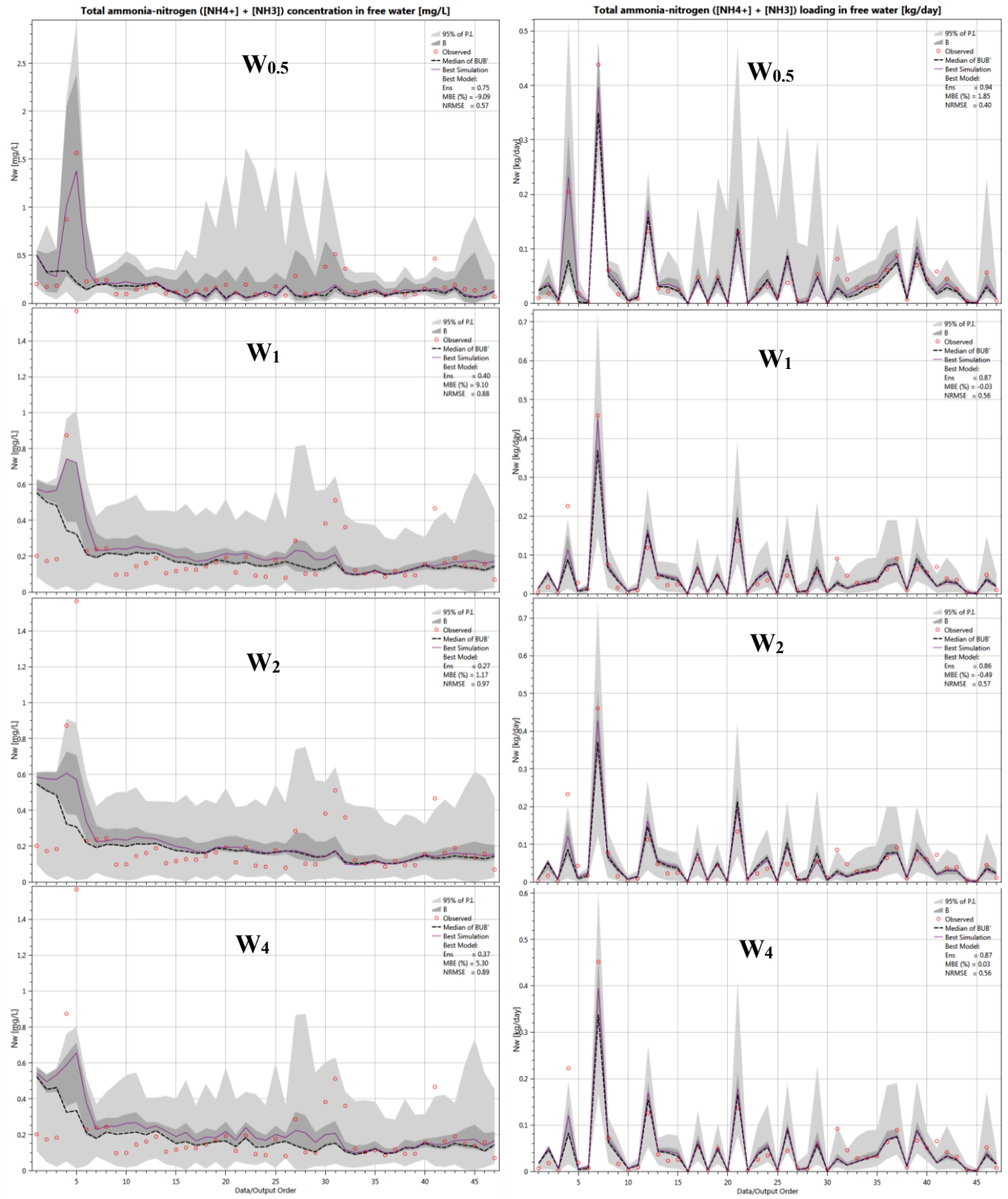

Figure 3.6. 95% prediction intervals (95% PI) of full MC simulations, behavioral simulations (B) and observed concentration and loading of total ammonia-nitrogen for synthetic wetlands

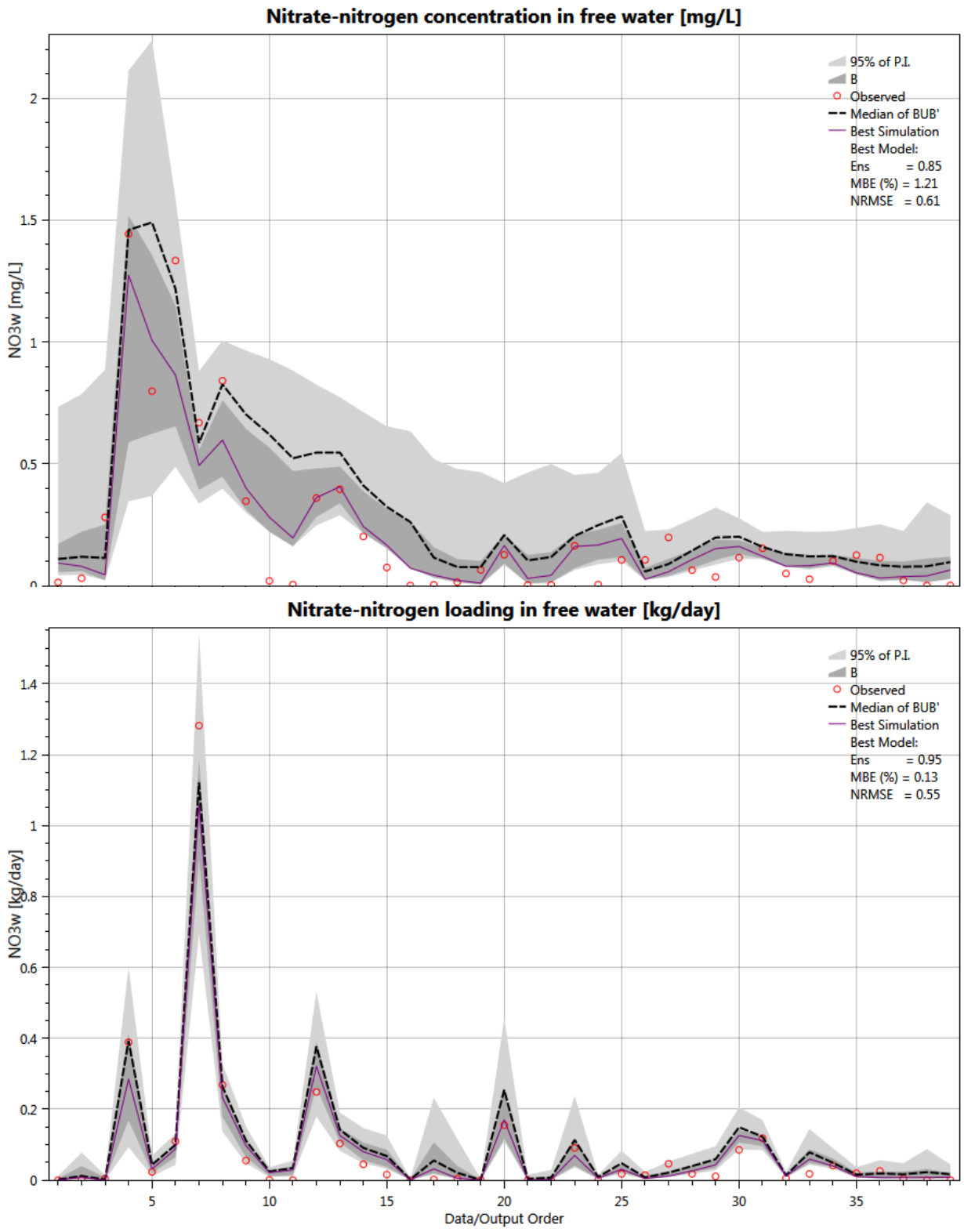

Figure 3.7. 95% prediction intervals (95% PI) of full MC simulations, behavioral simulations (B) and observed concentration and loading of nitrate-nitrogen for W_A

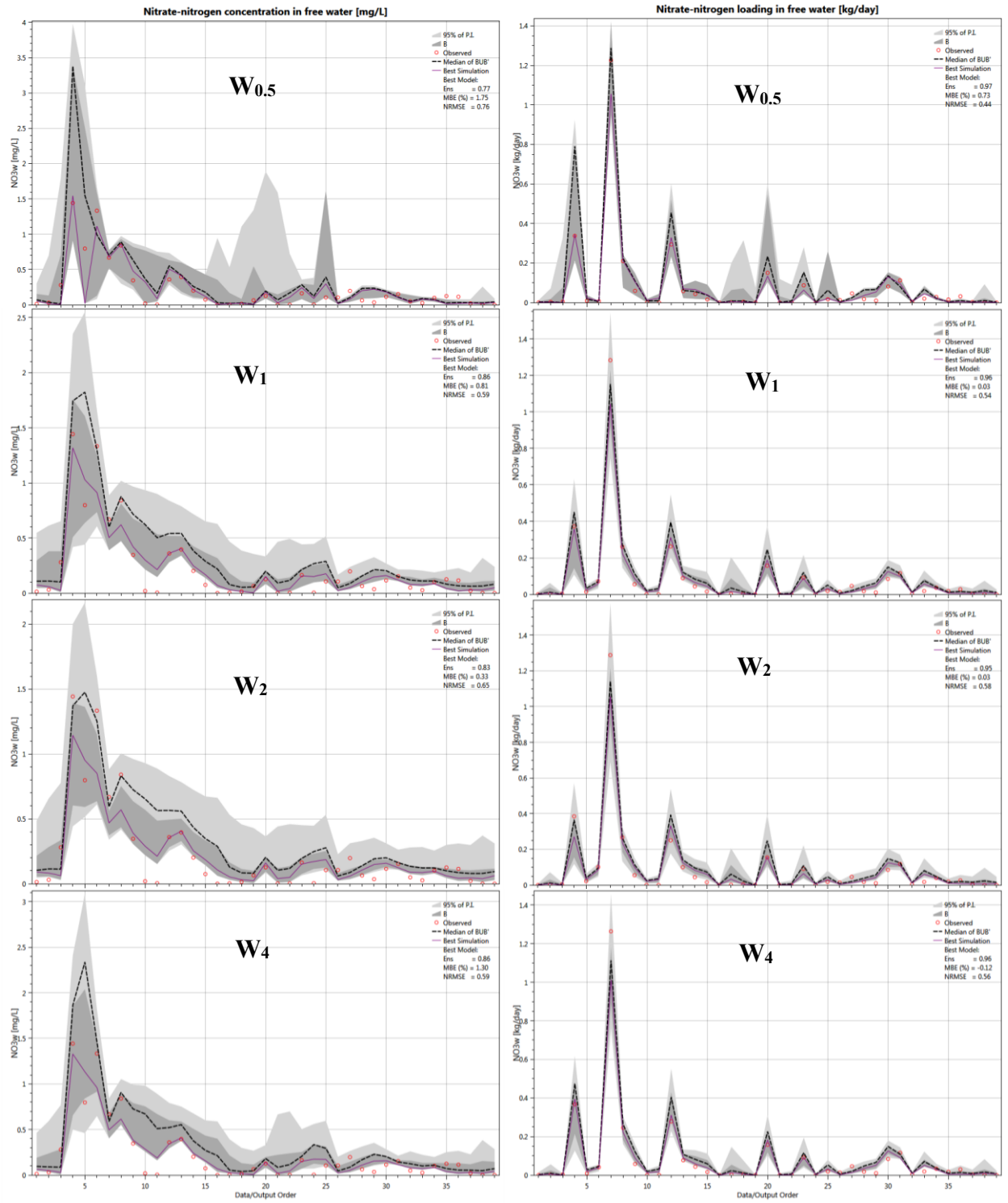

Figure 3.8. 95% prediction intervals (95% PI) of full MC simulations, behavioral simulations (B) and observed concentration and loading of nitrate-nitrogen for synthetic wetlands.

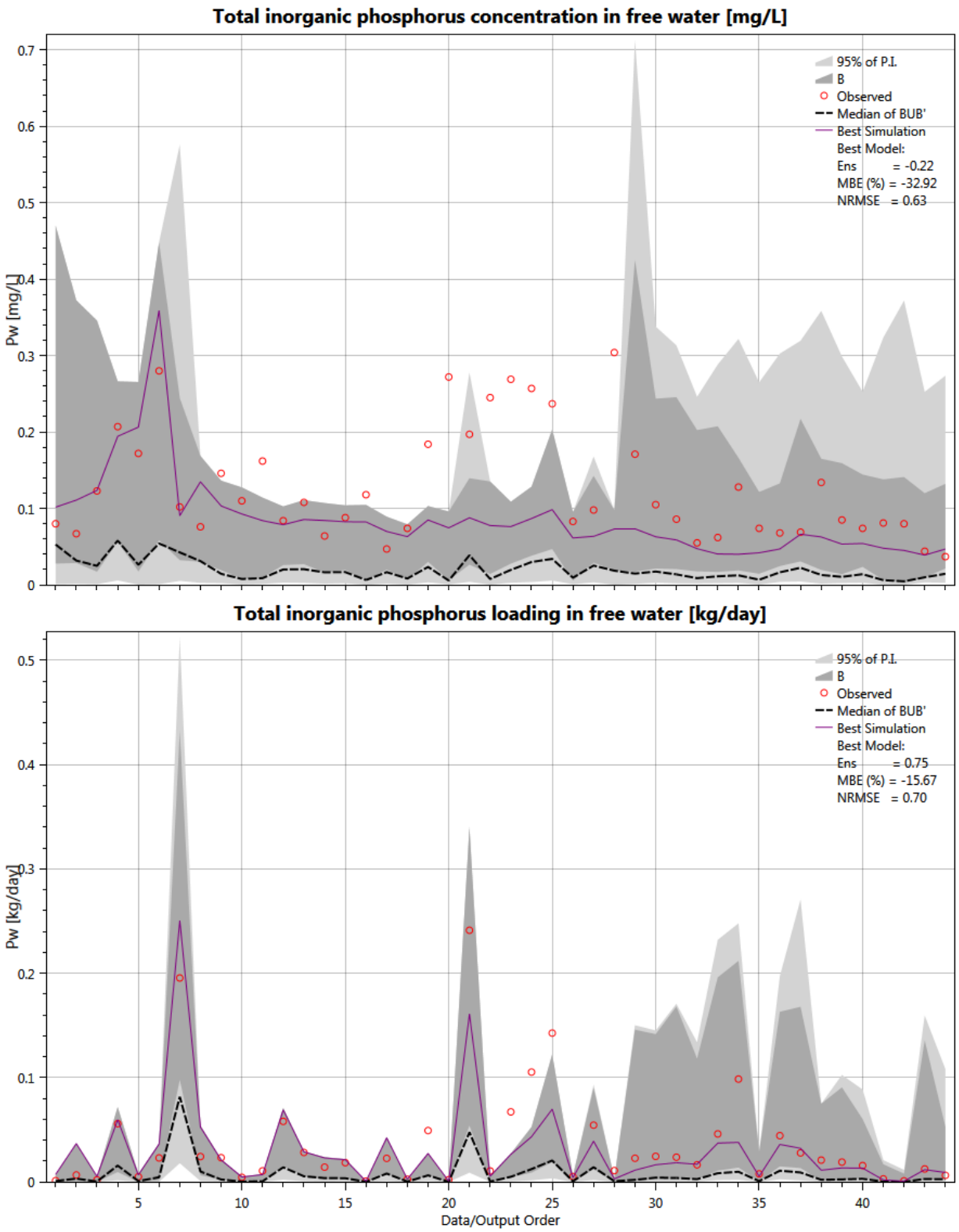

Figure 3.9. 95% prediction intervals (95% PI) of full MC simulations, behavioral simulations (B) and observed concentration and loading of total inorganic phosphorous for W_A.

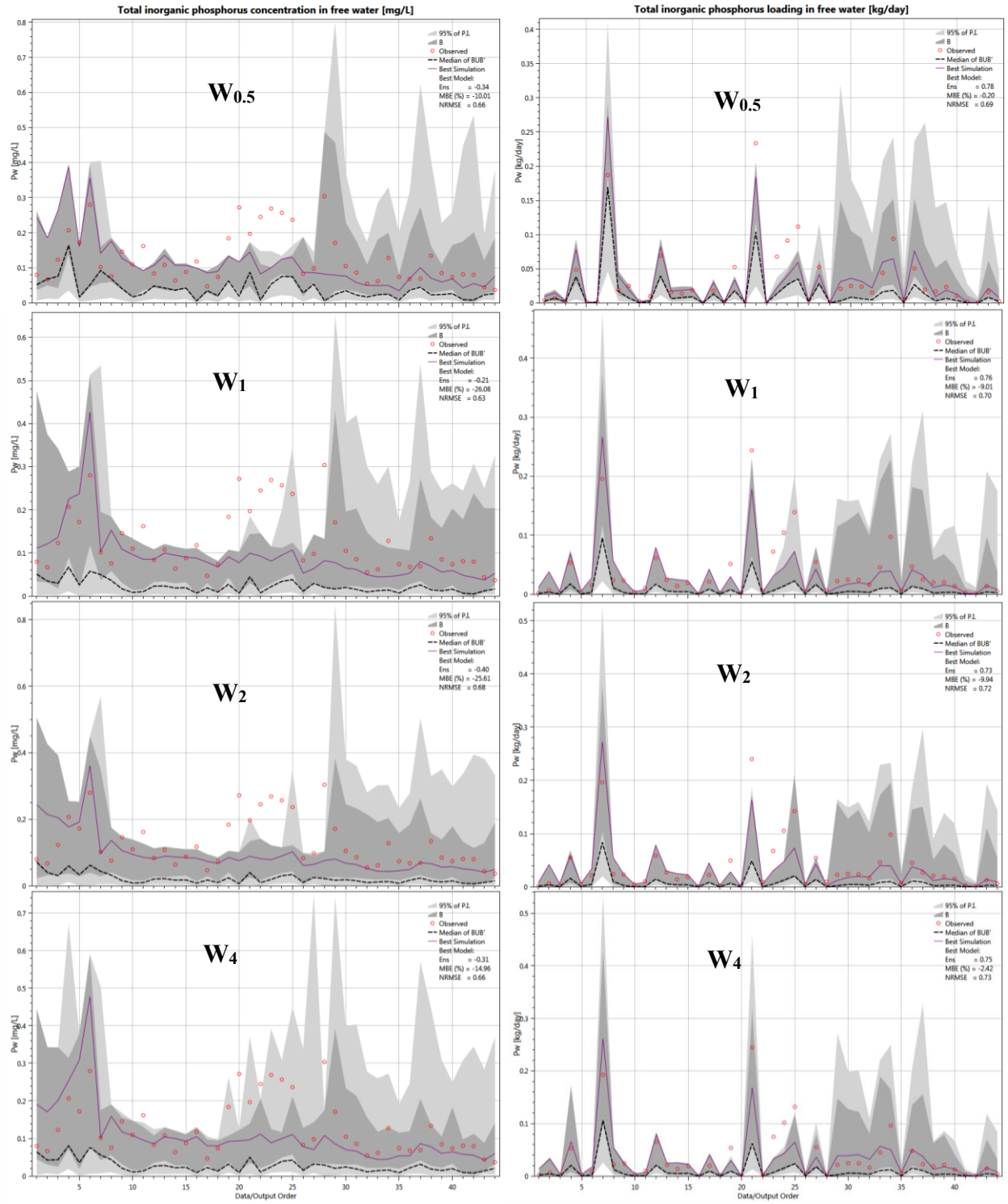

Figure 3.10. 95% prediction intervals (95% PI) of full MC simulations, behavioral simulations (B) and observed concentration and loading of total inorganic phosphorous for synthetic wetlands.

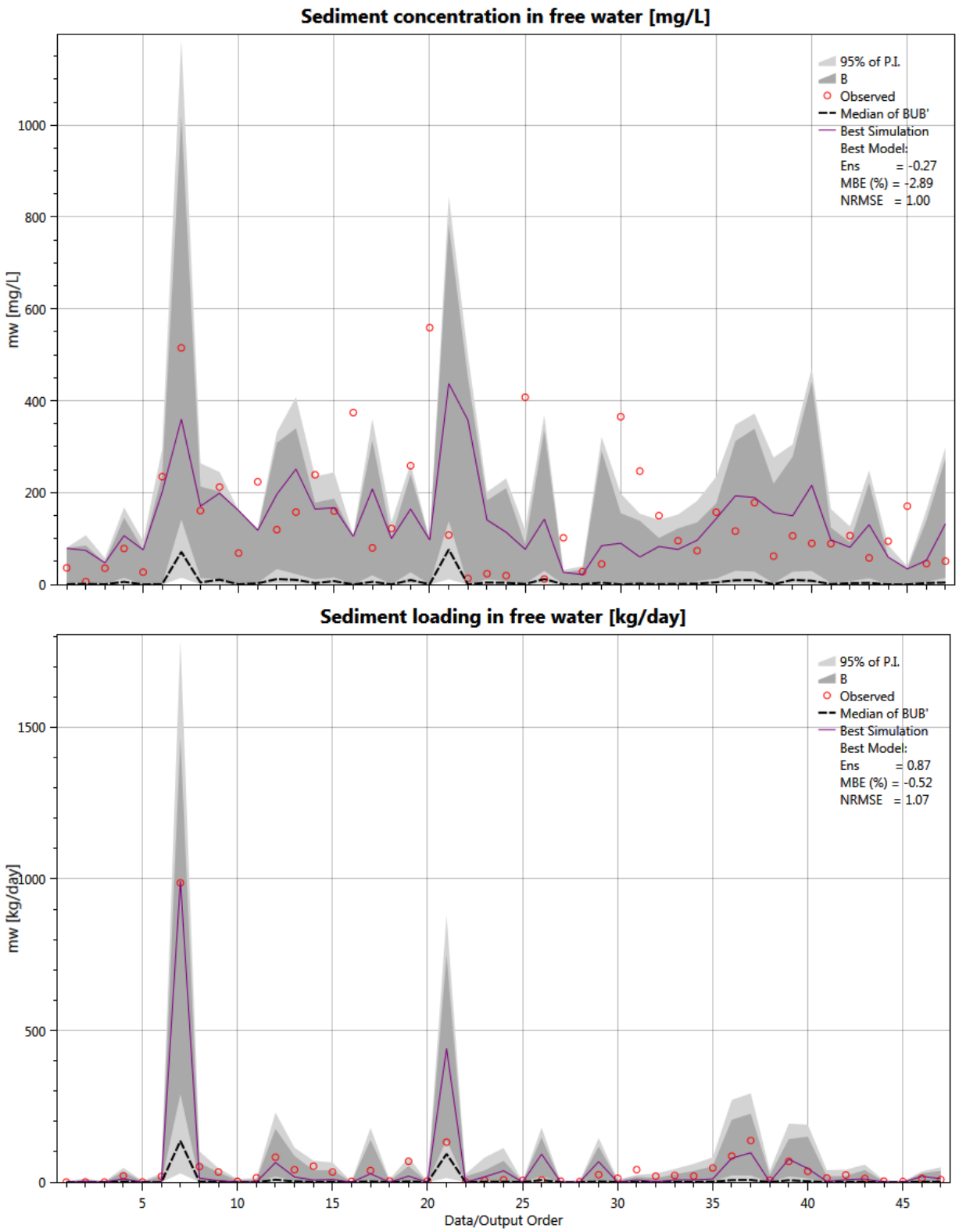

Figure 3.11. 95% prediction intervals (95% PI) of full MC simulations, behavioral simulations (B) and observed concentration and loading of sediment for WA.

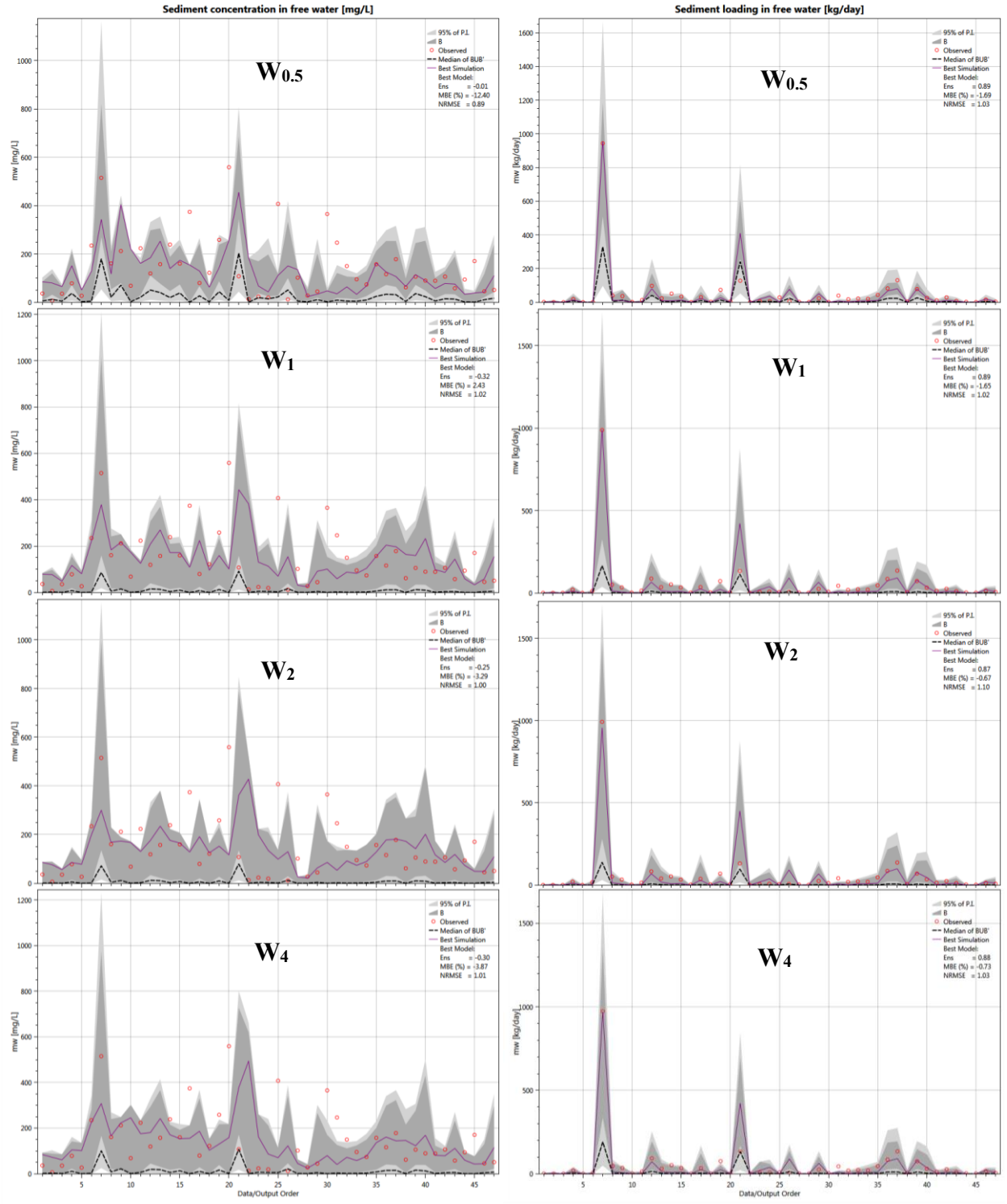

Figure 3.12. 95% prediction intervals (95% PI) of full MC simulations, behavioral simulations (B) and observed concentration and loading of sediment for synthetic wetlands.

3.1.3 Sensitivity Analysis

The Kolmogorov-Smirnov (K-S) test was applied to identify the most sensitive parameters with the actual wetland and the synthetic wetlands for ON_w, N_w, NO_{3w}, P_w, and m_w loadings. The confidence level chosen was 95% (α=0.05). For each test, a D^*_{max} value that correspond to p-value=0.05 was first determined. If a parameter had a D_{max} value larger than D^*_{max}, then that parameter was considered a sensitive parameter. With this approach, W_A wetland had 13, 17, 21, 12 and 7 sensitive parameters out of 38 parameters for ON_w, N_w, NO_{3w}, P_w, and m_w, respectively.

3.1.3.1 Particulate Organic Nitrogen (ON_w)

At α=0.05 level, 13 sensitive parameters ended being sensitive for W_A. Among them *a_vr_o*, *porw*, *vels_o*, *L2*, and *ana* had much higher sensitivities than others. Figure 3.13 shows the K-S test results of the most sensitive parameters for ON_w for all wetlands. Due to space limitation, parameters with very small D_{max} are not shown. Results for W_A was used as the base in sorting the parameters. The results, in general, indicate that resuspension and settling processes are the main processes and vegetation effects are the auxiliary processes of ON_w for the W_A wetland. For the three synthetic wetlands which are W_1, W_2, and W_4, the order of the sensitive parameters was similar to the W_A wetland. Wetland $W_{0.5}$ had a somewhat different behavior; the order of sensitive parameters became *porw, vels_o, ana, a_vr_o,* and *L2*. The parameters *porw*, *vels_o,* and *ana* became more sensitive while *a_vr_o* and *L2* lost their magnitude of sensitivities. This means that vegetation effect and settling processes have increased sensitivity while resuspension has lost its significance in $W_{0.5}$. Similar to the $r - factor$ based results, we can say that as long as assumed geometry is not highly different from the actual bathymetry, similar processes end up being dominant.

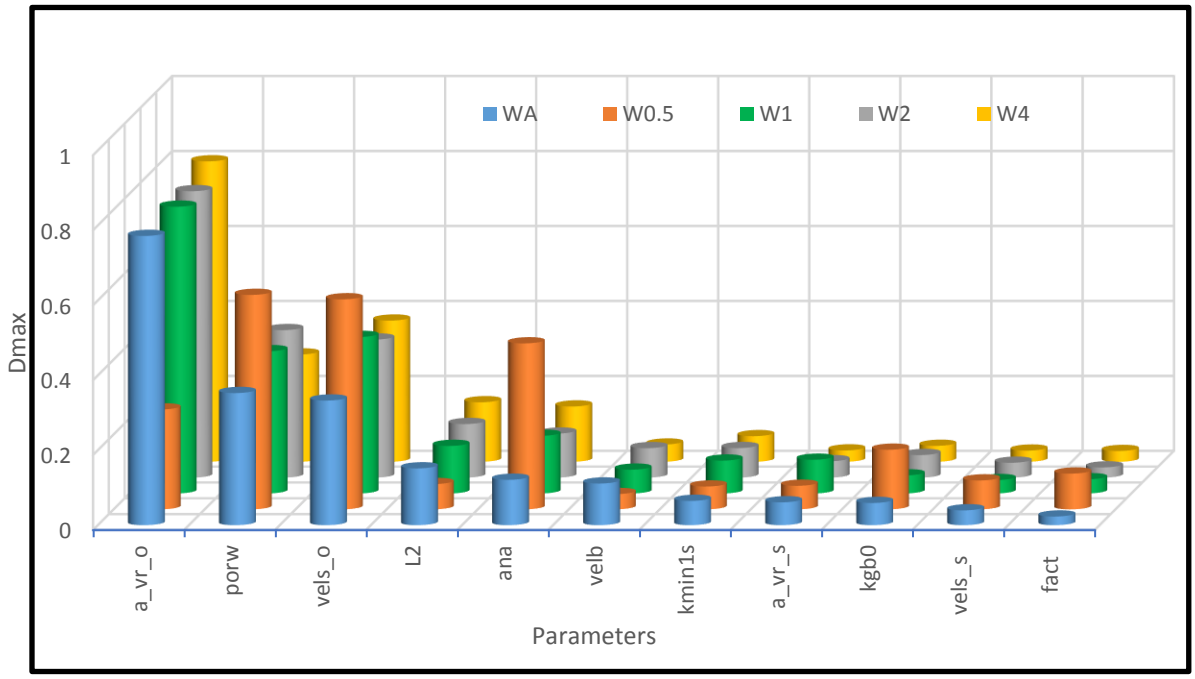

Figure 3.13. Particulate organic nitrogen K-S test results for wetlands W_A, $W_{0.5}$, W_1, W_2, and W_4

One follow up question to the above analysis is how the distributions of the behavior sets (***B***) compare for these highly sensitive parameters. For this, median and coefficient of variation (CV) values of the top sensitive parameters *a_vr_o*, *porw*, *vels_o*, *L2*, and *ana* were compared among all wetlands for the behavior data set of ON_w. Coefficient of variation is calculated by the formula below;

$$CV = \frac{\sigma}{\mu} \dots\dots\dots\dots\dots\dots\dots\dots\dots\dots (36)$$

where σ is standard deviation of ***B,*** μ is the mean of ***B.***

The median and CV values of behavioral part of the most sensitive parameters are provided in Table 3.5. The median and CV values of ***BUB'*** are also shown for comparison purposes. The table also shows the relative change in median and CV values of the synthetic wetlands with respect to values of the actual wetland. The median values of $W_{0.5}$ wetland has the greatest

deviation from the median values of the actual wetland, and W_2 wetland has the closest median values. Comparisons of CV values reveal that the CV values are almost same for all wetlands except for the $W_{0.5}$ wetland. Note the significant reduction and increase in value of the resuspension parameter *a_vr_o* and the settling parameter *vels_o*, respectively, in $W_{0.5}$. To sum up, wetlands most similar to the W_A wetland are W_2, W_4, and W_1 based on the most sensitive parameters for ON_w. $W_{0.5}$ is the least similar to the W_A wetland. To further support this interpretation, probability density function (PDF) graphs were compared in Figure 3.14. The difference in PDFs of ***B*** and ***B*U*B*'** are clear. Further, one can also see that PDFs of W_A, W_1, W_2 and W_4 are similar to each other, and PDFs of $W_{0.5}$ is different from all of them.

Table 3.5. Median (*Mdn*) and Coefficient of Variation (*CV*) values of the top sensitive parameters of the behavior set (B) for ON_w for different bathymetries. Percent change indicate relative change with respect to values of W_A.

	BUB'		**W_A**		**$W_{0.5}$**		**W_1**		**W_2**		**W_4**	
Parameter	***Mdn***	***CV***	***Mdn***	***CV***	***Mdn***	***CV***	***Mdn***	***CV***	***Mdn***	***CV***	***Mdn***	***CV***
a_vr_o	0.02	15.5	0.84	0.67	0.07	0.93	0.75	0.64	0.71	0.67	1.04	0.68
change (%)					*-91%*	*39%*	*-11%*	*-5%*	*-16%*	*0%*	*24%*	*1%*
porw	0.8	0.11	0.88	0.07	0.91	0.04	0.88	0.07	0.88	0.06	0.87	0.08
change (%)					*4%*	*-38%*	*1%*	*-4%*	*0.4%*	*8%*	*-1%*	*22%*
vels_o	1.87	2.29	1.9	0.31	3.6	0.26	2.59	0.34	2.14	0.31	2.15	0.33
change (%)					*89%*	*-16%*	*36%*	*11%*	*12%*	*1%*	*13%*	*8%*
L2	27.5	0.47	21.5	0.55	28.7	0.42	22.3	0.51	21.4	0.54	20.8	0.55
change (%)					*34%*	*-23%*	*4%*	*-7%*	*-0.3%*	*-2%*	*-3%*	*-1%*
Ana	10.51	0.39	11.7	0.34	15.4	0.18	12.3	0.32	11.9	0.34	12.3	0.33
change (%)					*31%*	*-48%*	*6%*	*-7%*	*2%*	*0%*	*5%*	*-5%*

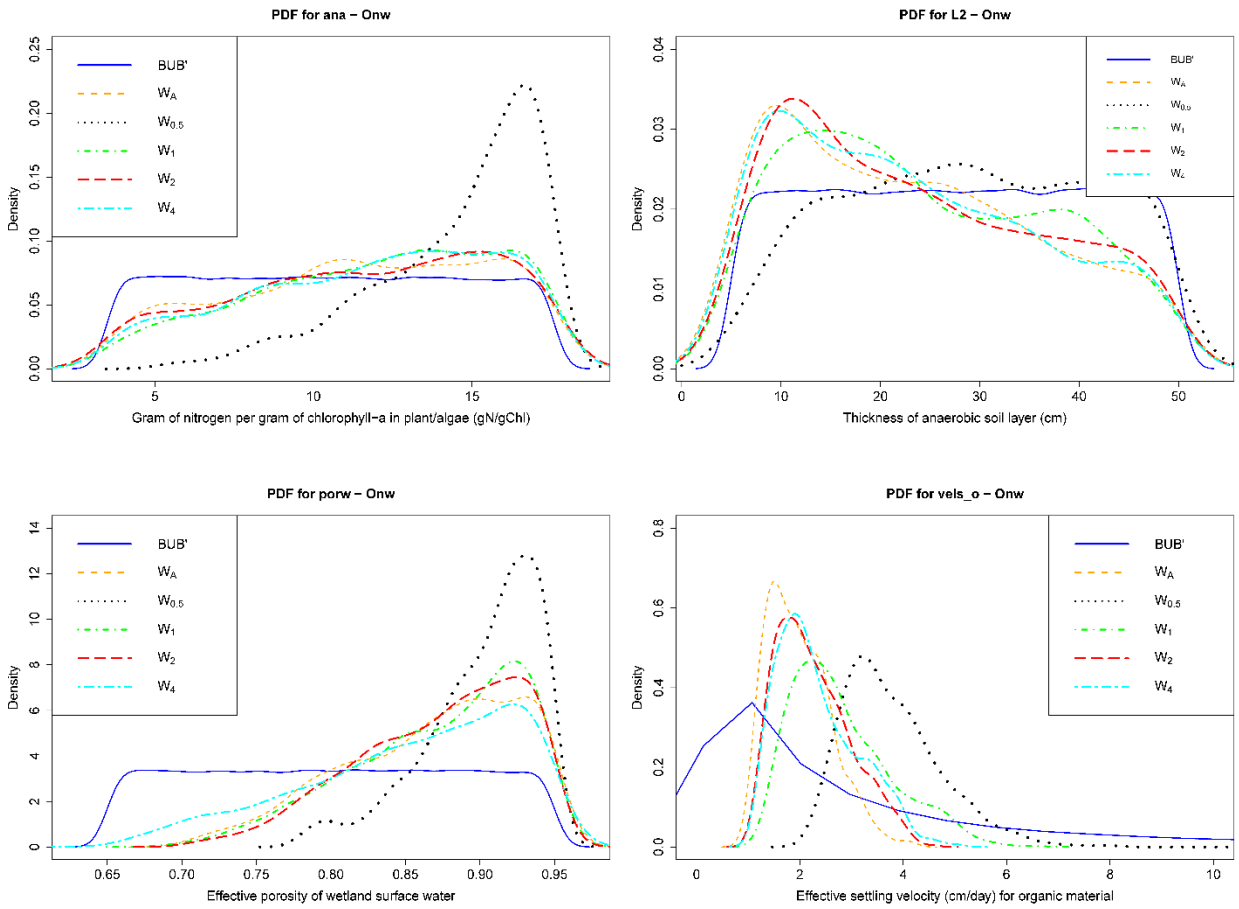

Figure 3.14. PDFs of the most sensitive parameters for ON_w

3.1.3.2 Total Ammonia-Nitrogen ($[NH_4^+] + [NH_3]$) (N_w)

At α=0.05 level, 17 sensitive parameters ended being sensitive for W_A. Among them *fact*, *c2*, *kd*, and *knw* had much higher sensitivities than others. Figure 3.15 shows the K-S test results of the most sensitive parameters for N_w for all wetlands. Due to space limitation, parameters with very small D_{max} are not shown. Due to space limitation, parameters with very small D_{max} are not shown. Results for W_A was used as the base in sorting the parameters. The results, in general, indicate that diffusion, nitrification and adsorption processes are the main processes of N_w for the W_A wetland. Equilibrium coefficient (*c2*) which is related to the temperature is surprisingly among the most sensitive parameters because temperature effect is not among the sensitive parameters in *Kalin et.*

all. (2013). For all wetlands, *fact* parameter is the most sensitive parameter. $W_{0.5}$ had a somewhat different behavior; the order of sensitive parameters became *fact, kd, kmin1s,* and *c2*. The parameters *kd* and *kmin1s* became more sensitive while *fact, knw* and *c2* lost their magnitude of sensitivities. This means that adsorption and mineralization processes have increased sensitivity while diffusion, nitrification and temperature effect have lost their significance in $W_{0.5}$. Similar to the $r - factor$ based results, we can say that as long as assumed geometry is not highly different from the actual bathymetry, similar processes end up being dominant.

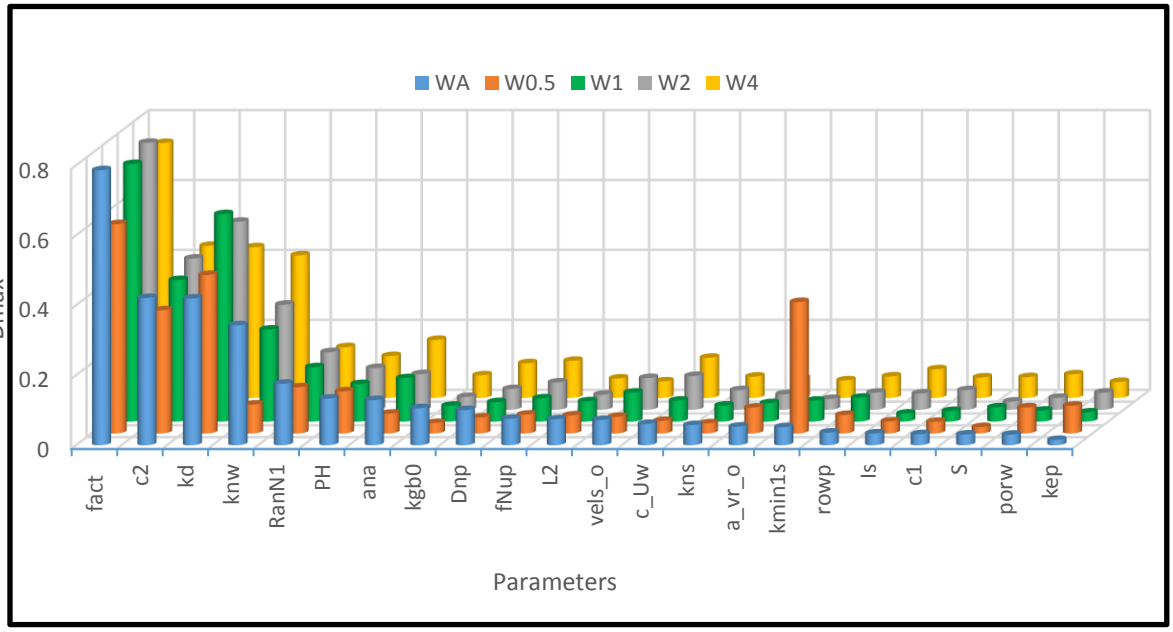

Figure 3.15. Total ammonia-nitrogen K-S test results for different bathymetries

The median and CV values of behavioral part of the most sensitive parameters *fact*, *c2*, *kd*, and *knw* are provided in Table 3.6. The median and CV values of ***BUB'*** are also shown for comparison purposes. The table also shows the relative change in median and CV values of the synthetic wetlands with respect to values of the actual wetland. The median values of $W_{0.5}$ wetland has the greatest deviation from the median values of the actual wetland and W_4 wetland has the

closest median values. Comparisons of CV values reveal that the CV values are almost same for all wetlands except for the $W_{0.5}$ wetland. Note the significant increase in value of the nitrification parameter *knw* and the adsorption parameter *kd*, respectively, in $W_{0.5}$. To sum up, wetlands most similar to the W_A wetland are W_4, W_2, and W_1 based on the most sensitive parameters for N_w. $W_{0.5}$ is the least similar to the W_A wetland. To further support this interpretation, probability density function (PDF) graphs were compared in Figure 3.16. The difference in PDFs of ***B*** and ***BUB'*** are clear. Further, one can also see that PDFs of W_A, W_1, W_2 and W_4 are similar to each other, and PDFs of $W_{0.5}$ is different from all of them.

Table 3.6. Median (*Mdn*) and Coefficient of Variation (*CV*) values of the top sensitive parameters of the behavior set (B) for N_w for different bathymetries. Percent change indicate relative change with respect to values of W_A.

	BUB'		**W_A**		**$W_{0.5}$**		**W_1**		**W_2**		**W_4**	
Parameter	***Mdn***	***CV***	***Mdn***	***CV***	***Mdn***	***CV***	***Mdn***	***CV***	***Mdn***	***CV***	***Mdn***	***CV***
fact	137	1.08	662	0.66	473	0.92	587	0.70	618	0.63	609	0.74
change (%)					*-29%*	*40%*	*-11%*	*7%*	*-7%*	*-4%*	*-8%*	*12%*
c2	2454	0.29	3139	0.13	3016	0.16	3072	0.14	3091	0.13	3140	0.13
change (%)					*-4%*	*17%*	*-2%*	*1%*	*-2%*	*-3%*	*0%*	*-5%*
kd	1.61	2.05	4.40	0.91	8.84	1.61	7.79	0.89	5.77	0.99	4.41	0.92
change (%)					*101%*	*76%*	*77%*	*-2%*	*31%*	*8%*	*0%*	*1%*
knw	6E-03	2.07	2.4E-03	1.08	5E-03	1.58	2.7E-03	1.29	2.8E-03	1.09	2E-03	1.11
change (%)					*103%*	*47%*	*10%*	*20%*	*12%*	*1%*	*-18%*	*3%*

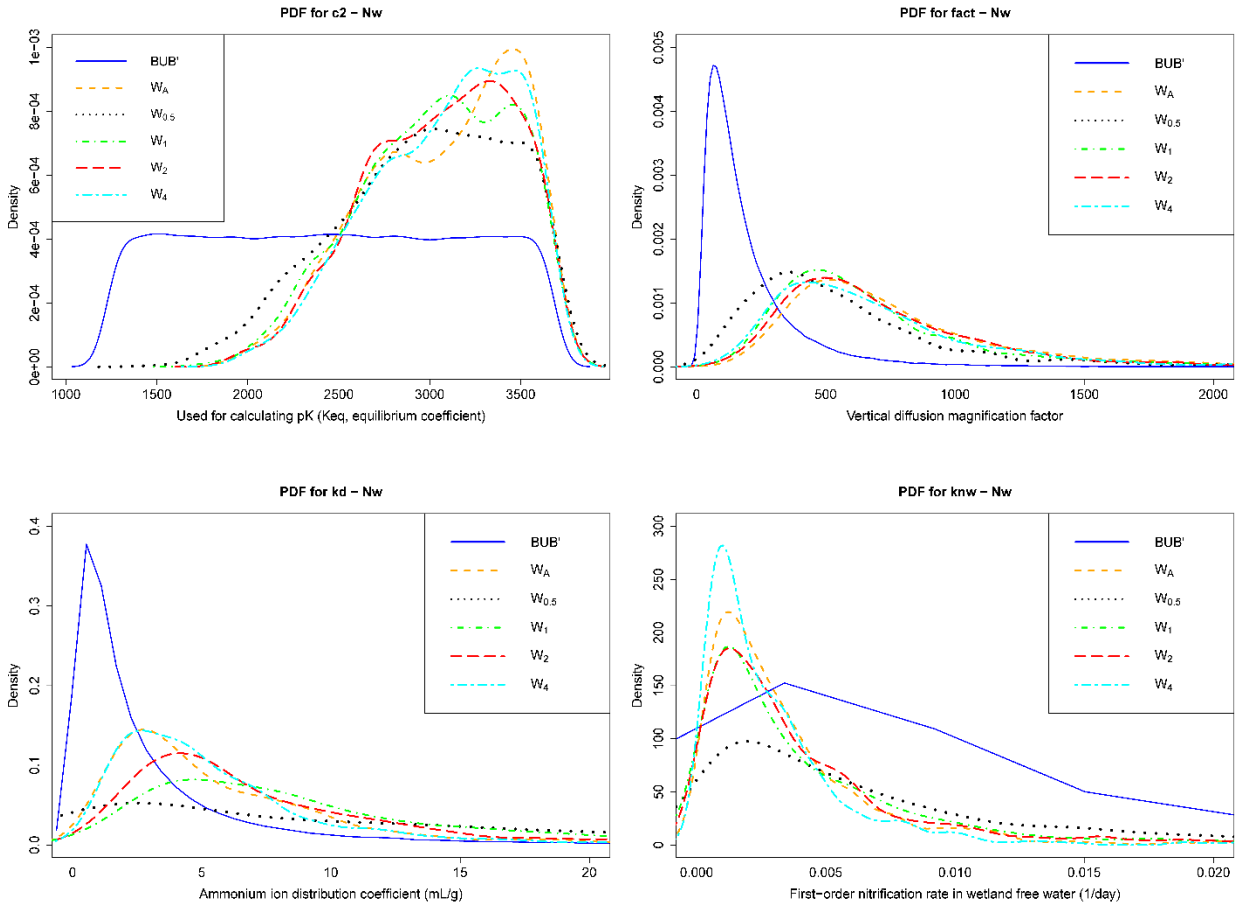

Figure 3.16. PDFs of the most sensitive parameters for N_w

3.1.3.3 Nitrate-Nitrogen (NO_{3w})

At α=0.05 level, 21 parameters ended being sensitive for W_A. Among them *ana*, *c2*, *kden*, *porw*, *fact*, *kgb0*, *PH*, and *L2* had much higher sensitivities than others. Figure 3.17 shows the K-S test results of the most sensitive parameters for NO_{3w} for all wetlands. Due to space limitation, parameters with very small D_{max} are not shown. Results for W_A was used as the base in sorting the parameters. The results, in general, indicate that vegetation, denitrification and diffusion are the main processes of NO_{3w} for the W_A wetland. For the two synthetic wetlands W_2 and W_4, the order of the sensitive parameters was similar to the W_A wetland. Wetlands $W_{0.5}$ and W_1 had somewhat different behavior; *fact* and *ana* became the most sensitive parameters. All the most sensitive

parameters for $W_{0.5}$ wetland lost their magnitude of sensitivities in larger scale compared to other wetlands except for the parameter *fact*. Most importantly *pH* is not a sensitive parameter for $W_{0.5}$ while it is very sensitive for others. Another interesting observation is about the *RanN1* parameter, which is not a sensitive parameter for actual wetland, but it became a sensitive parameter for synthetic wetlands. Similar to the $r - factor$ based results, we can say that as long as assumed geometry is not highly different from the actual bathymetry, similar processes end up being dominant.

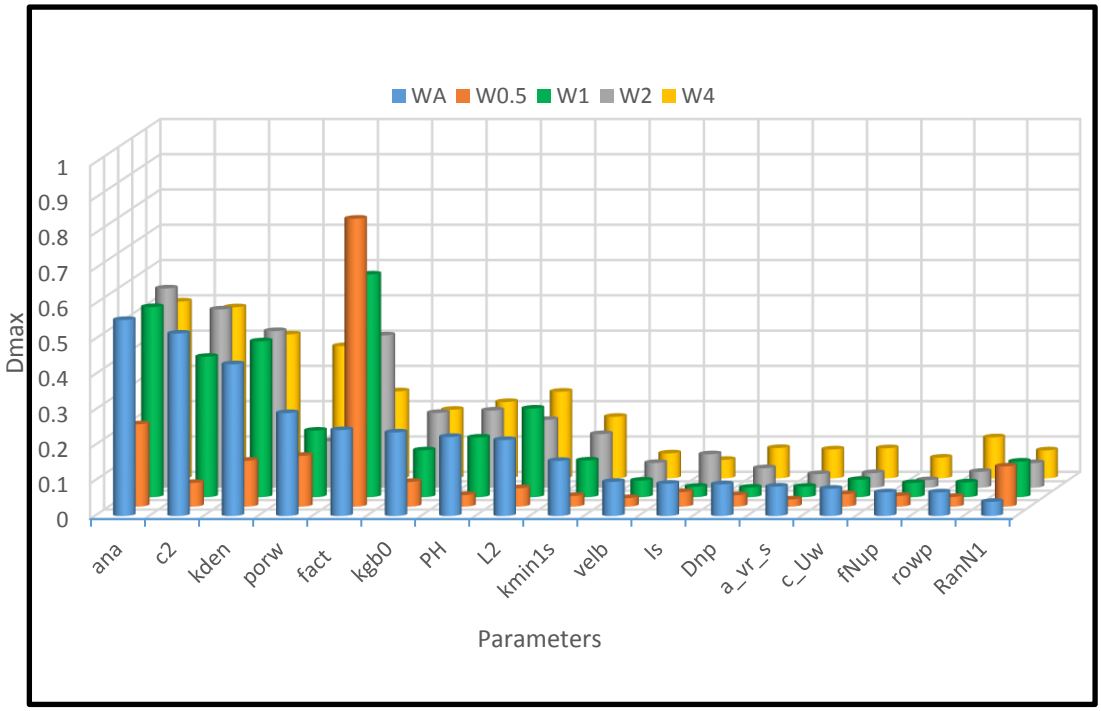

Figure 3.17. Nitrate-nitrogen K-S test results for different bathymetries

The median and CV values of the most sensitive parameters *ana*, *c2*, *kden*, *porw*, *fact*, *kgb0*, *PH*, and *L2* for the behavior set are provided in Table 3.7. The median and CV values of ***BUB'*** are also shown for comparison purposes. The table also shows the relative change in median and CV values of the synthetic wetlands with respect to values of the actual wetland. The median values

of $W_{0.5}$ wetland has the greatest deviation from the median values of the actual wetland, and W_4 wetland has the closest median values. Comparisons of CV values reveal that the CV values are almost the same for all wetlands except for $W_{0.5}$. Note the significant reduction and increase in value of the vegetation parameter ***ana*** and the diffusion parameter ***fact***, respectively, in $W_{0.5}$. To sum up, wetlands most similar to the W_A wetland are W_4, W_2, and W_1 based on the most sensitive parameters for NO_{3w}. $W_{0.5}$ is the least similar to the W_A wetland. To further support this interpretation, probability density function (PDF) graphs were compared in Figure 3.18. The difference in PDFs of ***B*** and ***B*U*B*'** are clear. Further, one can also see that PDFs of W_A, W_1, W_2 and W_4 are similar to each other, and PDFs of $W_{0.5}$ is different from all of them.

Table 3.7. Median (*Mdn*) and Coefficient of Variation (*CV*) values of the top sensitive parameters of the behavior set (B) for NO_{3w} for different bathymetries. Percent change indicate relative change with respect to values of W_A.

	BUB'		**WA**		**W0.5**		**W1**		**W2**		**W4**	
Parameter	***Mdn***	***CV***	***Mdn***	***CV***	***Mdn***	***CV***	***Mdn***	***CV***	***Mdn***	***CV***	***Mdn***	***CV***
ana	10.52	0.39	15.7	0.12	13.0	0.28	15.6	0.13	15.9	0.12	15.3	0.14
change (%)					*-17%*	*129%*	*0%*	*4%*	*2%*	*-6%*	*-3%*	*12%*
c2	2454	0.29	1620	0.22	2341	0.30	1689	0.30	1636	0.24	1648	0.25
change (%)					*44%*	*40%*	*4%*	*38%*	*1%*	*11%*	*2%*	*17%*
kden	0.08	0.55	0.03	0.61	0.09	0.45	0.03	0.83	0.03	0.68	0.04	0.57
change (%)					*176%*	*-25%*	*-20%*	*37%*	*-3%*	*12%*	*10%*	*-6%*
porw	0.80	0.11	0.73	0.10	0.84	0.10	0.75	0.10	0.77	0.11	0.72	0.08
change (%)					*15%*	*6%*	*3%*	*7%*	*5%*	*10%*	*-2%*	*-14%*
fact	137.2	1.08	171.9	0.52	1082.9	0.56	395.0	0.55	266.3	0.51	177.1	0.53
change (%)					*530%*	*8%*	*130%*	*5%*	*55%*	*-3%*	*3%*	*1%*
kgb0	0.0013	0.13	0.0014	0.12	0.0014	0.13	0.0014	0.13	0.0014	0.12	0.0013	0.12
change (%)					*-4%*	*10%*	*-2%*	*8%*	*0%*	*0%*	*-1%*	*-1%*
PH	6.35	0.17	7.1	0.14	6.4	0.17	6.9	0.15	7.0	0.14	7.1	0.14
change (%)					*-9%*	*21%*	*-3%*	*6%*	*-2%*	*0%*	*0%*	*3%*
L2	27.4	0.47	18.7	0.60	28.5	0.50	16.7	0.66	19.4	0.61	17.8	0.60
change (%)					*53%*	*-16%*	*-10%*	*10%*	*4%*	*2%*	*-5%*	*1%*

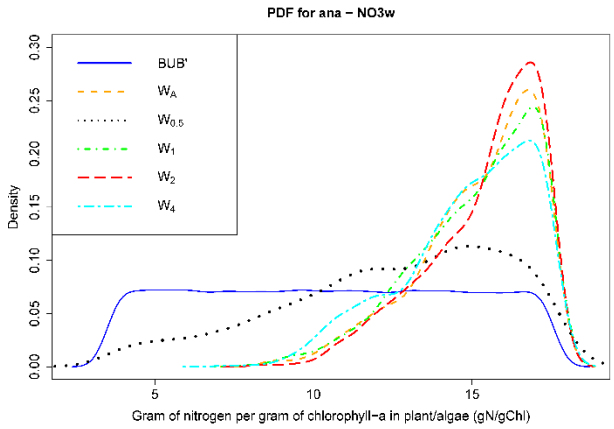
PDF for ana – NO3w
BUB'
W_A
$W_{0.5}$
W_1
W_2
W_4
Density
0.00
0.05
0.10
0.15
0.20
0.25
0.30
5
10
15
Gram of nitrogen per gram of chlorophyll−a in plant/algae (gN/gChl)

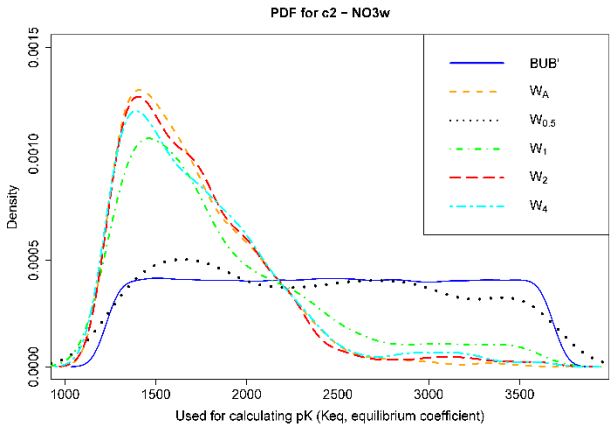
PDF for c2 – NO3w
BUB'
W_A
$W_{0.5}$
W_1
W_2
W_4
Density
0.0000
0.0005
0.0010
0.0015
1000
1500
2000
2500
3000
3500
Used for calculating pK (Keq, equilibrium coefficient)

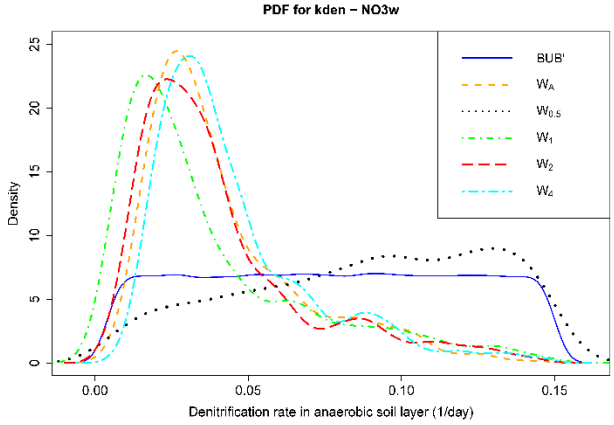
PDF for kden – NO3w
BUB'
W_A
$W_{0.5}$
W_1
W_2
W_4
Density
0
5
10
15
20
25
0.00
0.05
0.10
0.15
Denitrification rate in anaerobic soil layer (1/day)

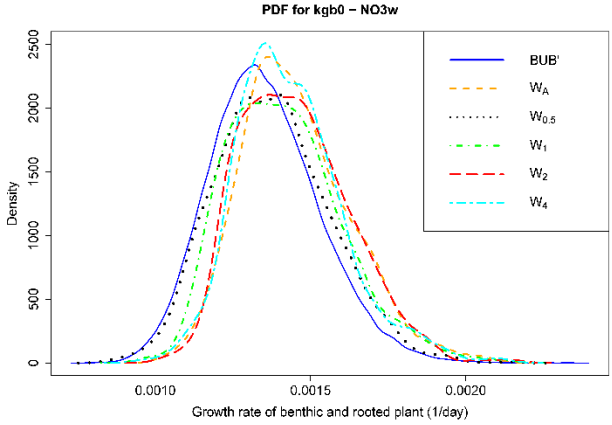
PDF for kgb0 – NO3w
BUB'
W_A
$W_{0.5}$
W_1
W_2
W_4
Density
0
500
1000
1500
2000
2500
0.0010
0.0015
0.0020
Growth rate of benthic and rooted plant (1/day)

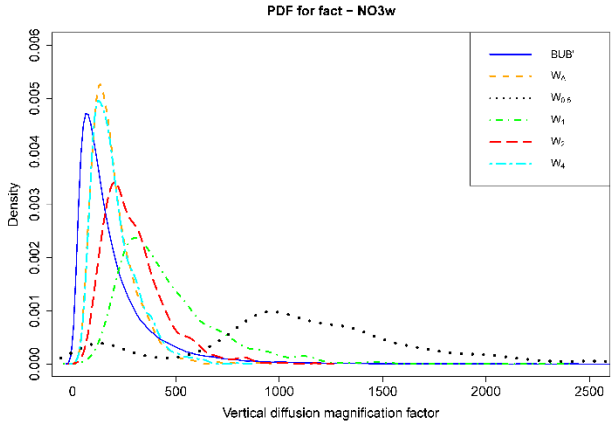
PDF for fact – NO3w
BUB'
W_A
$W_{0.5}$
W_1
W_2
W_4
Density
0.000
0.001
0.002
0.003
0.004
0.005
0.006
0
500
1000
1500
2000
2500
Vertical diffusion magnification factor

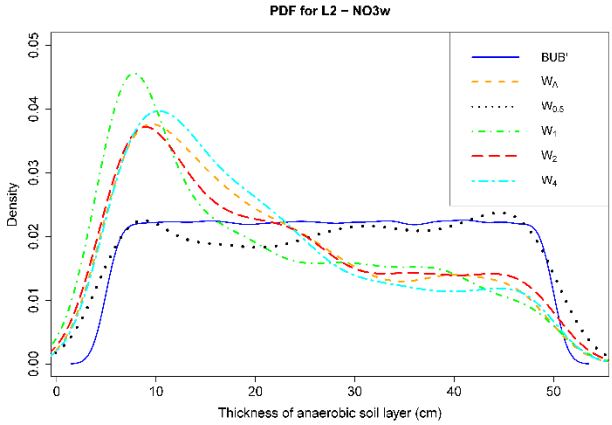
PDF for L2 – NO3w
BUB'
W_A
$W_{0.5}$
W_1
W_2
W_4
Density
0.00
0.01
0.02
0.03
0.04
0.05
0
10
20
30
40
50
Thickness of anaerobic soil layer (cm)

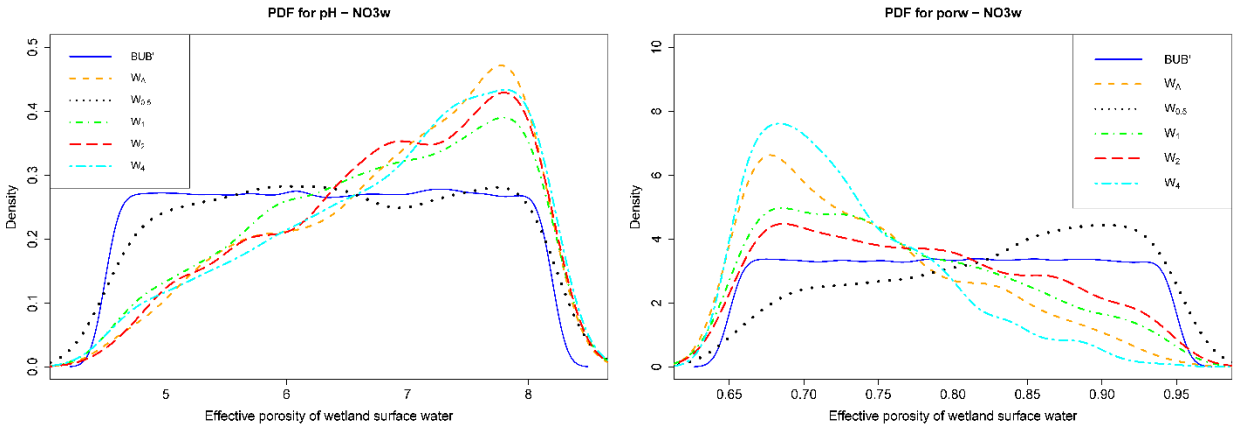

Figure 3.18. PDFs of the most sensitive parameters for NO_{3w}.

3.1.3.4 Total Inorganic Phosphorus (P_w)

At α=0.05 level, 12 parameters ended being sensitive for W_A. Among them *Kw*, *fact*, and *vels_s* had much higher sensitivities than others. Figure 3.19 shows the K-S test results of the most sensitive parameters for P_w for all wetlands. Due to space limitation, parameters with very small D_{max} are not shown. Results for W_A was used as the base in sorting the parameters. The results, in general, indicate that phosphorous sorption is the main processes and diffusion and settling effects are the auxiliary processes of P_w for the W_A wetland. For the all synthetic wetlands, the order of the sensitive parameters was similar to the W_A wetland. Interestingly *c_Uw* parameter is sensitive for $W_{0.5}$ wetland. However, this parameter is insensitive for other wetlands.

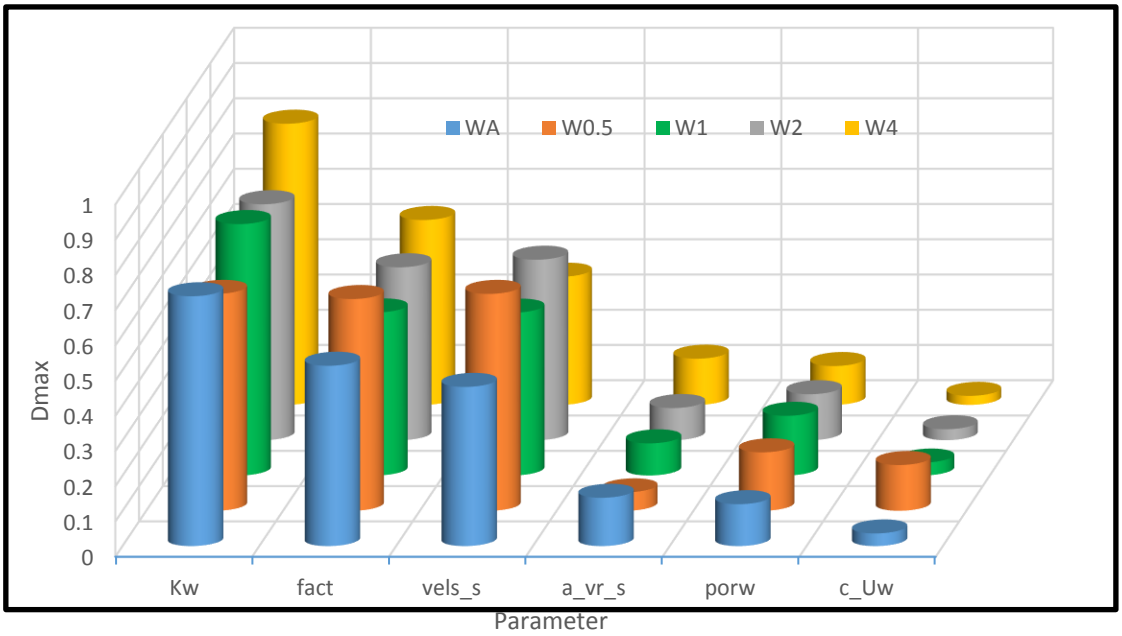

Figure 3.19. Total Inorganic phosphorous K-S test results for different bathymetries.

The median and CV values of behavioral part of the most sensitive parameters *Kw*, *fact*, and *vels_s* are provided in Table 3.8. The median and CV values of ***BUB'*** are also shown for comparison purposes. The table also shows the relative change in median and CV values of the synthetic wetlands with respect to values of the actual wetland. The median values of $W_{0.5}$ wetland has the greatest deviation from the median values of the actual wetland, and W_2 wetland has the closest median values. Comparisons of CV values reveal that the CV values are almost same for all wetlands except for the $W_{0.5}$ wetland. Note the significant reduction and increase in value of the settling parameter *vels_s* and the sorption parameter *Kw*, respectively, in $W_{0.5}$. To sum up, wetlands most similar to the W_A wetland are W_1, W_2, and W_4 based on the most sensitive parameters for P_w. $W_{0.5}$ is the least similar to the W_A wetland. To further support this interpretation, probability density function (PDF) graphs were compared in Figure 3.20. The difference in PDFs

of ***B*** and ***BUB'*** are clear. Further, one can also see that PDFs of W_A, W_1, W_2 and W_4 are similar to each other, and PDFs of $W_{0.5}$ is different from all of them.

Table 3.8. Median (*Mdn*) and Coefficient of Variation (*CV*) values of the top sensitive parameters of the behavior set (B) for P_w for different bathymetries. Percent change indicate relative change with respect to values of W_A.

	BUB'		**WA**		**W0.5**		**W1**		**W2**		**W4**	
Parameter	***Mdn***	***CV***	***Mdn***	***CV***	***Mdn***	***CV***	***Mdn***	***CV***	***Mdn***	***CV***	***Mdn***	***CV***
Kw	34975	1.58	3483	2.36	6833	1.11	3226	2.92	3977	2.71	3118	2.00
change (%)					*96%*	*-53%*	*-7%*	*24%*	*14%*	*15%*	*-10%*	*-15%*
fact	137.2	1.08	54.7	0.86	50.2	0.54	58.1	0.75	54.8	0.69	53.0	0.61
change (%)					*-8%*	*-36%*	*6%*	*-13%*	*0%*	*-19%*	*-3%*	*-29%*
vels_s	231.5	1.51	59.3	2.21	53.6	1.42	51.2	2.18	46.3	3.02	75.3	2.05
change (%)					*-10%*	*-36%*	*-14%*	*-1%*	*-22%*	*36%*	*27%*	*-7%*

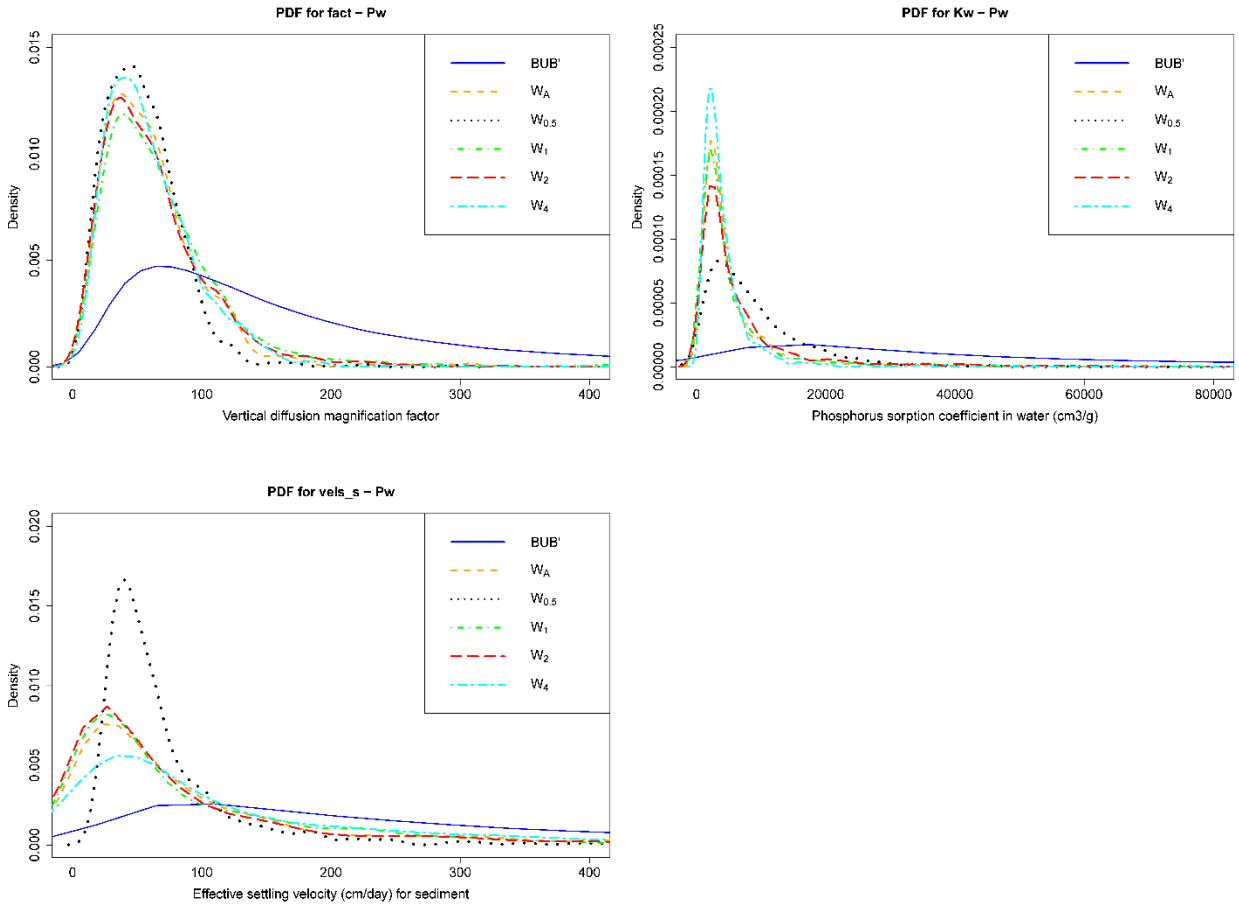

Figure 3.20. PDFs of the most sensitive parameters for P_w.

3.1.3.5 Sediment (m_w)

At α=0.05 level, 7 parameters ended being sensitive for W_A. Among them *a_vr_s*, *vels_s*, and *RanN1* had much higher sensitivities than others. Figure 3.21 shows the K-S test results of the most sensitive parameters for m_w for all wetlands. Due to space limitation, parameters with very small D_{max} are not shown. Results for W_A was used as the base in sorting the parameters. The results, in general, indicate that resuspension and settling processes are the main processes of m_w for the W_A wetland. Resuspension rate is the most important parameter because studied wetland received high agricultural runoff discharge into the wetland.

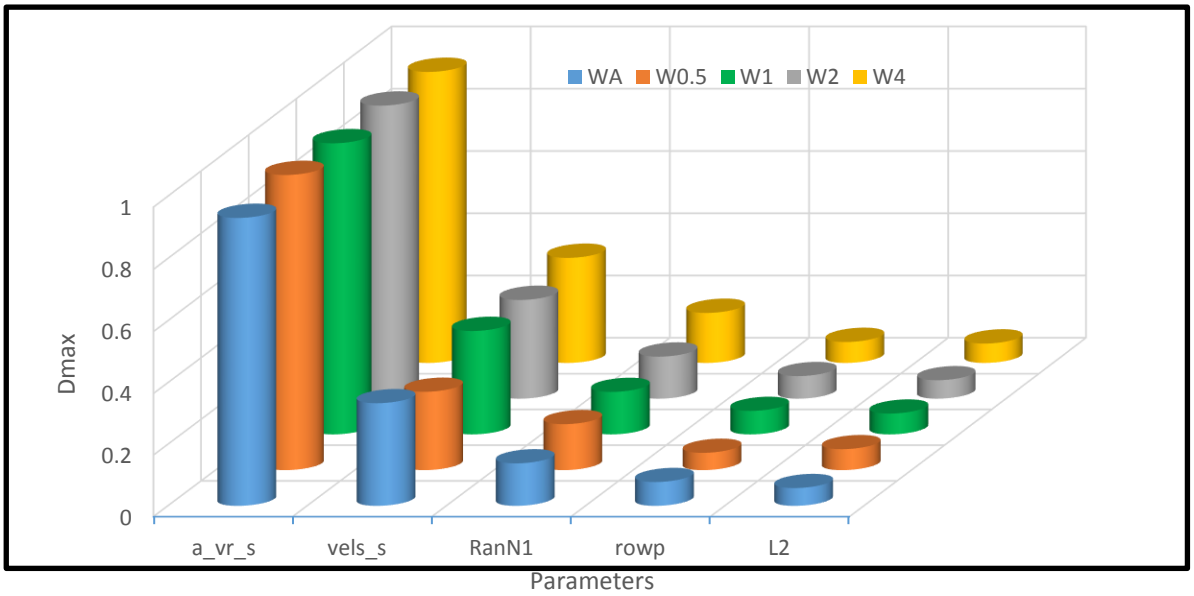

Figure 3.21. Sediment K-S test results for different bathymetries.

The median and CV values of behavioral part of the most sensitive parameters *a_vr_s*, *vels_s*, and *RanN1* are provided in Table 3.9. The median and CV values of ***BUB'*** are also shown for comparison purposes. The table also shows the relative change in median and CV values of the synthetic wetlands with respect to values of the actual wetland. The median values of $W_{0.5}$ wetland has the greatest deviation from the median values of the actual wetland, and W_4 wetland has the closest median values. Comparisons of CV values reveal that the CV values are almost same for all wetlands except for the $W_{0.5}$ wetland. Note the significant increase and reduction in value of the resuspension parameter ***a_vr_o*** and the settling parameter ***vels_o***, in $W_{0.5}$ and W_1, respectively. To sum up, wetlands most similar to the W_A wetland are W_4, W_2, and W_1 based on the most sensitive parameters for ON_w. $W_{0.5}$ is the least similar to the W_A wetland. To further support this interpretation, probability density function (PDF) graphs were compared in Figure 3.22. The difference in PDFs of ***B*** and ***BUB'*** are clear. Further, one can also see that PDFs of W_A, W_1, W_2 and W_4 are similar to each other, and PDFs of $W_{0.5}$ is different from all of them.

Table 3.9. Median (*Mdn*) and Coefficient of Variation (*CV*) values of the top sensitive parameters of the behavior set (B) for m_w for different bathymetries. Percent change indicate relative change with respect to values of W_A.

	BUB'		**W_A**		**$W0.5$**		**W_1**		**W_2**		**W_4**	
Parameter	***Mdn***	***CV***	***Mdn***	***CV***	***Mdn***	***CV***	***Mdn***	***CV***	***Mdn***	***CV***	***Mdn***	***CV***
a_vr_s	2.14E-03	4.38	0.09	0.79	0.10	0.76	0.09	0.69	0.09	0.78	0.09	0.82
change (%)					*12%*	*-3%*	*8%*	*-12%*	*8%*	*-1%*	*6%*	*4%*
vels_s	231.5	1.51	112.1	0.88	153.4	0.80	105.6	0.95	123.0	0.90	113.8	0.96
change (%)					*37%*	*-9%*	*-6%*	*8%*	*10%*	*2%*	*2%*	*9%*
RanN1	0.50	0.58	0.38	0.68	0.37	0.67	0.38	0.66	0.38	0.65	0.35	0.68
change (%)					*-2%*	*0%*	*-1%*	*-2%*	*0%*	*-4%*	*-7%*	*1%*

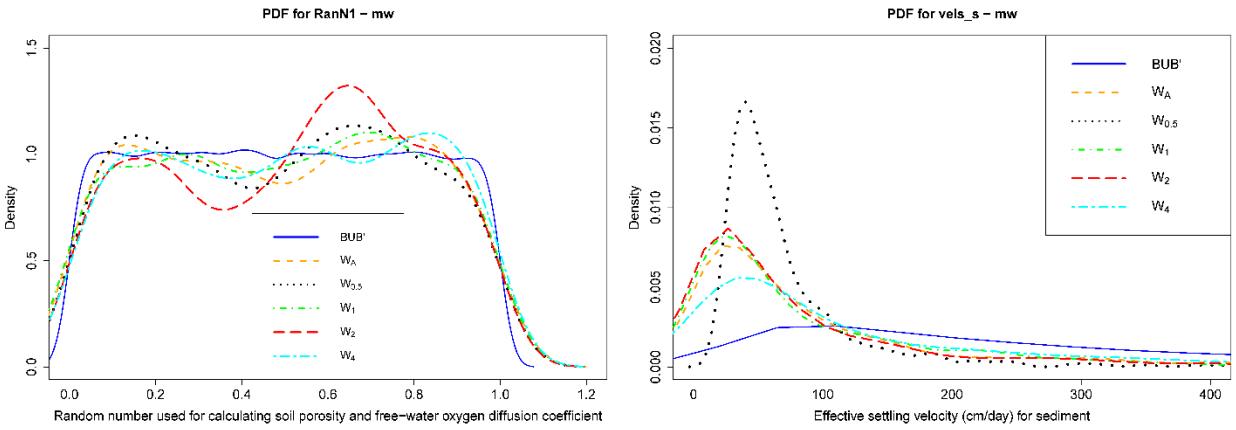

Figure 3.22. PDFs of the most sensitive parameters for m_w.

3.2 Temperature Analysis

3.2.1 Model Performance and Uncertainties

As it was mentioned before, the focus of this study is on pollutant loads, but results for concentrations are presented too in several occasions. Comparison of model performances based on T_{org} and T_{new} reveals that the average E_{NS} values of the behavioral set simulations are almost the same except for a very small but likely statistically insignificant improvement in P_w. Table 3.10

shows the minimum, maximum and average loading-based E_{NS} values of the behavioral set simulations for all constituents.

Table 3.10. Minimum, Maximum and Average E_{NS} Values of Behavioral Part for all Constituents for temperature analysis

	Onw			Nw			NO3w			Pw			mw		
	Min	**Max**	**Avr**	**Min**	**Max**	**Avr**	**Min**	**Max**	**Avr**	**Min**	**Max**	**Avr**	**Min**	**Max**	**Avr**
Torg	0.47	0.50	0.48	0.84	0.86	0.84	0.96	0.97	0.97	0.56	0.79	0.61	0.76	0.90	0.81
Tnew	0.47	0.50	0.48	0.84	0.86	0.85	0.96	0.97	0.96	0.58	0.75	0.63	0.77	0.90	0.81

Figures 3.23 and 3.24 show the 95% prediction interval bands of MC simulations (***BUB***') for loads and concentrations, the behavioral bands (***B***) and the observed data. $r-factors$ were also calculated for each parameter for each case to compare the model uncertainty of the parameters (Table 3.11). Although it is known that temperature has a very important effect on reaction rates and process dynamics, figures reveals that relaxing the temperature conversion equations' coefficients does not have significant impact on the uncertainty of ON_w, N_w, and m_w loads. This can be interpreted that changes in temperature can be compensated by other parameters (which will be scrutinized later). However, $r-factors$ show that the uncertainty of NO_{3w} increased while the uncertainty of P_w decreased slightly for loadings. This means that temperature analysis has a positive effect on P_w loads and a negative effect on NO_{3w} loads from the uncertainty reduction perspective. Results for concentrations were similar to loads with the exception of Nw, where $r-factor$ decreased for Nw.

Table 3.11. Concentration and loading based $r - factors$ for the temperature analysis.

	ON_w		N_w		$NO3_w$		P_w		m_w	
	Conc	**Load**	**Conc**	**Load**	**Conc**	**Load**	**Conc**	**Load**	**Conc**	**Load**
T_{org}	0.67	0.22	0.41	0.10	0.52	0.13	2.13	0.93	1.55	0.63
T_{new}	0.65	0.21	0.28	0.09	1.03	0.21	2.08	0.88	1.59	0.63

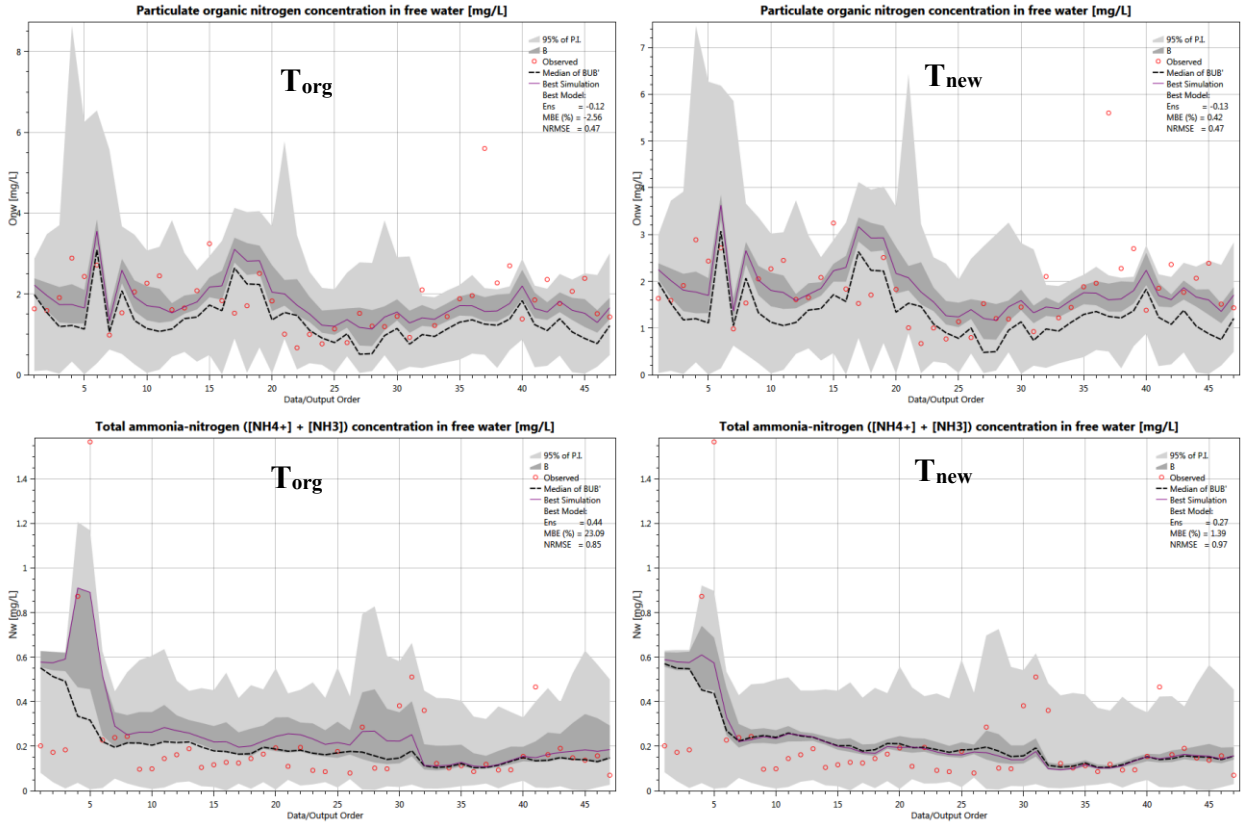

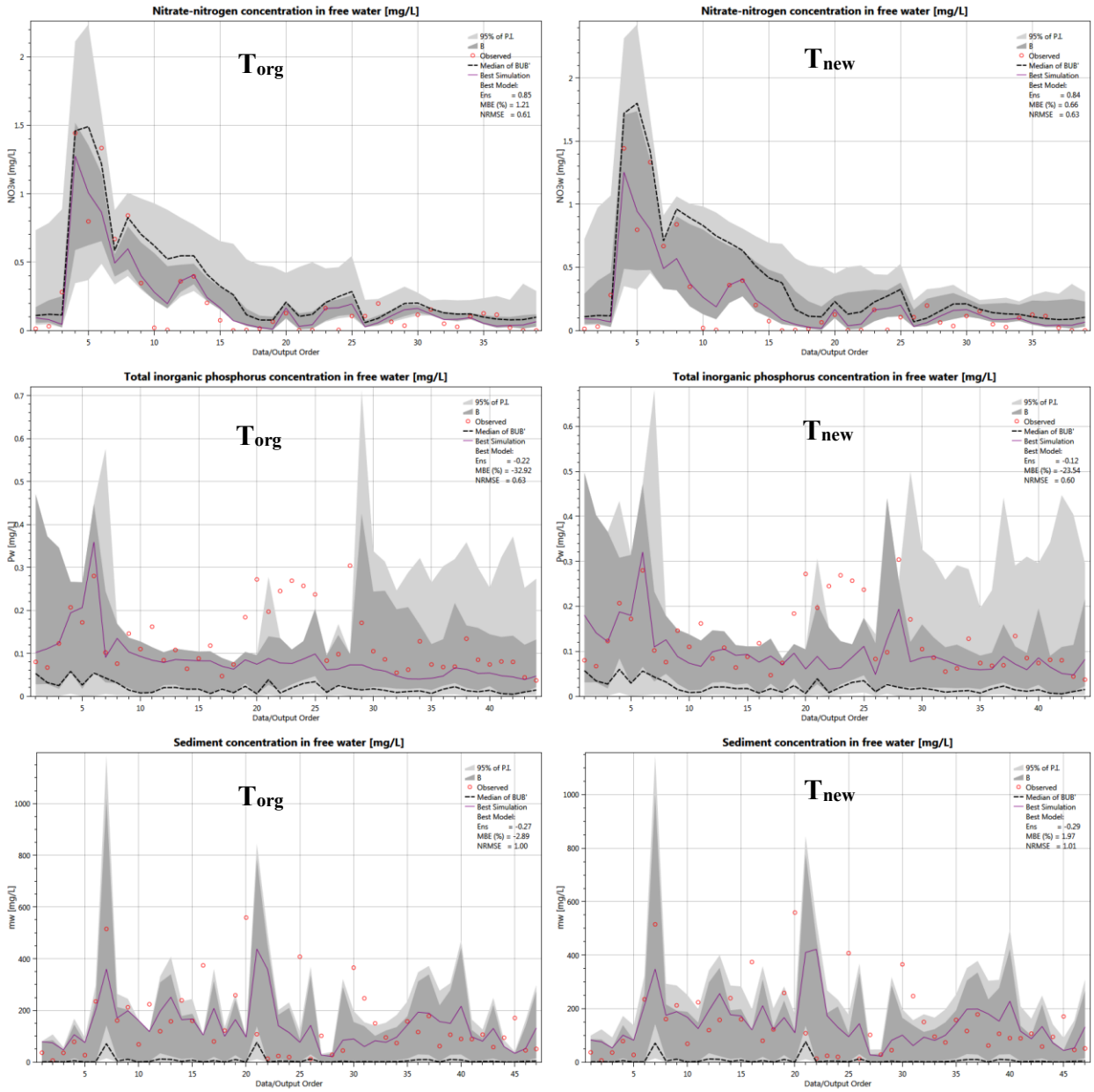

Figure 3.23. 95% PI vs Observed Concentrations of all constituents for temperature analysis

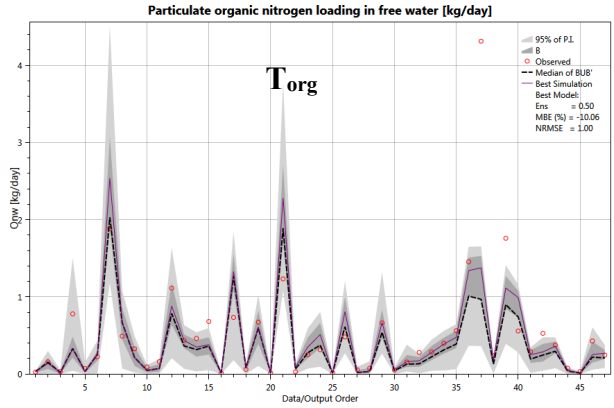
Particulate organic nitrogen loading in free water [kg/day]
Torg
95% of P.I.
B
Observed
Median of BUB'
Best Simulation
Best Model:
Ens = 0.50
MBE (%) = -10.06
NRMSE = 1.00
Qpw [kg/day]
Data/Output Order

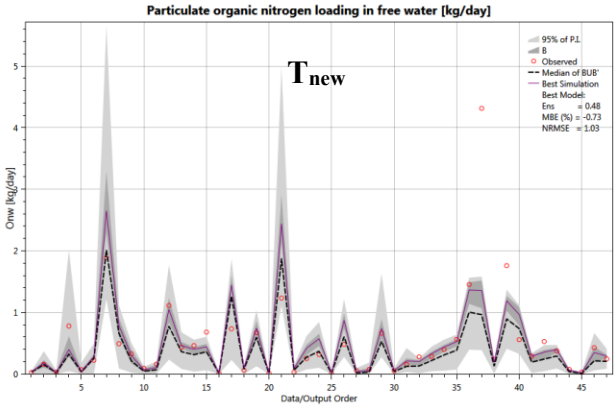
Particulate organic nitrogen loading in free water [kg/day]
Tnew
95% of P.I.
B
Observed
Median of BUB'
Best Simulation
Best Model:
Ens = 0.48
MBE (%) = -0.73
NRMSE = 1.03
Qnw [kg/day]
Data/Output Order

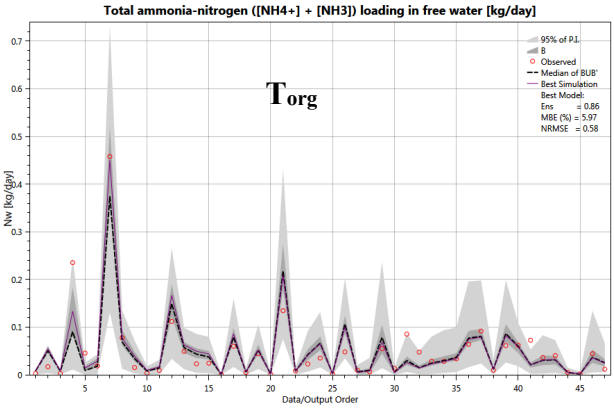
Total ammonia-nitrogen ([NH4+] + [NH3]) loading in free water [kg/day]
Torg
95% of P.I.
B
Observed
Median of BUB'
Best Simulation
Best Model:
Ens = 0.86
MBE (%) = 5.97
NRMSE = 0.58
Nw [kg/day]
Data/Output Order

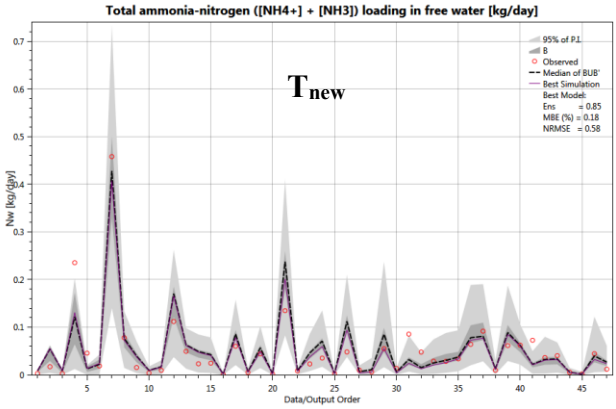
Total ammonia-nitrogen ([NH4+] + [NH3]) loading in free water [kg/day]
Tnew
95% of P.I.
B
Observed
Median of BUB'
Best Simulation
Best Model:
Ens = 0.85
MBE (%) = 0.18
NRMSE = 0.58
Nw [kg/day]
Data/Output Order

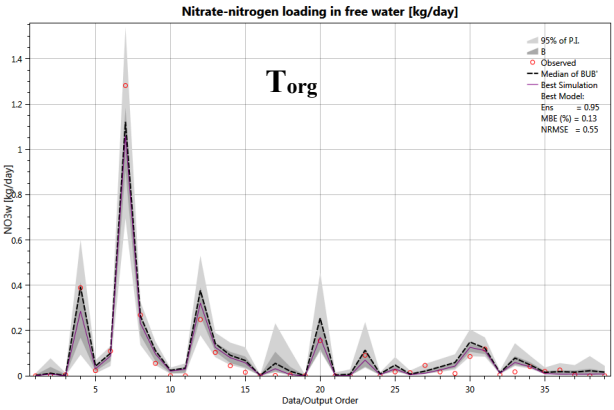
Nitrate-nitrogen loading in free water [kg/day]
Torg
95% of P.I.
B
Observed
Median of BUB'
Best Simulation
Best Model:
Ens = 0.95
MBE (%) = 0.13
NRMSE = 0.55
NO3w [kg/day]
Data/Output Order

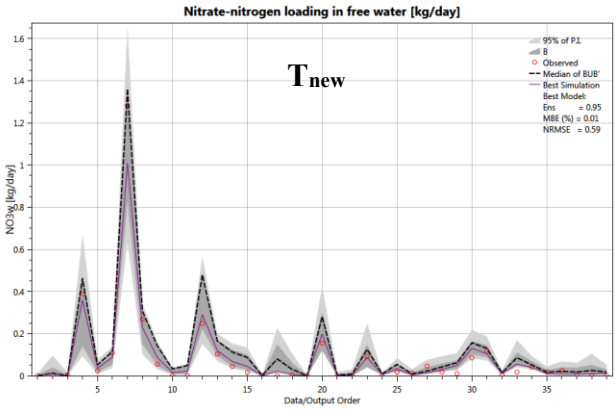
Nitrate-nitrogen loading in free water [kg/day]
Tnew
95% of P.I.
B
Observed
Median of BUB'
Best Simulation
Best Model:
Ens = 0.95
MBE (%) = 0.01
NRMSE = 0.59
NO3w [kg/day]
Data/Output Order

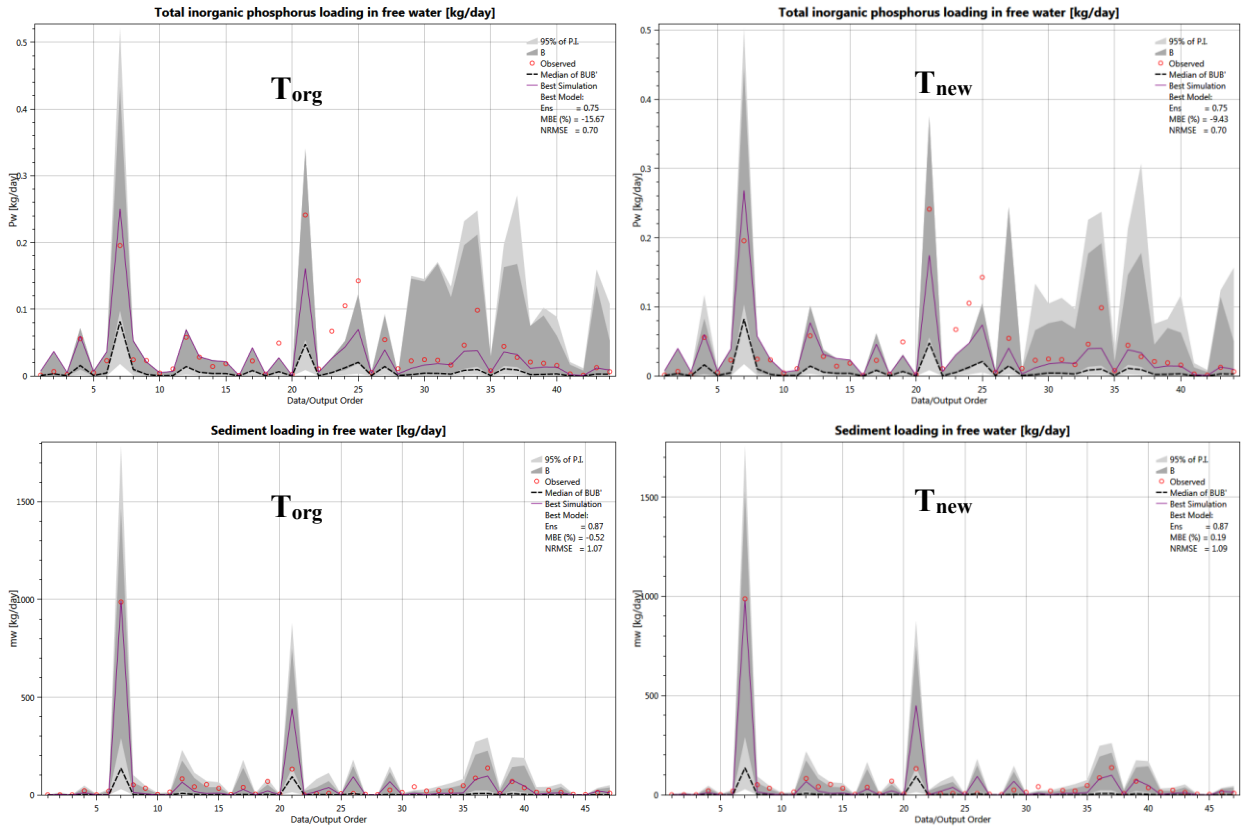

Figure 3.24. 95% PI vs observed loadings of all constituents for temperature analysis.

3.2.2 Sensitivity Analysis

The sensitivity analysis results of the original temperature model and the new model were compared through the K-S test. In addition to performing this analysis for the whole study period of two years, the same analysis was repeated for years 1 and 2 to see if years with differing wetland hydrology can affect the results. There is a 3-month dry season in the first year while total precipitation for these two years are roughly the same.

3.2.2.1 Particulate Organic Nitrogen (ON_w)

The top sensitive parameters for ON_w with the new temperature model are, in order, *a_vr_o*, *porw*, *vels_o*, *ana*, and *L2*. Figure 3.25 and Figure 3.26 show the K-S test results of ON_w for temperature

analysis, for the whole year and year 1 and 2, respectively. As can be seen, the temperature conversion equation coefficients did not show up sensitive when the whole period was considered. However, when we look at individual years, they became sensitive for the 1st year. When the whole period is considered, updating the temperature conversion equation did not change the dominant model processes. Order of sensitive parameters and their D_{max} values are almost the same. When individual years are considered, *vels_o* is the most sensitive parameter for the 1st year while it is the second most sensitive parameter in 2nd year. In 2nd year, *a_vr_o* and *L2* have increased sensitivities compared to year 1. On the other hand, *ana* and *porw* became more sensitive in year 1. The temperature conversion equation coefficients are sensitive in 1st year only, and the parameter a_T (D_{max}=0.11) is more sensitive than b_T (D_{max}=0.06).

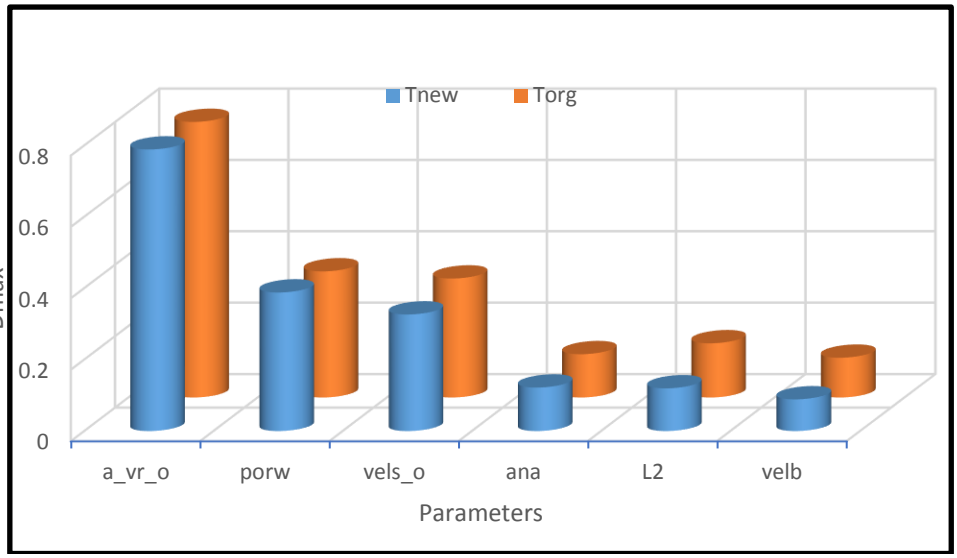

Figure 3.25. ON_w K-S test results for temperature analysis.

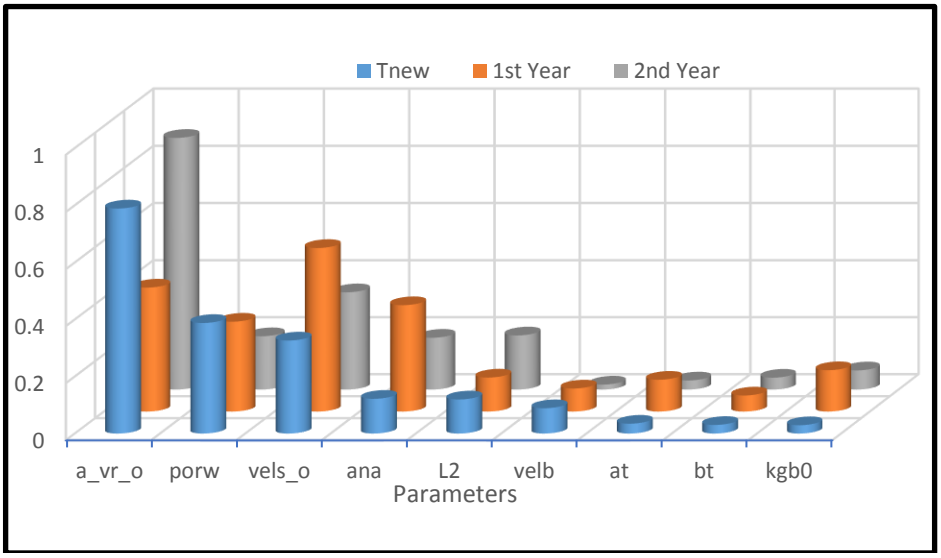

Figure 3.26. ON_w K-S test results for interannual analysis.

For a more detailed analysis with the top sensitive parameters, which are *a_vr_o*, *porw*, *vels_o*, *L2*, and *ana*, median and CV values of these sensitive parameters are compared for ON_w. The median and CV values of these parameters are shown in Table 3.12. The only significant difference is the change in the median value of *a_vr_o*. The new equation leads to 16% higher estimate for the median of this parameter. The table also shows results of interannual comparisons. The median and CV values for interannual analysis exhibit big differences from each other and T_{new} values, except for the parameter *porw*. CV values are highly different from each other. To sum up, relaxing the coefficients in the temperature conversion equation does not affect sensitive parameters for ON_w dramatically when the whole period is considered. The probability density function (PDF) graphs shown in Figure 3.27 also supports this conclusion. However, interannual variability in hydrology can affect these conclusions.

Table 3.12. Median (*Mdn*) and Coefficient of Variation (*CV*) values of the top sensitive parameters of the behavior set (***B***) for ON_w for temperature analysis

	BUB'		**T_{org}**		**T_{new} (Yr1+Yr2)**		**T_{new} (Yr1)**		**T_{new} (Yr2)**	
Parameter	***Mdn***	***CV***	***Mdn***	***CV***	***Mdn***	***CV***	***Mdn***	***CV***	***Mdn***	***CV***
a_vr_o	0.02	15.54	0.84	0.67	0.98	0.66	0.0037	1.35	2.41	0.71
porw	0.80	0.11	0.88	0.07	0.88	0.07	0.86	0.07	0.85	0.09
vels_o	1.87	2.29	1.90	0.31	1.82	0.32	1.05	0.12	2.16	0.42
L2	27.5	0.47	21.45	0.55	22.3	0.54	31.02	0.40	19.28	0.58
ana	10.5	0.39	11.69	0.34	11.9	0.33	14.04	0.19	12.86	0.30

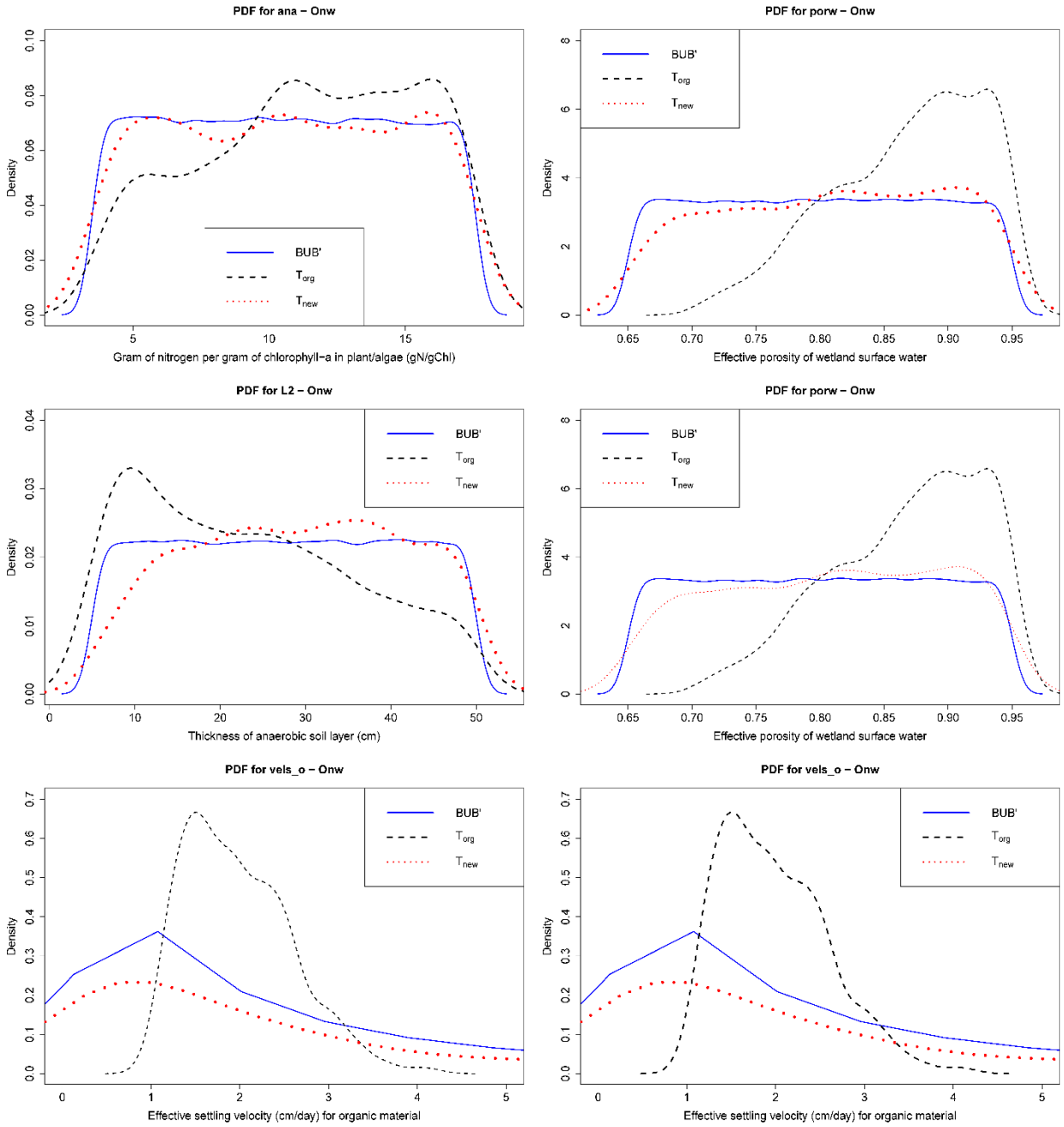

Figure 3.27. PDFs of the most sensitive parameters of ON_w for temperature analysis.

3.2.2.2 Total Ammonia-Nitrogen ($[NH_4^+] + [NH_3]$) (N_w)

The top sensitive parameters for N_w with the new temperature model are, in order, *fact*, *kd*, *c2*, and *knw*. Figure 3.28 and Figure 3.29 show the K-S test results of N_w for temperature analysis, for the whole year and year 1 and 2, respectively. As can be seen, the temperature conversion equation

coefficients a_T and b_T showed up sensitive when the whole period was considered. However, when we look at individual years, their sensitive strengths (D_{max}) increased substantially for the 2st year. When the whole period is considered, updating the temperature conversion equation impacted sensitivity of *knw*. Nitrification rate became less sensitive with updated temperature conversion equation. In spite these, the order of sensitive parameters and their D_{max} values (except k_{nw}) are almost the same. For the interannual analysis, *fact* and *kd* are the most sensitive parameters for the 1st year while *c2* and *kmin1s* are the most sensitive parameters for the 2nd year. The parameters *fact*, *kd*, and *knw* are still sensitive for 2nd year, but they lost their sensitivity strength (D_{max}) significantly compared to 1st year. Another interesting result from the K-S test is that although *kmin1s* was almost not a sensitive parameter when the whole year was considered, it became highly sensitive individual years, especially so for year 2.

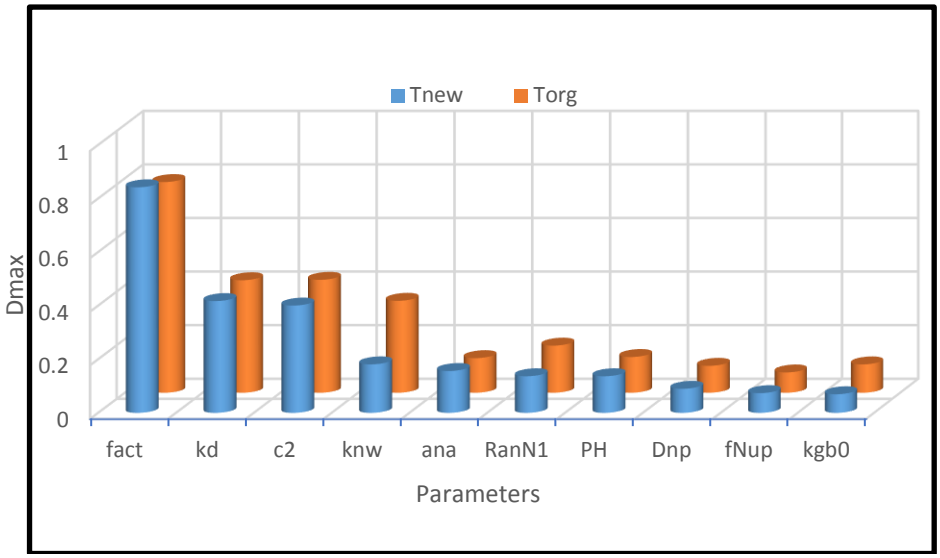

Figure 3.28. Nw K-S test results for temperature analysis.

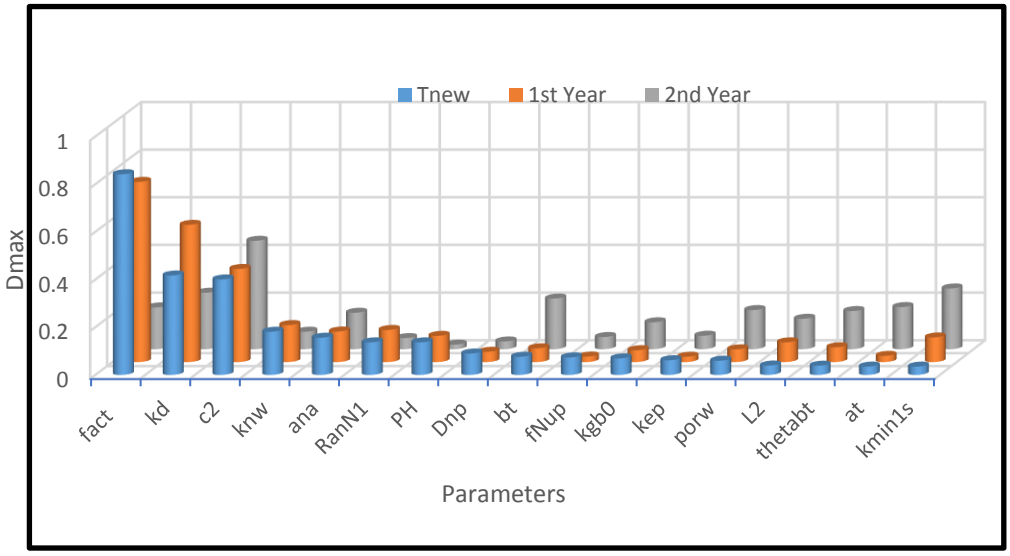

Figure 3.29. N_w K-S test results for interannual analysis.

For a more detailed analysis with the top sensitive parameters, which are *fact*, *kd*, *c2*, and *knw*, median and CV values of these sensitive parameters are compared for N_w. The median and CV values of these parameters are shown in Table 3.13. The most significant difference is the change in the median value of *knw* with 55% change compared to its value in T_{org}. The table also consists of interannual comparisons. The median and CV values for interannual analysis show big differences from each other and T_{new} values. CV values are also completely different from each other. To sum up, relaxing the coefficients in the temperature conversion equation does not affect sensitive parameters for N_w dramatically when the whole period is considered except for the parameter *knw*. The probability density function (PDF) graphs shown in Figure 3.30 also supports this conclusion. However, interannual variability in hydrology can affect these conclusions.

Table 3.13. Median (Mdn) and Coefficient of Variation (CV) values of the top sensitive parameters of the behavior set (B) for N_w for temperature analysis

Parameter	BUB'		T_{org}		T_{new} (Yr1+Yr2)		T_{new} (Yr1)		T_{new} (Yr2)	
	Mdn	***CV***	***Mdn***	***CV***	***Mdn***	***CV***	***Mdn***	***CV***	***Mdn***	***CV***
fact	137	1.08	662	0.66	799.3	0.63	637	0.62	191	1.22
c2	2454	0.29	3139	0.13	3090	0.14	3066	0.14	1927	0.20
kd	1.61	2.05	4.4	0.91	3.87	0.88	9.42	1.31	3.46	1.83
knw	0.006	2.07	0.002	1.08	0.004	1.56	0.004	1.72	0.006	2.59

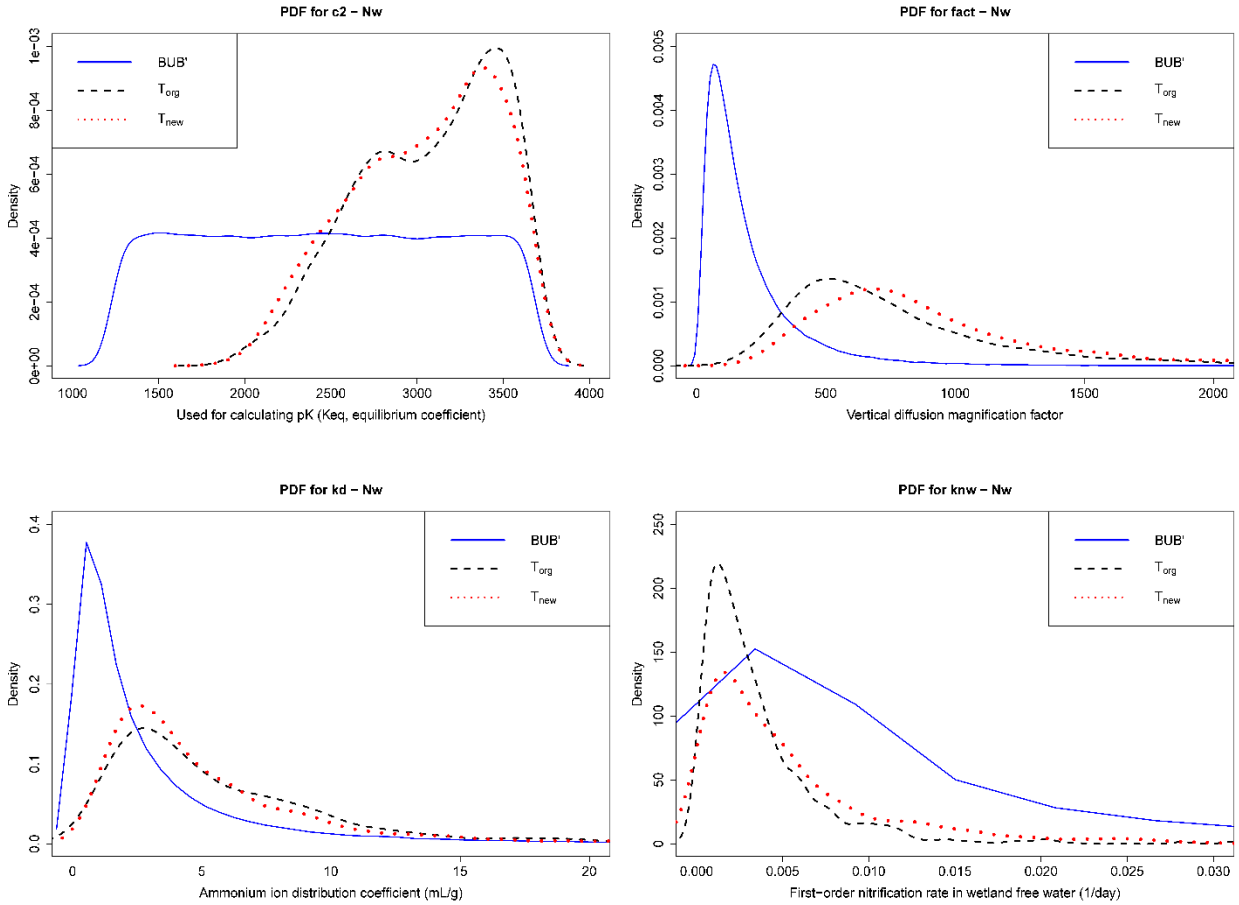

Figure 3.30. PDFs of the most sensitive parameters of N_w for temperature analysis.

3.2.2.3 Nitrate-Nitrogen (NO_{3w})

The top sensitive parameters for NO_{3w}, with the new temperature model are, in order, *ana*, *c2*, *kgb0*, *porw*, *PH*, *fact*, a_T, and b_T. Figure 3.31 and Figure 3.32 show the K-S test results of NO_{3w} for temperature analysis, for the whole year and year 1 and 2, respectively. As can be seen, the temperature conversion equation coefficients were among the sensitive parameters when the whole period was considered. When we look at individual years, b_T became more sensitive for 2nd year. When the whole period is considered, updating the temperature conversion equation do not have significant impact on sensitivity rankings except the parameters *kden* and *L2*. Order of sensitive parameters and their D_{max} values are almost the same except for these two parameters. For the interannual analysis, *porw* is the most sensitive parameter for the 1st year while it is the seventh most sensitive parameter in 2nd year. In 2nd year, *fact*, *c2*, and b_T have increased sensitivities compared to year 1. On the other hand, *L2* and *kd* became more sensitive in year 1.

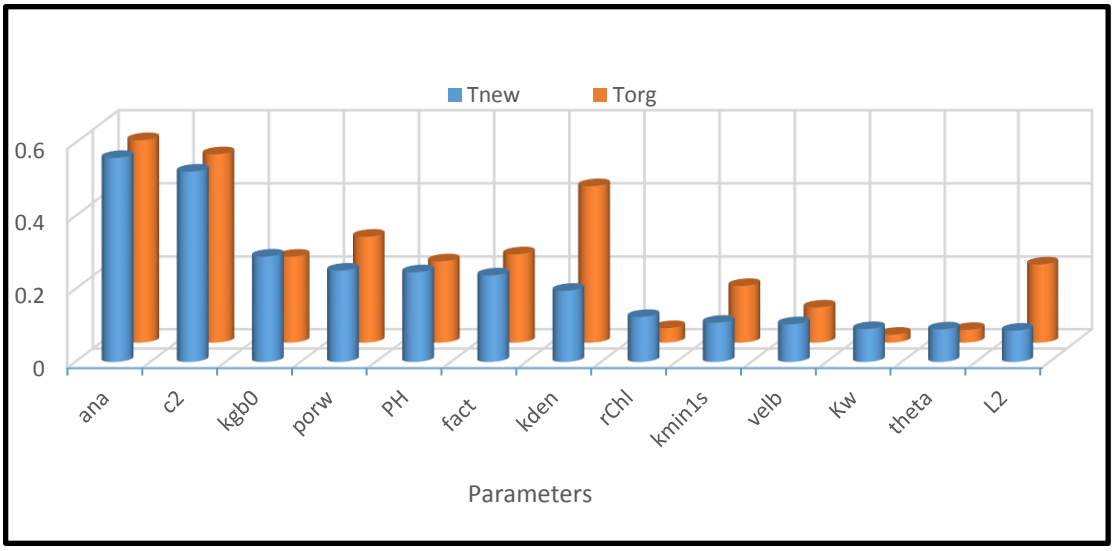

Figure 3.31. NO_{3w} K-S test results for temperature analysis.

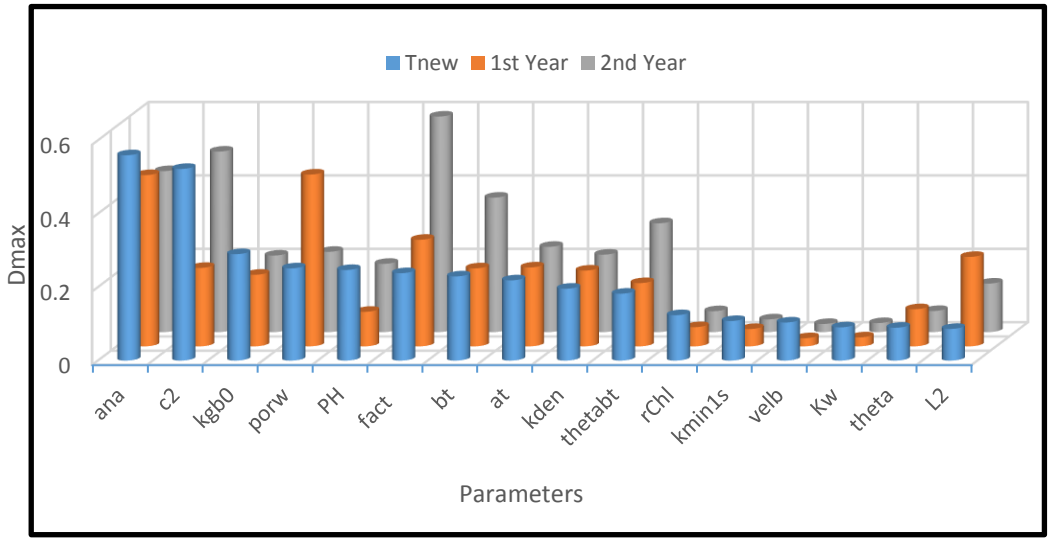

Figure 3.32. NO_{3w} K-S test results for interannual analysis.

For a more detailed analysis with the top sensitive parameters, which are *ana*, *c2*, *kgb0*, *porw*, *pH*, *fact*, a_T, and b_T median and CV values of these sensitive parameters are compared for NO_{3w}. The median and CV values of the most sensitive parameters are shown in Table 3.14 and Table 3.15. The most significant difference is the change in the median value of *kden*. The new equation leads to 195% higher estimate for the median of this parameter. The table also consists of interannual comparisons. The median and CV values for interannual analysis show big differences from each other and T_{new} values, except for the parameter *ana*. CV values are also completely different from each other. To sum up, relaxing the coefficients in the temperature conversion equation affects sensitive parameters for NO_{3w} dramatically when the whole period is considered. The probability density function (PDF) graphs shown in Figure 3.33 also supports this conclusion. Further, when the analysis is broken down into individual years, sensitivity orders and their strength can show dramatic changes.

Table 3.14. Median (*Mdn*) and Coefficient of Variation (*CV*) values of the top sensitive parameters of the behavior set (B) for NO_{3w} for temperature analysis

	BUB'		**T_{org}**		**T_{new}**	
Parameter	***Mdn***	***CV***	***Mdn***	***CV***	***Mdn***	***CV***
ana	10.5	0.39	15.67	0.12	15.7	0.12
c2	2454	0.29	1620	0.22	1629	0.23
kden	0.08	0.55	0.03	0.61	0.10	0.37
porw	0.80	0.11	0.73	0.10	0.74	0.10
fact	137	1.08	172	0.52	181.4	0.60
kgb0	1.3E-03	0.13	1.4E-03	0.12	1.5E-03	0.13
PH	6.4	0.17	7.07	0.14	7.1	0.13

Table 3.15. Median (*Mdn*) and Coefficient of Variation (*CV*) values of the top sensitive parameters of the behavior set (B) for NO_{3w} for interannual analysis

	T_{new} (Yr1)		**T_{new} (Yr2)**	
Parameter	***Mdn***	***CV***	***Mdn***	***CV***
ana	15.42	0.17	14.91	0.20
c2	1974	0.32	1608	0.29
kgb0	0.001	0.12	0.001	0.14
porw	0.70	0.07	0.86	0.09
PH	6.65	0.16	6.97	0.14
fact	195	0.50	446	0.79
bt	0.63	0.33	0.73	0.27
at	6.91	0.35	7.39	0.34
L2	36.97	0.34	31.47	0.41

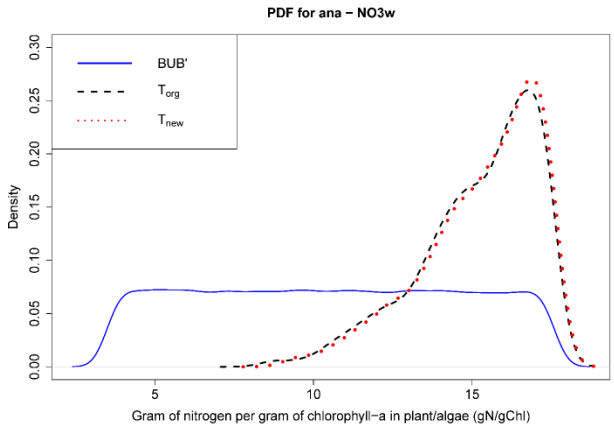
PDF for ana – NO3w
BUB'
Torg
Tnew
Density
Gram of nitrogen per gram of chlorophyll−a in plant/algae (gN/gChl)

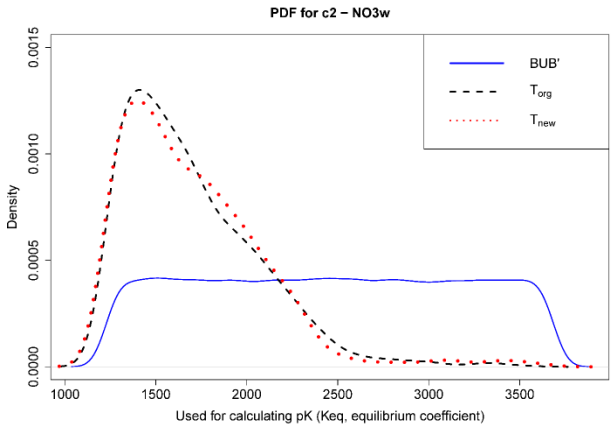
PDF for c2 – NO3w
BUB'
Torg
Tnew
Density
Used for calculating pK (Keq, equilibrium coefficient)

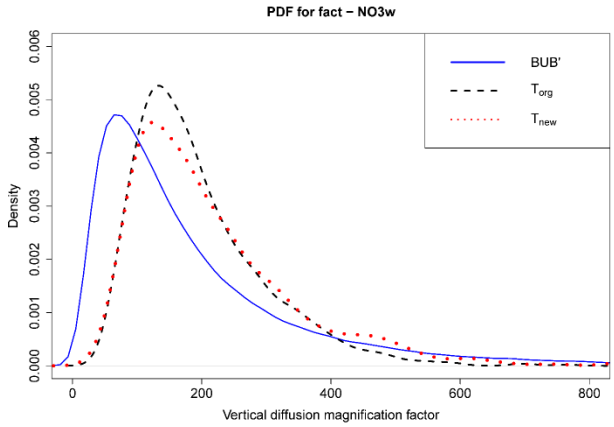
PDF for fact – NO3w
BUB'
Torg
Tnew
Density
Vertical diffusion magnification factor

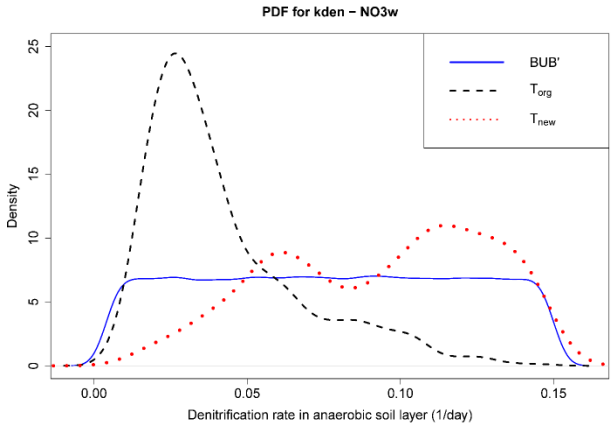
PDF for kden – NO3w
BUB'
Torg
Tnew
Density
Denitrification rate in anaerobic soil layer (1/day)

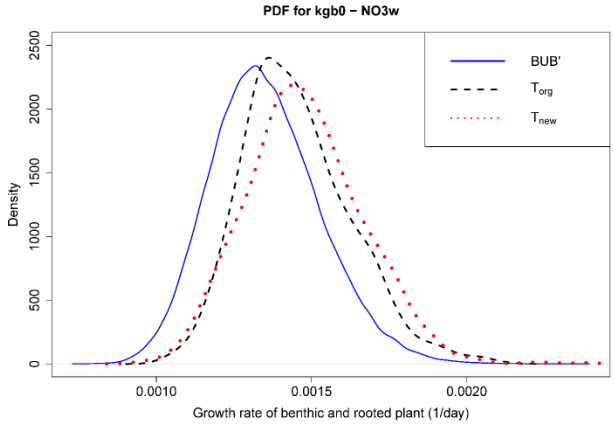
PDF for kgb0 – NO3w
BUB'
Torg
Tnew
Density
Growth rate of benthic and rooted plant (1/day)

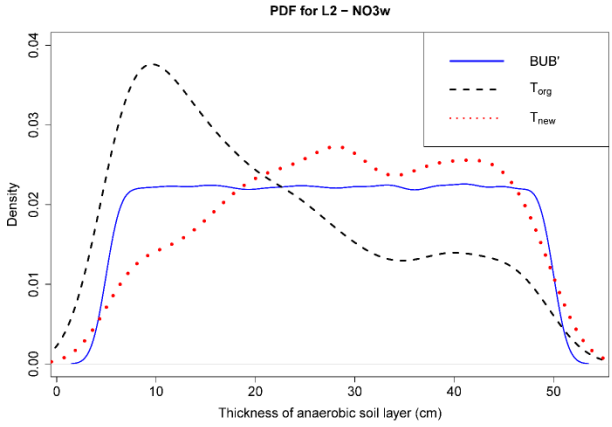
PDF for L2 – NO3w
BUB'
Torg
Tnew
Density
Thickness of anaerobic soil layer (cm)

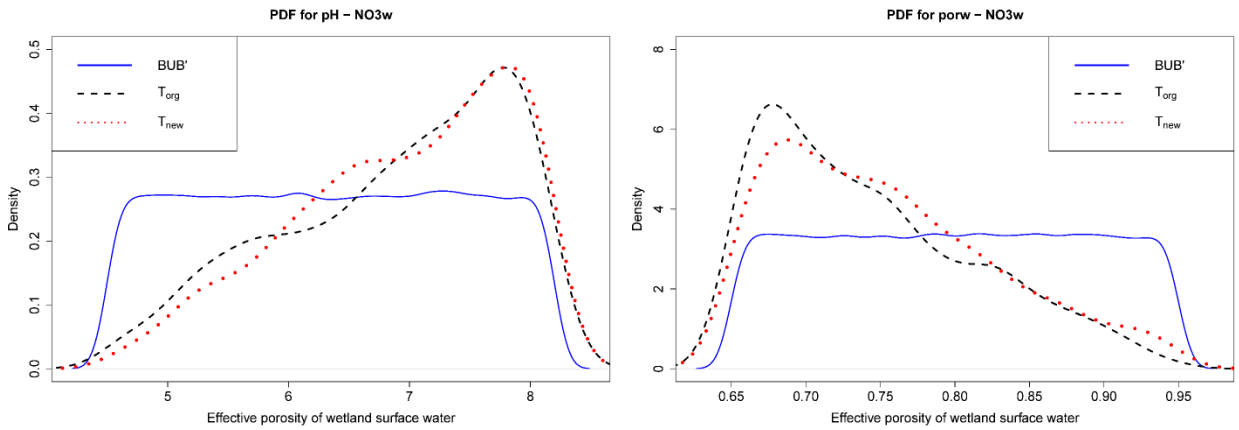

Figure 3.33. PDFs of the most sensitive parameters of NO_{3w} for temperature analysis.

3.2.2.4 Total Inorganic Phosphorous (P_w)

The top sensitive parameters for P_w with the new temperature model are, in order, *Kw*, *fact*, *vels_s*, and *porw*. Figure 3.34 and Figure 3.35 show the K-S test results of P_w for temperature analysis, for the whole year and year 1 and 2, respectively. As can be seen, the temperature conversion equation coefficients showed up sensitive when the whole period was considered. However, when we look at individual years, their strength of sensitivities were reduced, especially b_T. Updating the temperature conversion equation did not change the significant model processes. Order of sensitive parameters and their D_{max} values are almost the same. This was the case regardless of whether we considered the whole year or individual years.

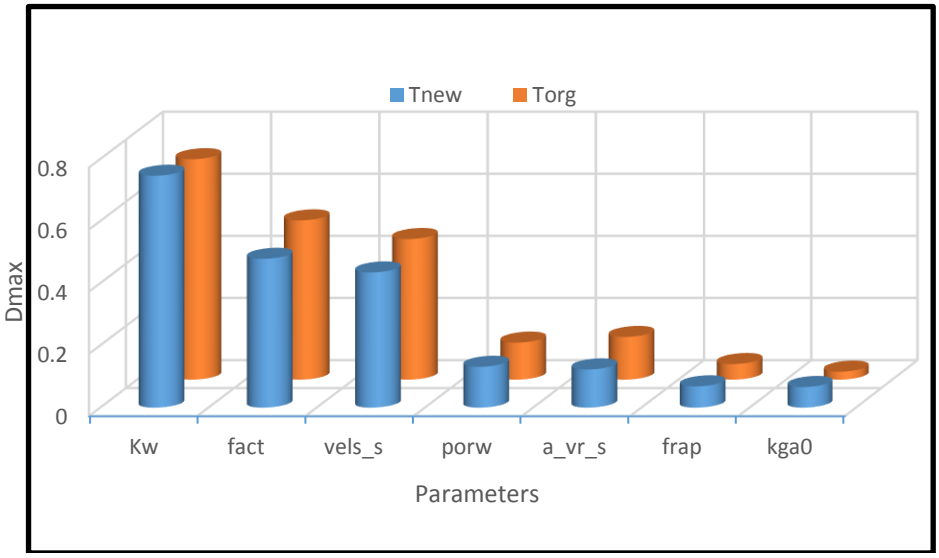

Figure 3.34. P_w K-S test results for temperature analysis.

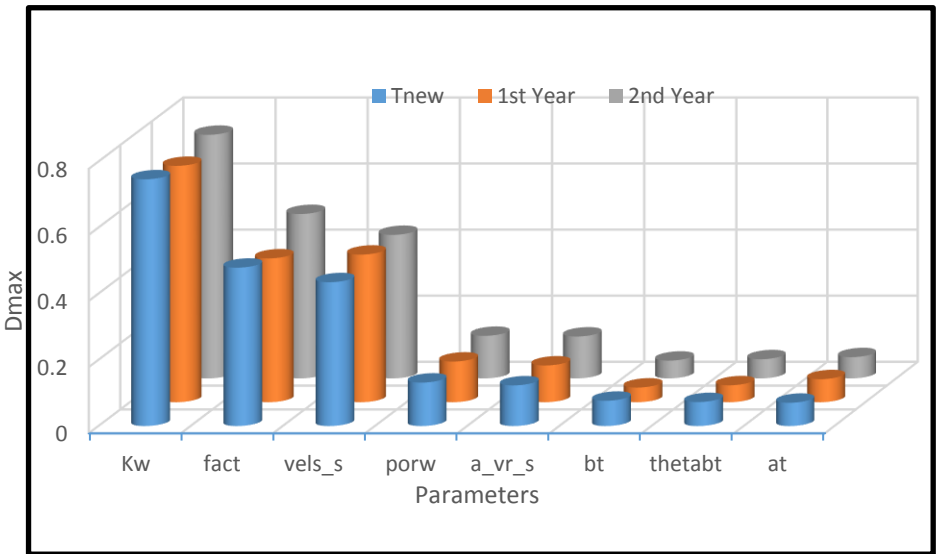

Figure 3.35. Pw K-S test results for interannual analysis.

For a more detailed analysis with the top sensitive parameters, which are *Kw*, *fact*, and *vels_s*, median and CV values of these sensitive parameters are compared for P_w. The median and CV values of these parameters are shown in Table 3.16. The most significant difference is the change in the median value of *vels_s*. The new equation leads to 13% lower estimate for the median

of this parameter. The table also consists of interannual comparisons. The median and CV values for interannual analysis does not show big differences from each other and T_{new} values, except for the parameter *Kw*. To sum up, relaxing the coefficients in the temperature conversion equation does not affect sensitive parameters for P_w dramatically. The probability density function (PDF) graphs shown in Figure 3.36 also supports this conclusion.

Table 3.16. Median (*Mdn*) and Coefficient of Variation (*CV*) values of the top sensitive parameters of the behavior set (B) for P_w for temperature analysis.

	BUB'		**T_{org}**		**T_{new}**		**T_{new} (Yr1)**		**T_{new} (Yr2)**	
Parameter	***Mdn***	***CV***	***Mdn***	***CV***	***Mdn***	***CV***	***Mdn***	***CV***	***Mdn***	***CV***
Kw	34975	1.58	3483	2.36	3276	2.66	3509	3.02	3336	2.19
fact	137.2	1.08	54.7	0.86	56.4	0.90	63.6	0.71	55.2	0.63
vels_s	231.5	1.51	59.3	2.21	66.8	2.08	54.6	2.12	61.3	2.11

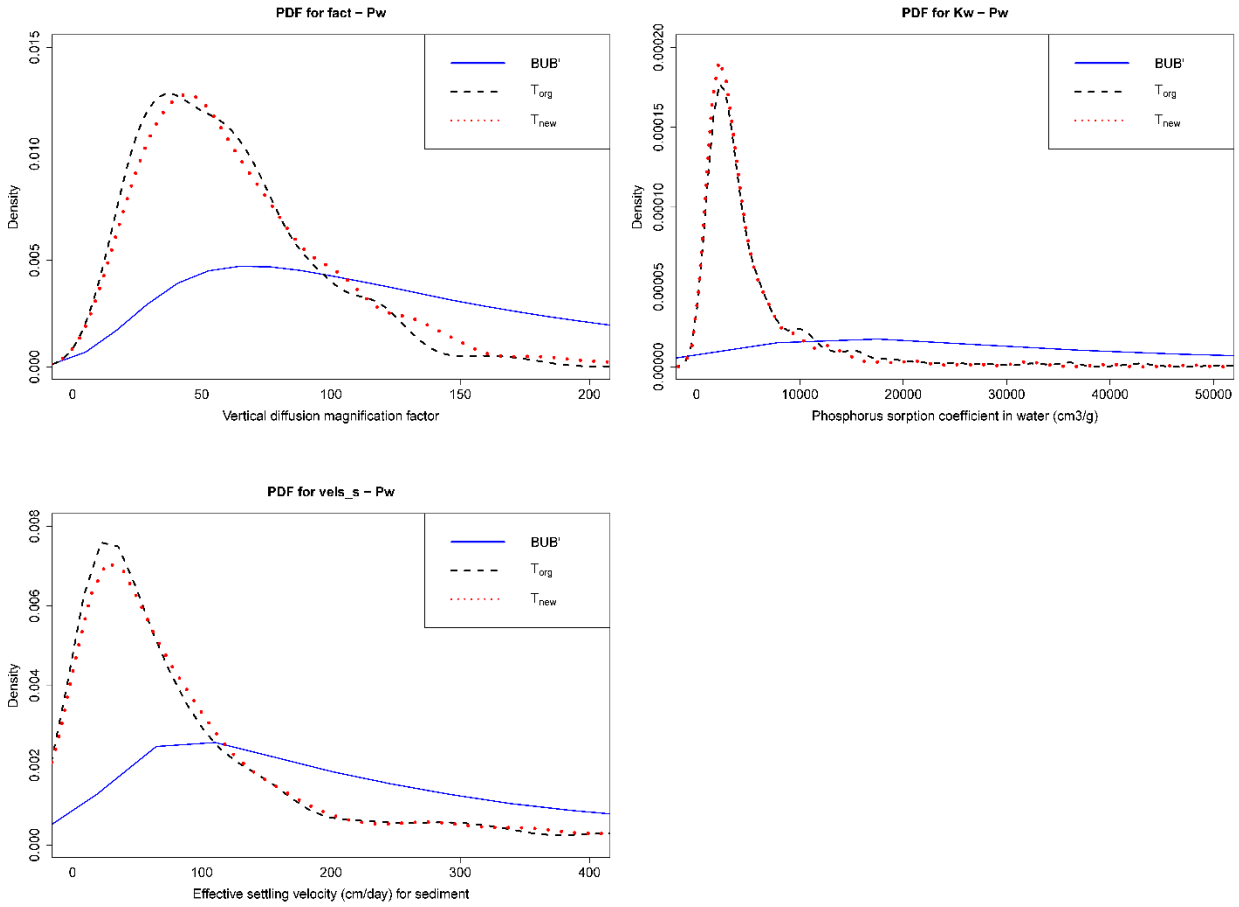

Figure 3.36. PDFs of the most sensitive parameters of P_w for temperature analysis

3.2.2.5 Sediment (m_w)

The top sensitive parameters for m_w with the new updated model are, in order, *a_vr_s*, *vels_s*, and *RanN1*. Figure 3.37 and Figure 3.38 show the K-S test results of m_w for temperature analysis, for the whole year and year 1 and 2, respectively. As can be seen, the temperature conversion equation coefficients did not show up in the list of sensitive parameters at all. The order and the strength of the parameter sensitivities also did not change much, except for porw in year 2 having increased level of sensitivity.

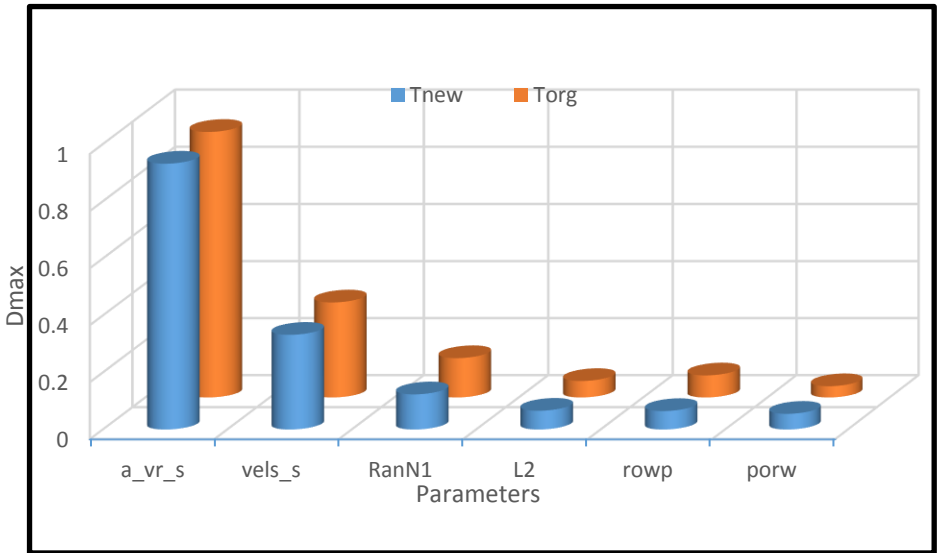

Figure 3.37. m_w K-S test results for temperature analysis.

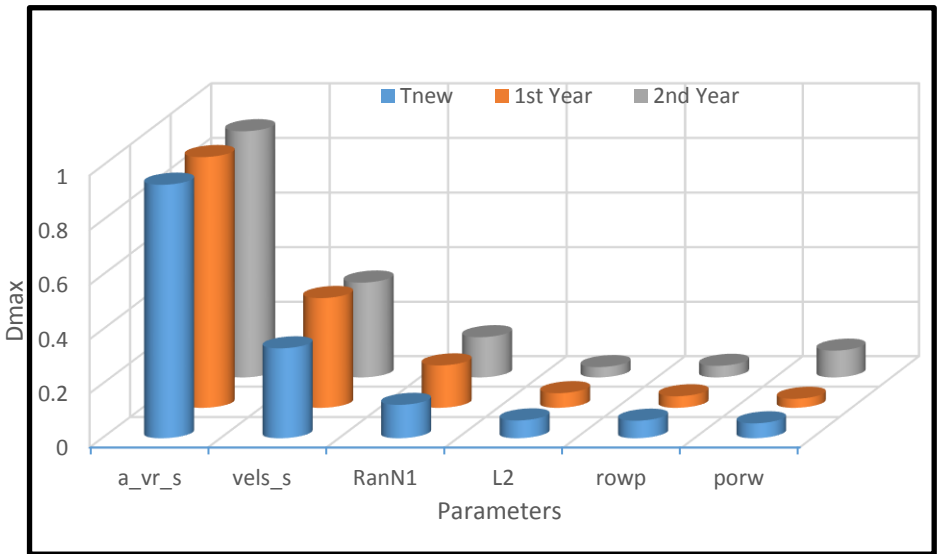

Figure 3.38. m_w K-S test results for interannual analysis.

For a more detailed analysis with the top sensitive parameters, which are *a_vr_s*, *vels_s*, and *RanN1*, median and CV values of these sensitive parameters are compared for m_w. The median and CV values of these parameters are shown in Table 3.17. The most significant difference is the change in the median value of *RanN1*. The new equation leads to 13% higher estimate for the

median of this parameter. The table also consists of interannual comparisons. The median and CV values of settling velocity parameter for interannual analysis show big differences from each other and T_{new} values. Other parameter do not have much differences. To sum up, relaxing the coefficients in the temperature conversion equation does not affect sensitive parameters for m_w dramatically when the whole period is considered. The probability density function (PDF) graphs shown in Figure 3.39 also supports this conclusion. However, interannual variability in hydrology can affect these conclusions.

Table 3.17. Median (*Mdn*) and Coefficient of Variation (*CV*) values of the top sensitive parameters of the behavior set (B) for m_w for temperature analysis

	BUB'		**T_{org}**		**T_{new}**		**T_{new} (Yr1)**		**T_{new} (Yr2)**	
Parameter	***Mdn***	***CV***	***Mdn***	***CV***	***Mdn***	***CV***	***Mdn***	***CV***	***Mdn***	***CV***
a_vr_s	0.002	4.38	0.09	0.79	0.09	0.87	0.09	0.97	0.06	0.88
vels_s	231	1.51	112	0.88	111	0.99	84	1.19	284	0.62
RanN1	0.50	0.58	0.38	0.68	0.39	0.65	0.37	0.68	0.38	0.67

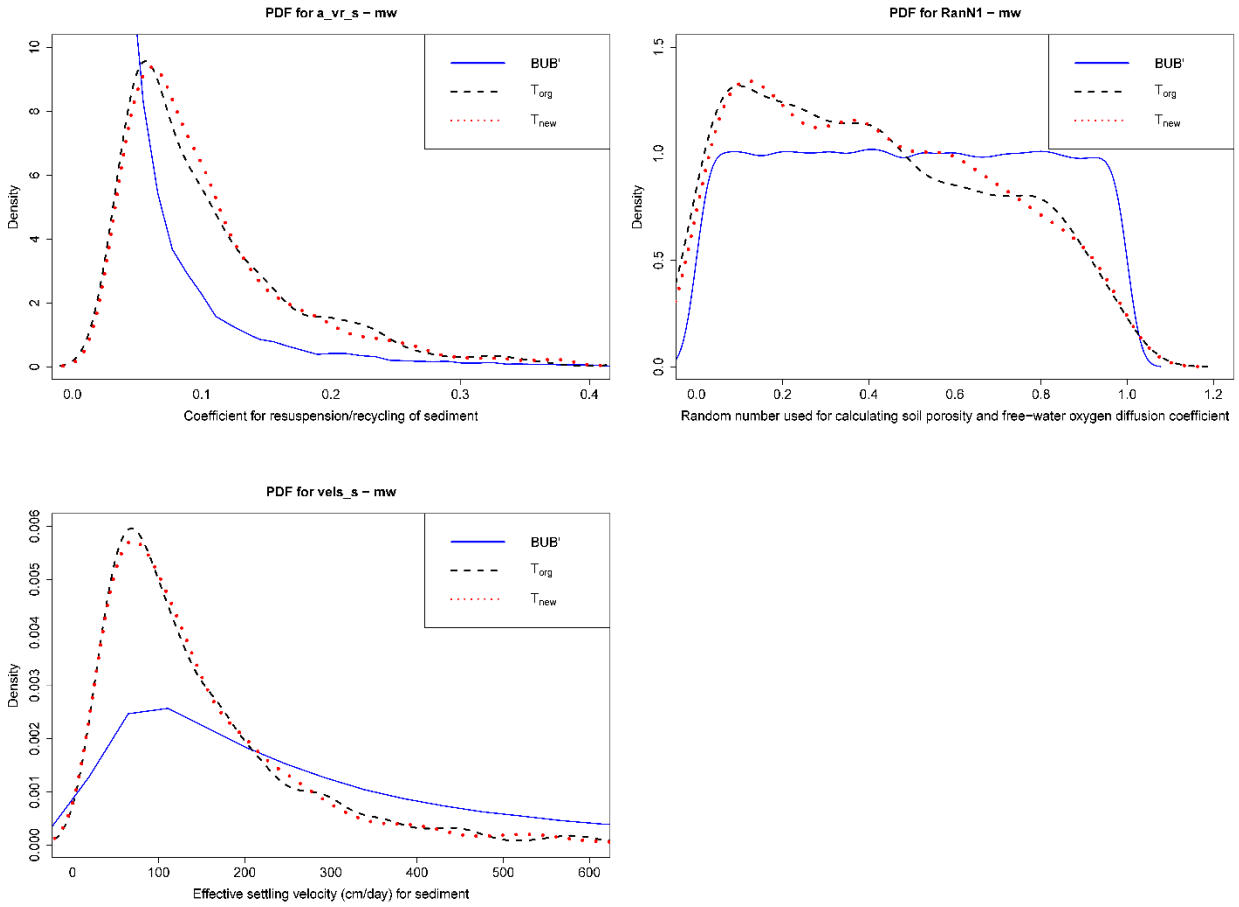

Figure 3.39. PDFs of the most sensitive parameters of m_w for temperature analysis.

3.3 Temporal Resolution Analysis

3.3.1 Model Performances and Uncertainty

Table 3.18 shows the minimum, maximum and average loading based E_{NS} values of behavioral set simulations for all constituents. First row represents results of the model with the new temperature model (T_{new}; same as the values in Table 3.10). Second row represents the results with the same model, but temperature disaggregated into sub-daily values (T_{sub}; at interval of the numeric time step Δt). Last row is further improvement to this model with all the inflow provided in sub-daily time scale (QT_{sub}) instead of daily time scale (which is the existing situation in WetQual).

Changing the time resolution of temperature did not make any difference in terms of model performance. When inflow data was provided in sub-daily form, model performance significantly improved for ON_w, but deteriorated substantially for m_w. Both are particulate matter. Thus, it is hard to make any sense of this contrasting behavior. Model performances were insensitive to these changes for total ammonia, nitrate and phosphorous. One can conclude that these changes in the model affect model performances in particulate forms (positively or not), but not dissolved forms.

Table 3.18. Minimum, maximum and average E_{NS} values of Behavioral parts for all constituents for temporal analysis.

	ON_w			N_w			NO_{3w}			P_w			m_w		
	Min	**Max**	**Avg**	**Min**	**Max**	**Avg**	**Min**	**Max**	**Avg**	**Min**	**Max**	**Avg**	**Min**	**Max**	**Avg**
T_{new}	0.47	0.50	0.48	0.84	0.86	0.85	0.96	0.97	0.96	0.58	0.75	0.63	0.77	0.90	0.81
T_{sub}	0.47	0.50	0.48	0.85	0.87	0.85	0.97	0.98	0.98	0.56	0.76	0.61	0.77	0.89	0.81
QT_{sub}	0.56	0.62	0.58	0.83	0.91	0.85	0.98	0.98	0.98	0.53	0.81	0.62	0.44	0.82	0.60

Figure 3.40 to figure 3.44 show the 95% prediction intervals of all MC simulations, behavioral bands, and observed data for loads and concentrations for all three models. Visually, differences in uncertainty bands are not distinguishable for loads, but concentrations show discernable differences. In order to compare the model predictive uncertainties quantitatively, $r-factors$ were calculated for each constituent and are shown in Table 3.19. It can be seen that the loading-based uncertainty of the model slightly increases and decreases for P_w and NO_{3w}, respectively, when the temporal resolution of temperature is increased. It doesn't change much in others. When the sub-daily inflow is used along with sub-daily temperature, uncertainty increases in all, both in concentrations and loads. One of the most interesting result from uncertainty analysis for the temporal resolution application is the changes in NO_{3w}. Increasing temporal resolution of

temperature only led to reduced model uncertainty, but adding sub-daily inflow took the uncertainty levels back to the original level. This indicates the sensitivity of nitrate to temperature fluctuations.

Table 3.19. Concentration and loading based $r - factors$ of temporal analysis for all constituents.

	ON_w		N_w		NO_{3w}		P_w		m_w	
	Conc	**Load**	**Conc**	**Load**	**Conc**	**Load**	**Conc**	**Load**	**Conc**	**Load**
$\mathbf{T_{new}}$	0.65	0.21	0.28	0.09	1.03	0.21	2.08	0.88	1.59	0.63
$\mathbf{T_{sub}}$	0.70	0.23	0.68	0.08	0.74	0.15	2.45	1.06	1.76	0.69
$\mathbf{QT_{sub}}$	0.81	0.38	0.53	0.20	1.00	0.21	3.41	1.25	1.89	0.87

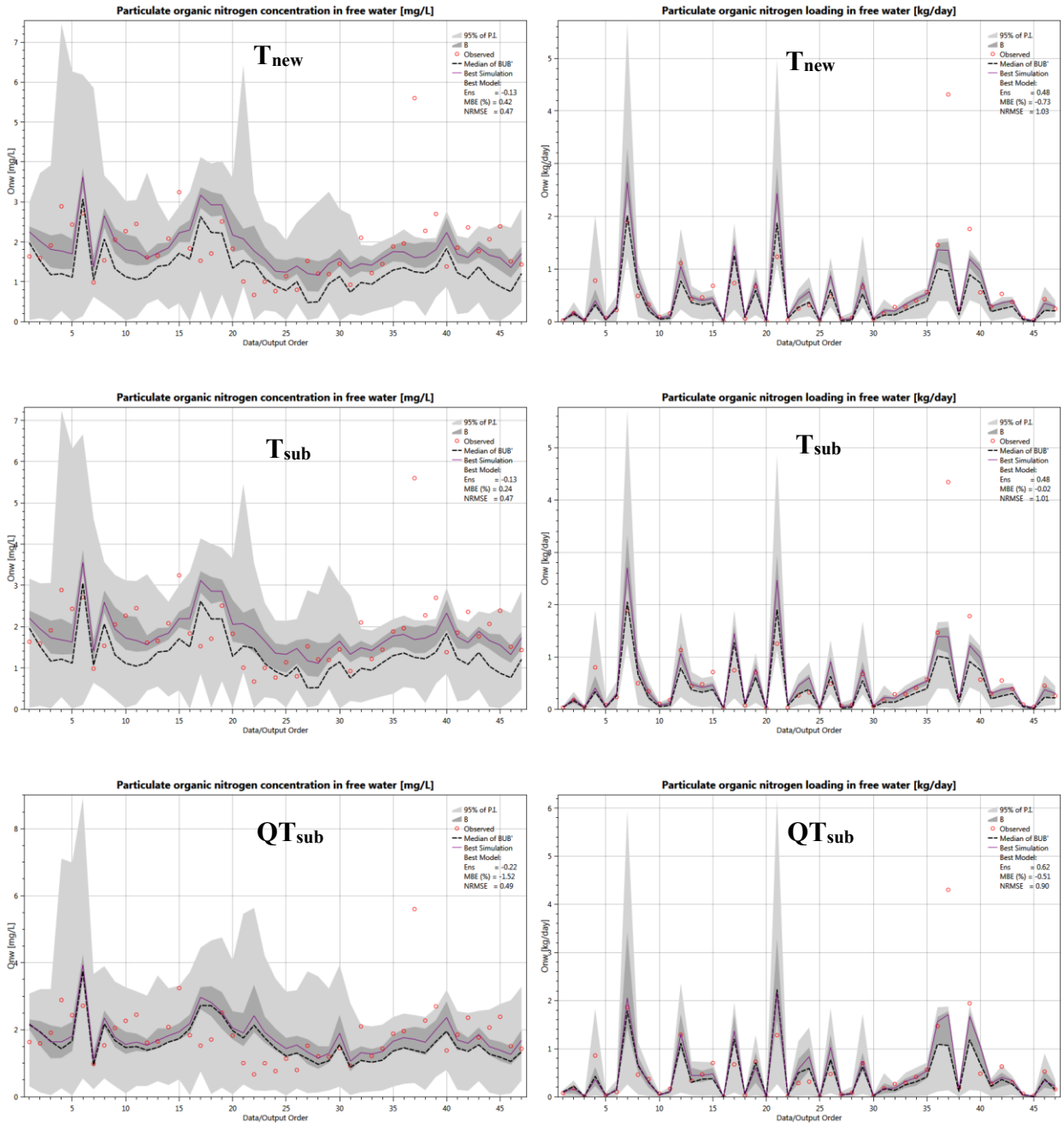

Figure 3.40. 95% prediction intervals (P.I) of all MC simulations, behavioral bands, and observed data for loads and concentrations of ONw for all three time resolution models.

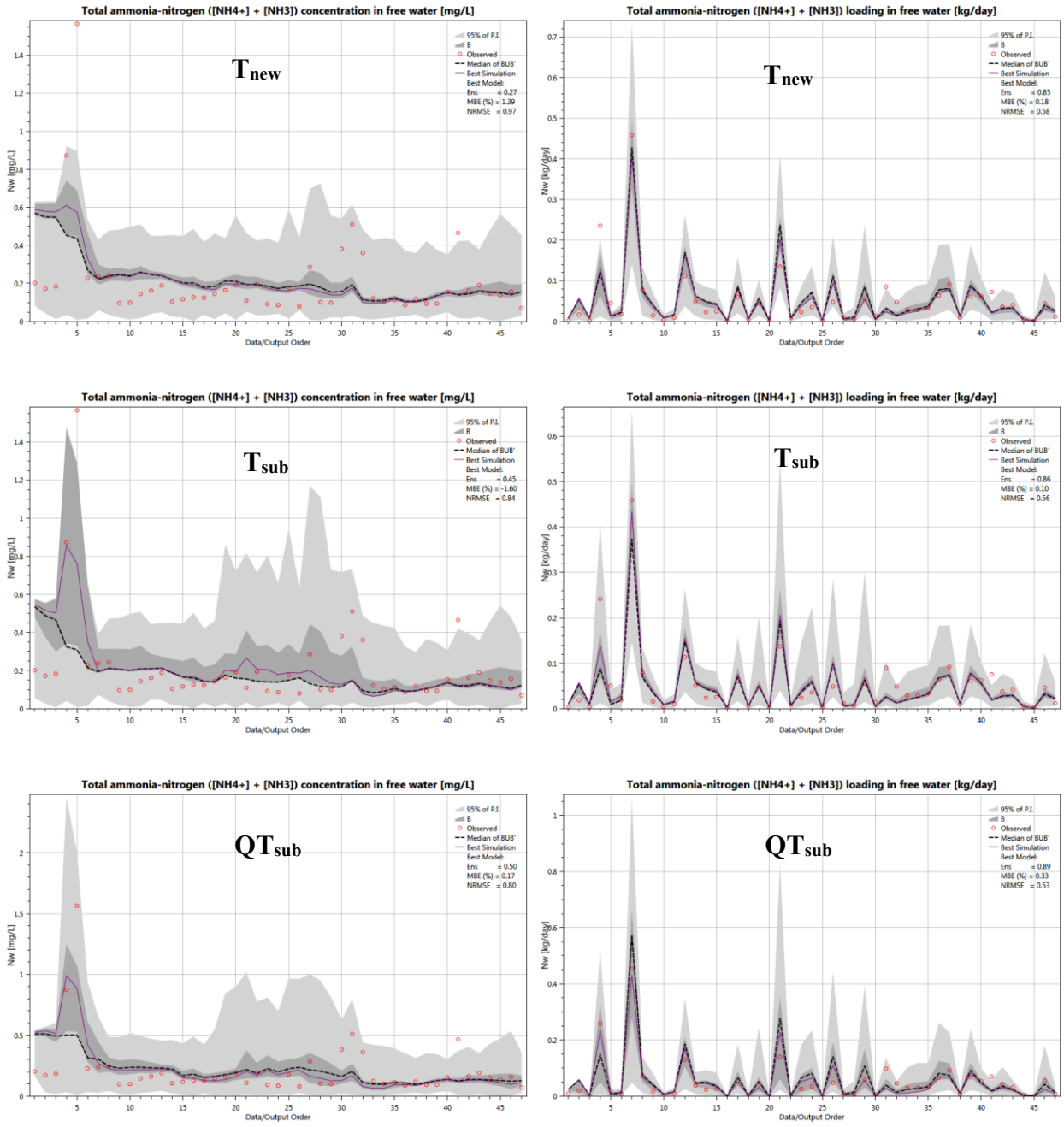

Figure 3.41. 95% prediction intervals (P.I) of all MC simulations, behavioral bands, and observed data for loads and concentrations of Nw for all three time resolution models.

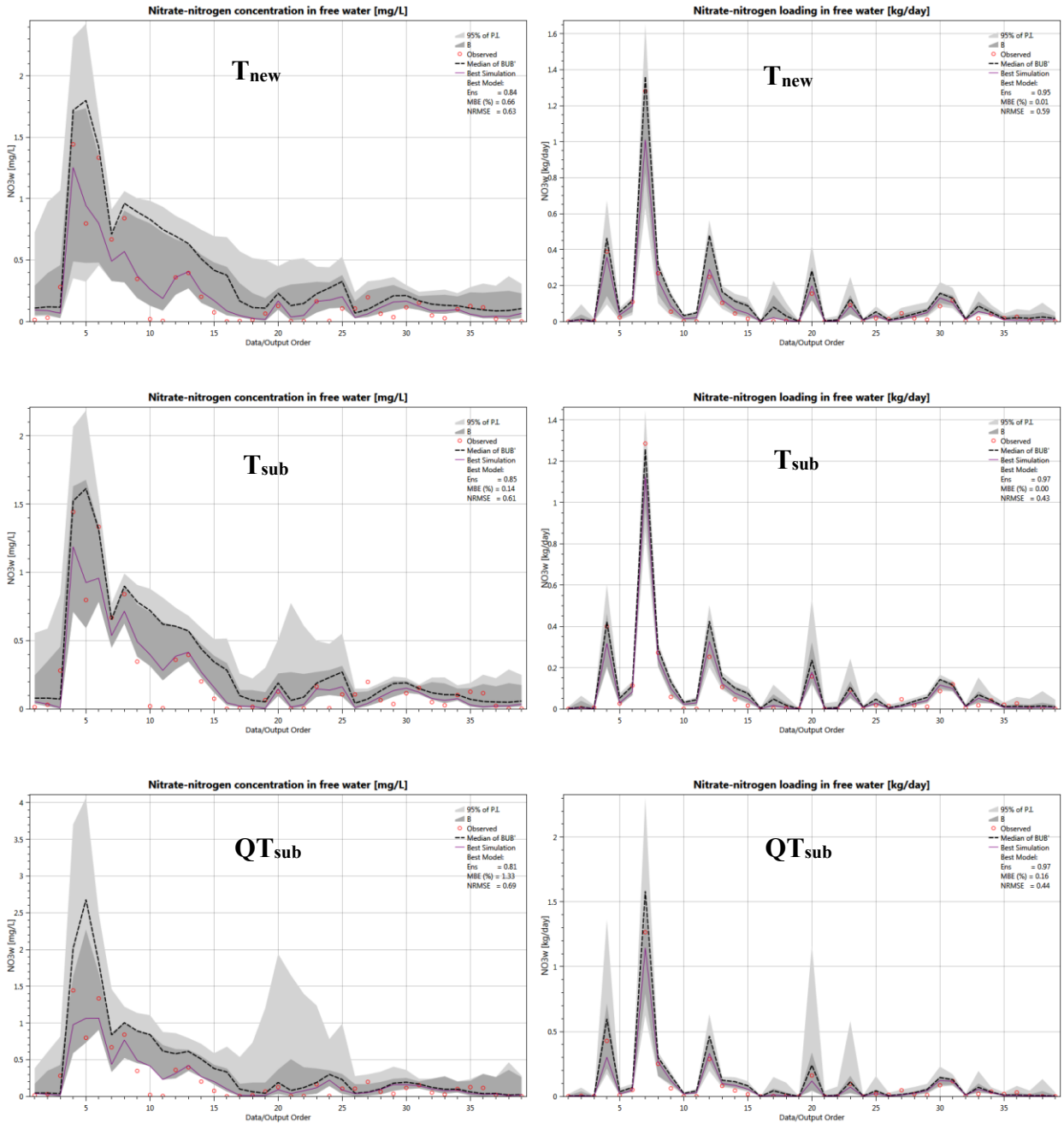

Figure 3.42. 95% prediction intervals (P.I) of all MC simulations, behavioral bands, and observed data for loads and concentrations of NO3w for all three time resolution models.

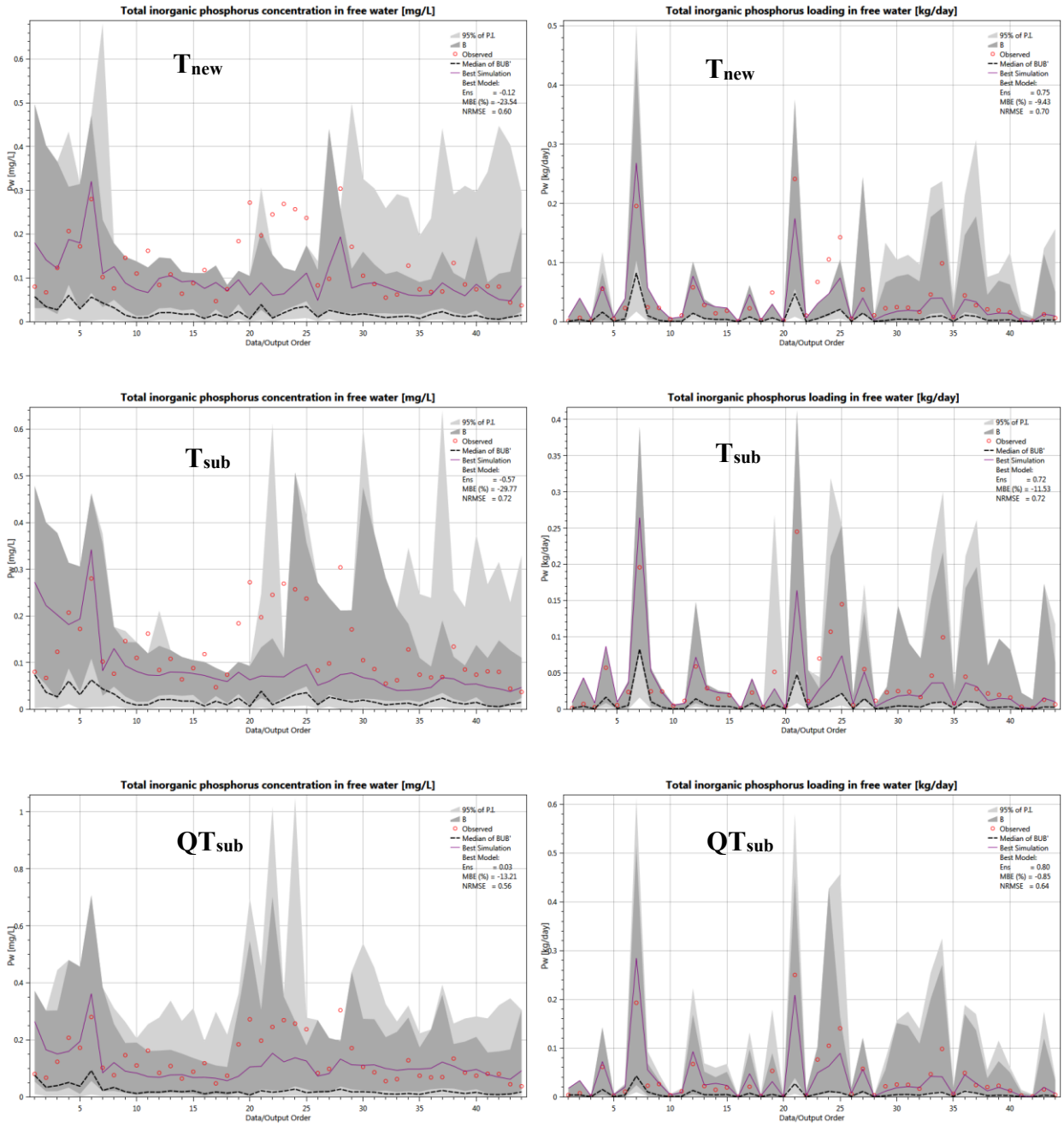

Figure 3.43. 95% prediction intervals (P.I) of all MC simulations, behavioral bands, and observed data for loads and concentrations of Pw for all three time resolution models.

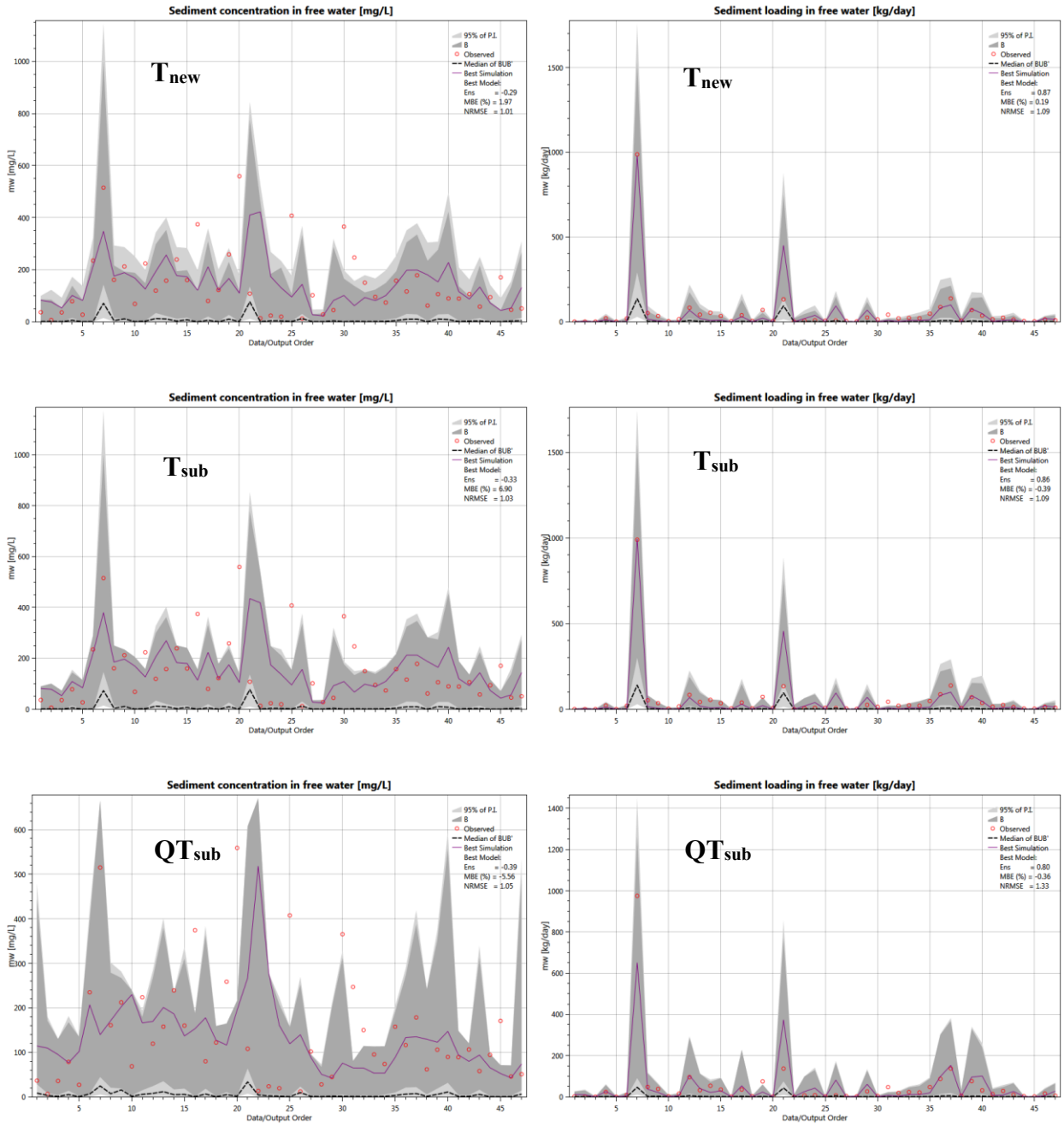

Figure 3.44. 95% prediction intervals (P.I) of all MC simulations, behavioral bands, and observed data for loads and concentrations of mw for all three time resolution models.

3.3.2 Sensitivity Analysis

The Kolmogorov-Smirnov (K-S) test was applied to identify the sensitive parameters for each of the three time resolution models. As explained before, the temperature data is in sub-daily temporal resolution for the T_{sub} model and temperature and inflow data are both in sub-daily temporal resolution for QT_{sub}.

3.3.2.1 Particulate Organic Nitrogen (ON_w)

The top sensitive parameters for T_{new} are *a_vr_o*, *porw*, *vels_o*, *ana*, and *L2*, in order (Figure 3.45). The results for T_{sub} are almost identical to T_{new}. The resuspension parameter *a_vr_o* stays as the most sensitive parameter for all applications. The settling velocity parameter *vels_o* becomes the second most sensitive parameter in QT_{sub} and the difference between this and the third sensitive parameter (*L2*) is significant. These results show that resuspension and settling of organic materials become the two dominant processes when the temporal resolution of inflow increases. On the other hand, *porw* has lost its magnitude of sensitivity when the inflow resolution was increased. It is interesting to see that sensitivity to *L2* gradually increased moving from T_{new} to QT_{sub}. This means that increasing the time resolutions of temperature and inflow data elevates the importance of the anaerobic soil layer thickness.

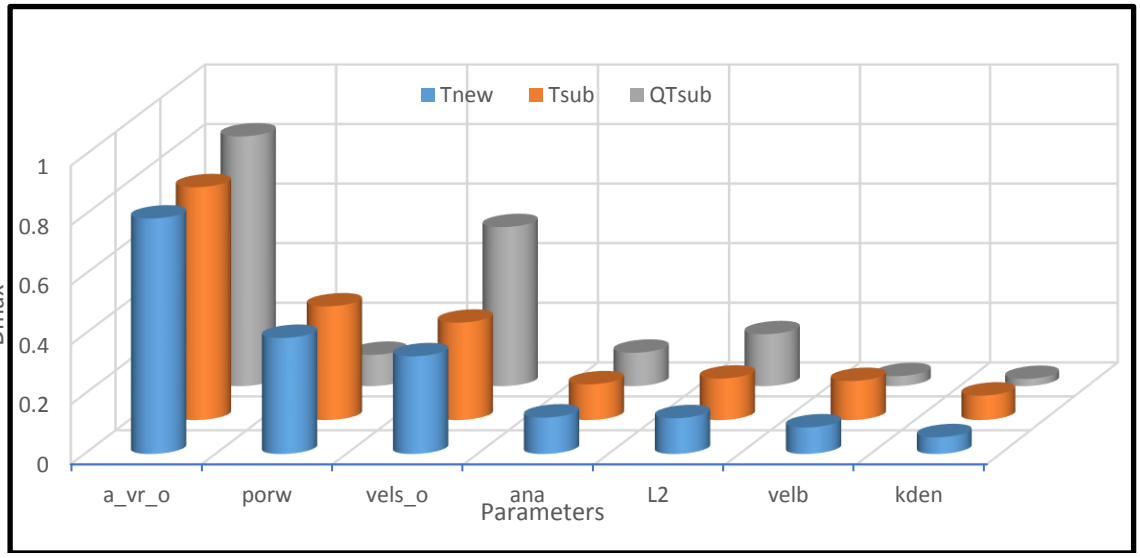

Figure 3.45. ON_w K-S test results for temporal resolution analysis.

To do detailed analysis with the most sensitive parameters *a_vr_o*, *porw*, *vels_o*, *L2*, and *ana* median and coefficient of variation (CV) values of these sensitive parameters were compared among all applications (Table 3.20). Between T_{new} and T_{sub}, median of the parameter values in the behavior set remains almost the same. There is some reduction in value of the resuspension parameter (12%). On the other hand, the median values of the resuspension and settling related parameters for QT_{sub} exhibit large deviations from the median values for T_{new} (59% and 101% increases, respectively). The increases in values of these parameter indicate that increasing the temporal resolution of inflow further raises the importance of these two processes. The CV values of parameters in behavior sets for T_{new} and T_{sub} are almost identical, while the values for QT_{sub} are all larger (e.g. 53% larger for *porw*, 18% larger for *a_vr_o*). To sum up, increasing the time resolution of temperature does not have much impact on ON_w processes, but changing temporal resolution of inflow has big impact on the sensitivity of model parameters. The PDFs of the most sensitive parameter shown in Figure 3.46 further support this conclusion.

Table 3.20. Median (*Mdn*) and coefficient of variations (*CV*) of the most sensitive parameters for ON_w under various temporal resolution analysis. Percent change indicates how a value has changed with respect to T_{new} values.

	BUB'		**T_{new}**		**T_{sub}**		**QT_{sub}**	
Parameter	***Mdn***	***CV***	***Mdn***	***CV***	***Mdn***	***CV***	***Mdn***	***CV***
a_vr_o	0.02	0.12	0.98	0.66	0.87	0.67	1.56	0.78
%change					*-12%*	*2%*	*59%*	*18%*
porw	0.80	0.0011	0.88	0.07	0.88	0.06	0.83	0.10
%change					*0%*	*-3%*	*-6%*	*53%*
vels_o	1.86	0.02	1.82	0.32	1.77	0.33	3.66	0.37
%change					*-3%*	*3%*	*101%*	*16%*
L2	27.5	0.0047	22.3	0.54	21.8	0.53	19.9	0.57
%change					*-2%*	*-1%*	*-11%*	*7%*
ana	10.5	0.0039	11.9	0.33	11.8	0.34	11.7	0.34
%change					*-1%*	*1%*	*-2%*	*2%*

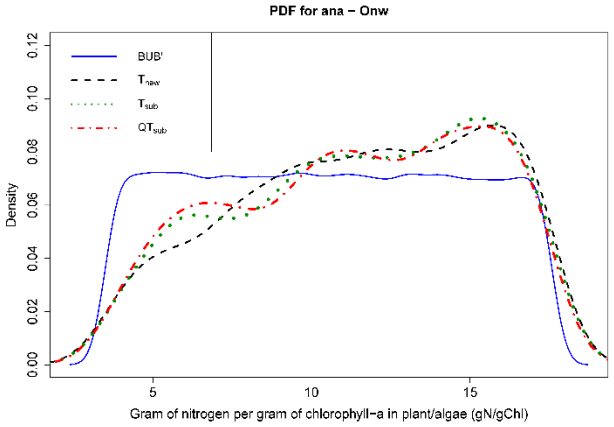

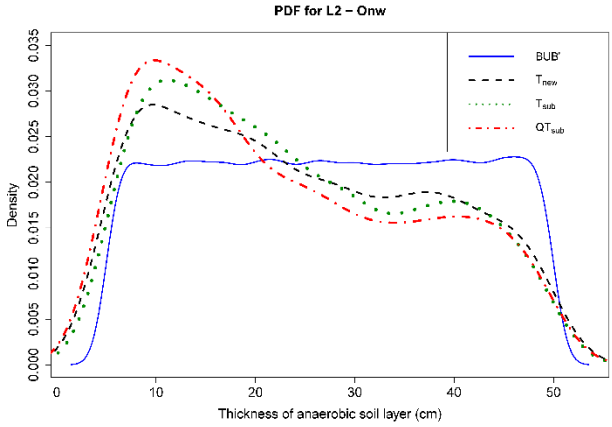

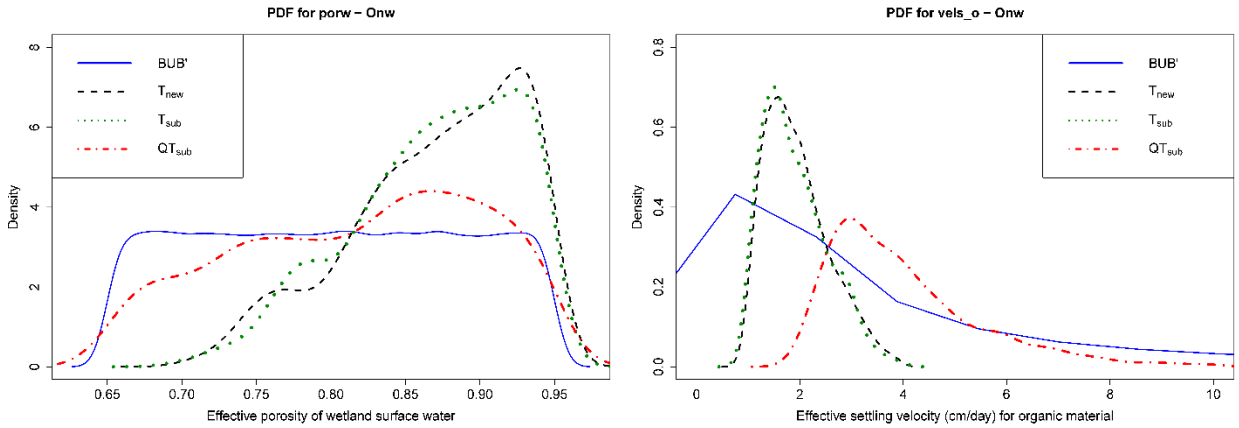

Figure 3.46. PDFs of the most sensitive parameters of ON_w for temporal resolution analysis.

3.3.2.2 Total Ammonia-Nitrogen ($[NH_4^+] + [NH_3]$) (N_w)

The most sensitive parameters of T_{new} for N_w are *fact*, *kd*, and *c2*. Figure 3.47 shows the K-S test results of the most sensitive parameters for N_w with bar chart that shows the D_{max} values having p-values lower than 0.05. Changing time resolution causes big fluctuations for sensitive parameters. The most sensitive parameters for T_{sub} are b_T, *c2*, *L2*, and *fact*, while the most sensitive parameters for QT_{sub} are *ana*, *L2*, *kd*, *kmin1s* and *knw*. In general, diffusive (*fact*) and adsorption (*kd*, *c2*) processes seem to lose their sensitivities with increased time resolution. Also, role of vegetation, mineralization and anaerobic layer thickness become highly sensitive when time resolution is increased.

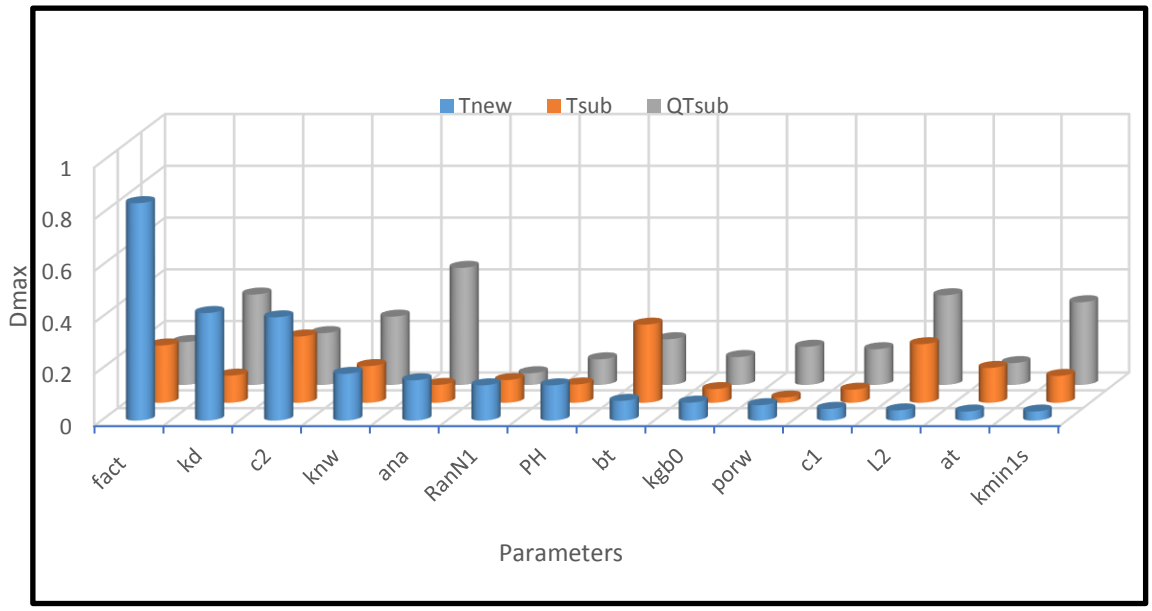

Figure 3.47. N_w K-S test results for temporal resolution analysis.

Table 3.21 compares the median and CV values of these sensitive parameters among the three applications for N_w. The median values of the behavior set parameters with T_{sub} and QT_{sub} show large deviations from the median values of the parameters with T_{new}. The differences are bigger with QT_{sub}. The biggest difference among the median values of the sensitive parameters is the change in nitrification parameter *knw* with a 267% increase with respect to its value in T_{new} while *knw* values for T_{sub} shows no difference. Comparison of CV values also show that the CV values for T_{new} and other two applications are completely different. With T_{sub}, CV values have all increased, except for one case. With QT_{sub}, they also mostly increased too, except for three cases. To sum up, changing the time resolution of temperature and the time resolution of temperature and inflow together have significant impacts on the sensitivity of parameters. The PDFs shown in Figure 3.48 portrays this situation clearly where shifts in parameter values and width of PDFs are highly noticeable.

Table 3.21. Median (*Mdn*) and Coefficient of Variation (*CV*) values of the top sensitive parameters of the behavior set (B) of N_w for temporal resolution analysis. Percent change indicate relative change with respect to values of T_{new}.

	BUB'		**T_{new}**		**T_{sub}**		**QT_{sub}**	
Parameter	***Mdn***	***CV***	***Mdn***	***CV***	***Mdn***	***CV***	***Mdn***	***CV***
fact	137	1.07	799	0.63	214	0.93	189	0.93
% change					*-73%*	*48%*	*-76%*	*47%*
kd	1.59	2.00	3.87	0.88	1.53	1.55	0.60	1.07
% change					*-60%*	*76%*	*-85%*	*22%*
c2	2456	0.29	3090	0.14	2951	0.23	2654	0.19
% change					*-4%*	*65%*	*-14%*	*42%*
knw	0.0059	2.25	0.0038	1.56	0.0038	1.87	0.0140	1.60
% change					*0%*	*19%*	*267%*	*2%*
bt	0.50	0.46	0.49	0.47	0.28	0.61	0.43	0.46
% change					*-42%*	*29%*	*-13%*	*-3%*
L2	27.5	0.47	26.0	0.48	18.3	0.58	14.4	0.61
% change					*-30%*	*22%*	*-45%*	*28%*
ana	10.5	0.39	8.55	0.43	10.0	0.38	15.1	0.18
% change					*17%*	*-11%*	*77%*	*-57%*
kmin1s	5.6E-05	2.06	5.7E-05	1.83	4.5E-05	1.88	2.2E-05	1.46
% change					*-21%*	*2%*	*-61%*	*-20%*

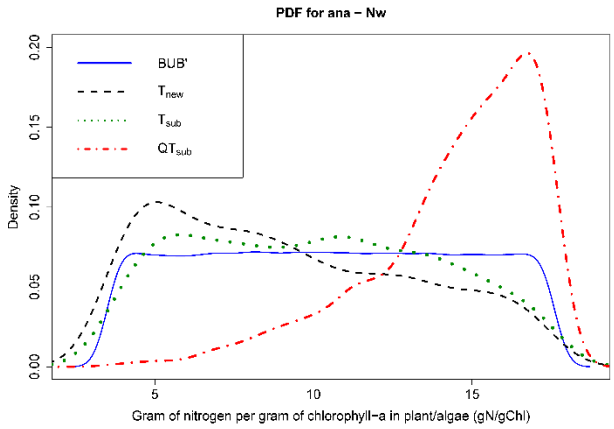
PDF for ana – Nw
BUB'
T_new
T_sub
QT_sub
Density
0.00
0.05
0.10
0.15
0.20
5
10
15
Gram of nitrogen per gram of chlorophyll-a in plant/algae (gN/gChl)

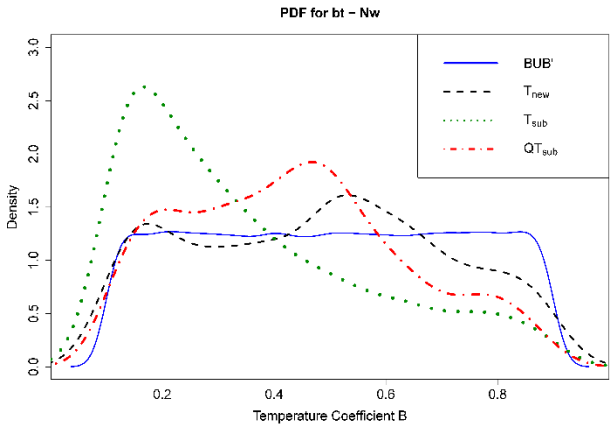
PDF for bt – Nw
BUB'
T_new
T_sub
QT_sub
Density
0.0
0.5
1.0
1.5
2.0
2.5
3.0
0.2
0.4
0.6
0.8
Temperature Coefficient B

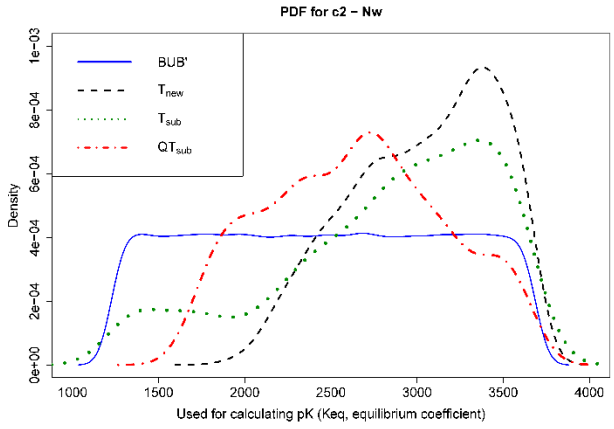
PDF for c2 – Nw
BUB'
T_new
T_sub
QT_sub
Density
0e+00
2e-04
4e-04
6e-04
8e-04
1e-03
1000
1500
2000
2500
3000
3500
4000
Used for calculating pK (Keq, equilibrium coefficient)

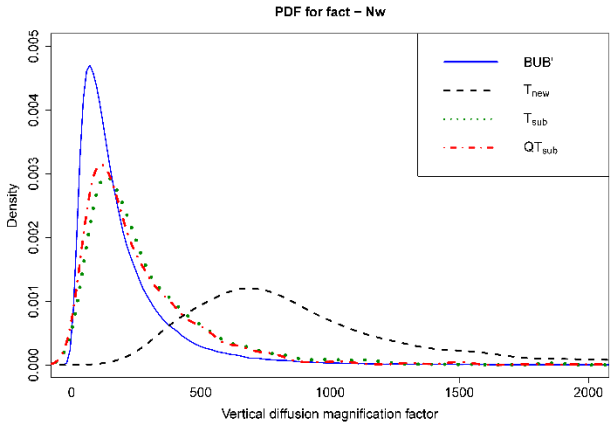
PDF for fact – Nw
BUB'
T_new
T_sub
QT_sub
Density
0.000
0.001
0.002
0.003
0.004
0.005
0
500
1000
1500
2000
Vertical diffusion magnification factor

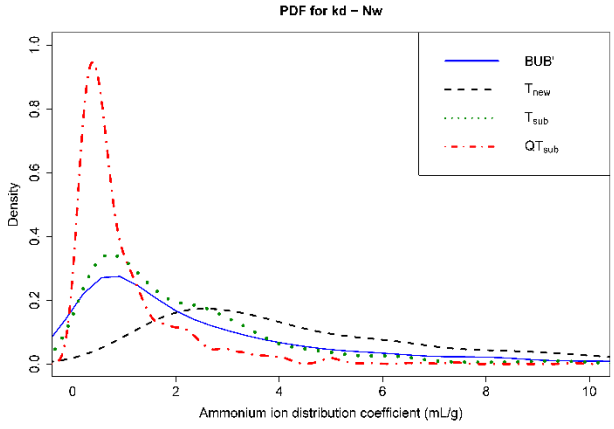
PDF for kd – Nw
BUB'
T_new
T_sub
QT_sub
Density
0.0
0.2
0.4
0.6
0.8
1.0
0
2
4
6
8
10
Ammonium ion distribution coefficient (mL/g)

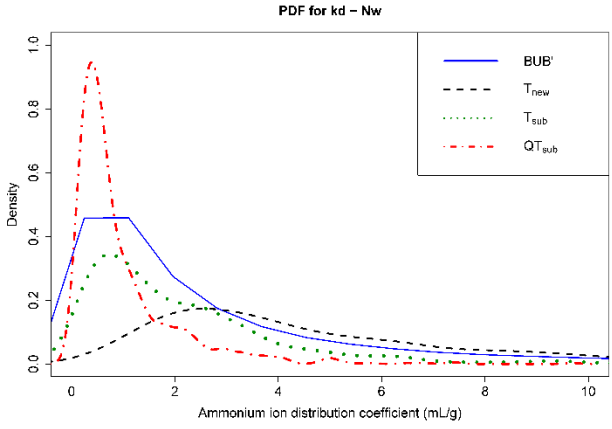
PDF for kd – Nw
BUB'
T_new
T_sub
QT_sub
Density
0.0
0.2
0.4
0.6
0.8
1.0
0
2
4
6
8
10
Ammonium ion distribution coefficient (mL/g)

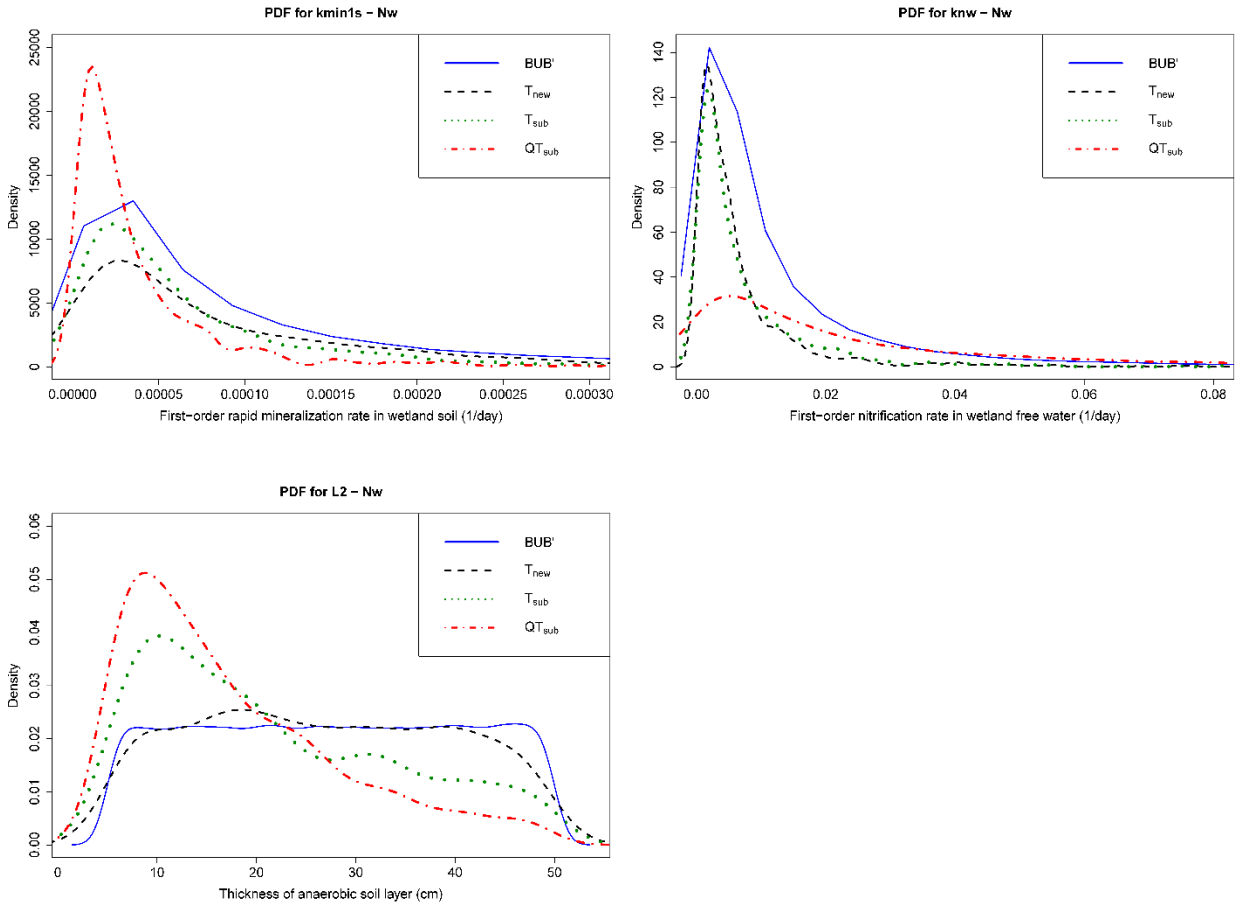

Figure 3.48. PDFs of the most sensitive parameters of N_w for temporal resolution analysis.

3.3.2.3 Nitrate-Nitrogen (NO_{3w})

The most sensitive parameters of T_{new} for NO_{3w} are *ana*, *c2*, *kgb0*, *porw*, *pH*, *fact*, a_T, b_T and k_{den}. Figure 3.49 shows the K-S test results for NO_{3w} with bar chart that shows the D_{max} values having p-values lower than 0.05. Changing time resolution causes massive fluctuations for order and strength of sensitive parameters. The most sensitive parameters for T_{sub}, in order, are b_T, *porw*, *fact*, *kden*, *L2*, and a_T, while the most sensitive parameters for QTsub are b_T, *ana*, *kden*, a_T, *porw*, and *fact*. In general, vegetation effect (*ana*, *kgb0*) and *pH* parameters seem to lose their sensitivities with increased time resolution. Also, temperature conversion equation's coefficients, nitrification and denitrification processes became highly sensitive when the time resolution increased.

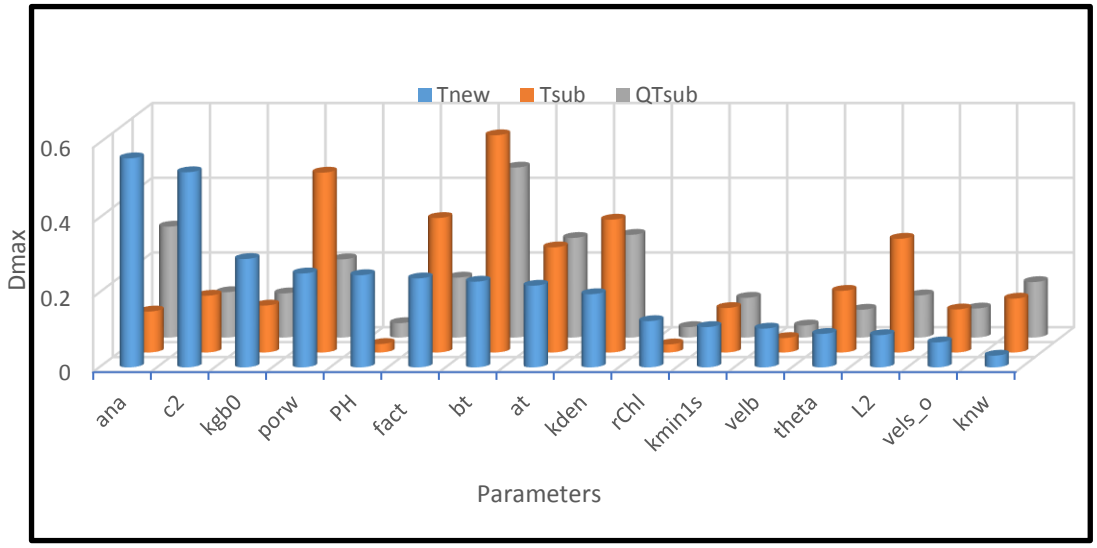

Figure 3.49. NO_{3w} K-S test results for temporal resolution analysis

Table 3.22 compares the median and CV values of these sensitive parameters among the three applications for NO_{3w}. The median values of the behavior set parameters with T_{sub} and QT_{sub} show large deviations from the median values of the parameters with T_{new}. The differences are slightly bigger with T_{sub}. The biggest difference among the median values of the sensitive parameters is the change in *c2* parameter with a 35% increase with respect to its value in T_{new} while *c2* values for T_{sub} shows 32% increase. Comparison of CV values also show that the CV values for T_{new} and other two applications are highly different. The biggest difference among the CV values of the sensitive parameters is the change in *ana* with a 197% increase with respect to its value in T_{new} while *ana* values for QT_{sub} shows 142% difference. To sum up, changing the time resolution of temperature and the time resolution of temperature and inflow together have significant impacts on the sensitivity of parameters. The PDFs shown in Figure 3.50 portrays this situation clearly where shifts in parameter values and width of PDFs are very clear.

Table 3.22. Median (*Mdn*) and coefficient of variations (*CV*) of the most sensitive parameters for NO_{3w} under various temporal resolution analysis. Percent change indicates how a value has changed with respect to T_{new} values.

	BUB'		**T_{new}**		**T_{sub}**		**QT_{sub}**	
Parameter	***Mdn***	***CV***	***Mdn***	***CV***	***Mdn***	***CV***	***Mdn***	***CV***
ana	10.54	0.39	15.7	0.12	11.9	0.35	14.2	0.29
% change					*-25%*	*197%*	*-9%*	*142%*
c2	2456	0.29	1629	0.23	2154	0.33	2193	0.32
% change					*32%*	*44%*	*35%*	*39%*
kgb0	0.0013	0.13	0.0015	0.13	0.0014	0.12	0.0014	0.12
% change					*-6%*	*-9%*	*-5%*	*-2%*
porw	0.80	0.11	0.74	0.10	0.70	0.07	0.75	0.10
% change					*-6%*	*-29%*	*1%*	*2%*
PH	6.34	0.17	7.07	0.13	6.38	0.17	6.45	0.16
% change					*-10%*	*30%*	*-9%*	*27%*
fact	137	1.07	181	0.60	216	0.56	137	0.70
% change					*19%*	*-7%*	*-25%*	*16%*
at	5.50	0.47	7.14	0.35	7.53	0.30	7.37	0.32
% change					*5%*	*-16%*	*3%*	*-10%*
bt	0.50	0.46	0.64	0.33	0.80	0.13	0.77	0.19
% change					*25%*	*-61%*	*20%*	*-41%*

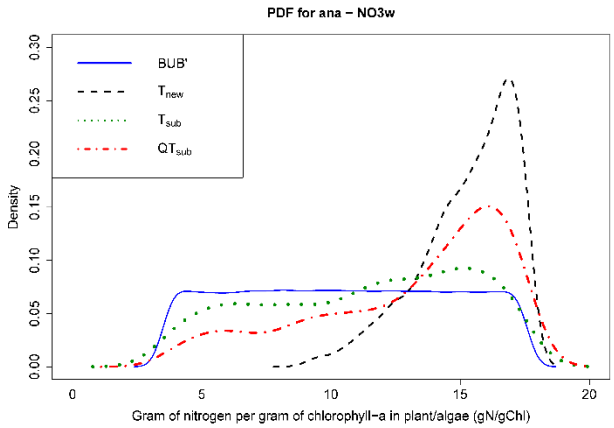
PDF for ana – NO3w
BUB'
T_new
T_sub
QT_sub
Density
Gram of nitrogen per gram of chlorophyll-a in plant/algae (gN/gChl)

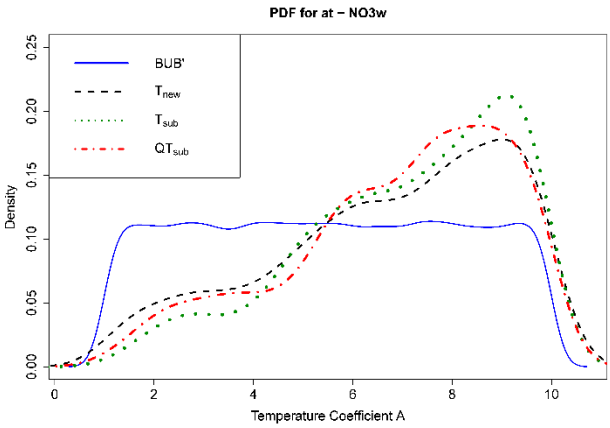
PDF for at – NO3w
BUB'
T_new
T_sub
QT_sub
Density
Temperature Coefficient A

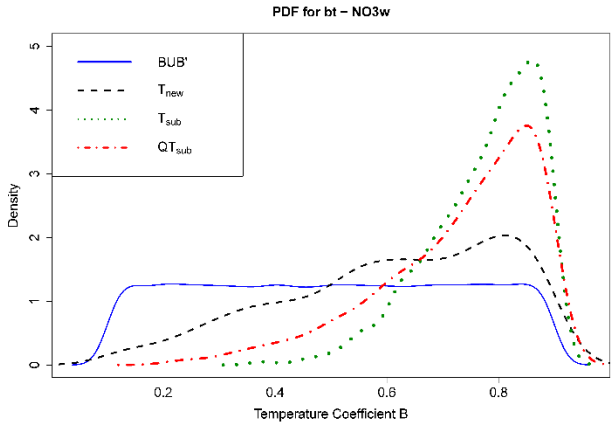
PDF for bt – NO3w
BUB'
T_new
T_sub
QT_sub
Density
Temperature Coefficient B

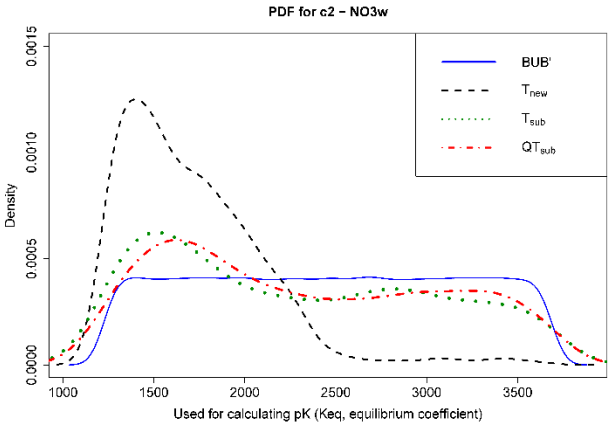
PDF for c2 – NO3w
BUB'
T_new
T_sub
QT_sub
Density
Used for calculating pK (Keq, equilibrium coefficient)

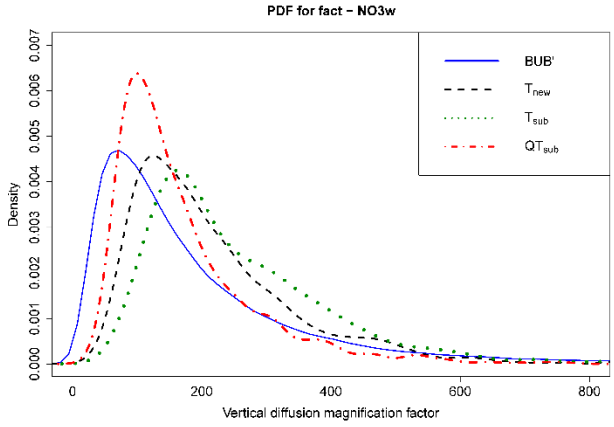
PDF for fact – NO3w
BUB'
T_new
T_sub
QT_sub
Density
Vertical diffusion magnification factor

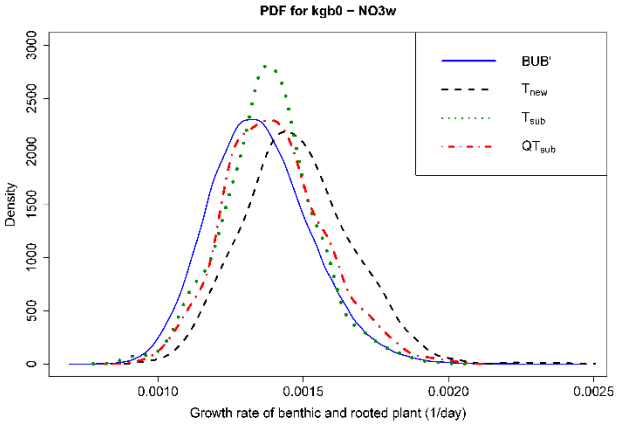
PDF for kgb0 – NO3w
BUB'
T_new
T_sub
QT_sub
Density
Growth rate of benthic and rooted plant (1/day)

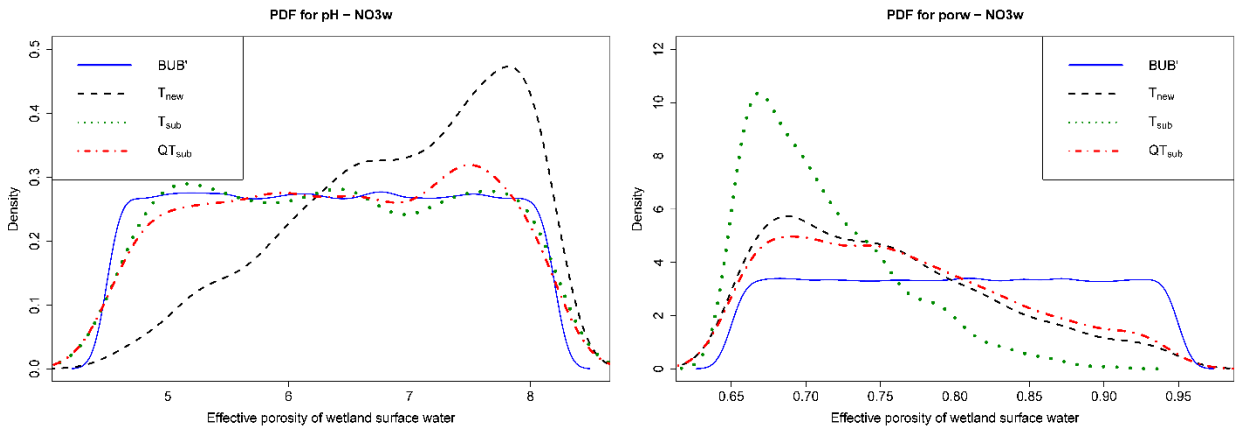

Figure 3.50. PDFs of the most sensitive parameters of NO_{3w} for temporal resolution analysis.

3.3.2.4 Total Inorganic Phosphorous (P_w)

The top sensitive parameters for T_{new} are *Kw*, *fact*, *vels_s*, *porw*, and *a_vr_s*, in order (Figure 3.51). The results for T_{sub} are almost identical to T_{new}. Phosphorous sorption parameter *Kw and* diffusion parameter *fact* stay as the most sensitive parameters for all applications and these parameters see increase in their magnitude of sensitivity when time resolution of inflow increases. The settling velocity parameter *vels_s* becomes less sensitive in QT_{sub}.

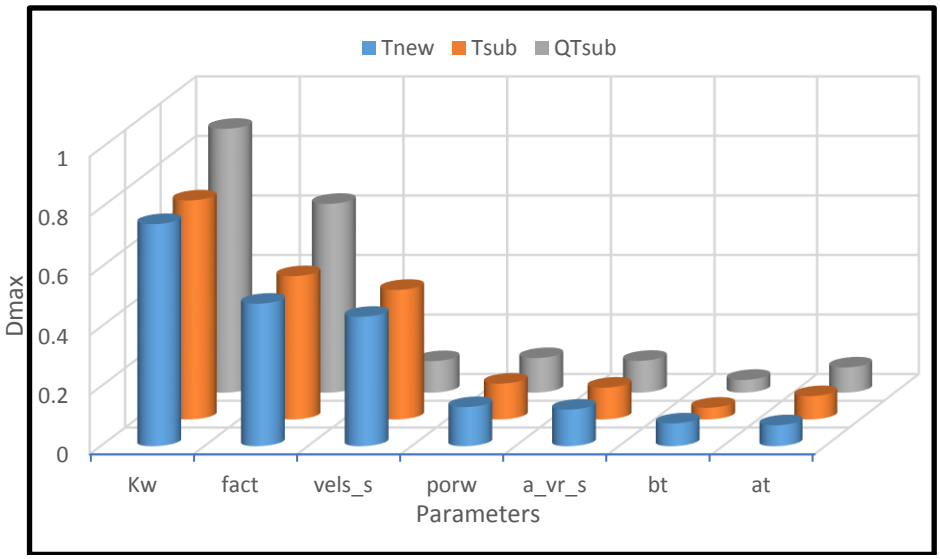

Figure 3.51. P_w K-S test results for temporal resolution analysis.

To do detailed analysis with the most sensitive parameters *Kw*, *fact*, *vels_s*, and *porw*, median and CV values of these sensitive parameters were compared among all applications for P_w (Table 3.23). Between T_{new} and T_{sub}, median of the parameter values in the behavior set remains almost the same. There is some reduction in value of the settling parameter (13%). On the other hand, the median values of the diffusion and settling related parameters for QT_{sub} exhibit large deviations from the median values for T_{new} (23% reduction and 168% increases, respectively). The changes in values of these parameter indicate that increasing the temporal resolution of inflow amplify the importance of these two processes. The CV values of parameters in behavior sets for all applications are almost identical for sorption parameter while the CV values of other parameters are completely different. The largest deviations from CV values is 37% reduction for diffusion parameter in QT_{sub}. To sum up, increasing the time resolution of temperature does not have much impact on P_w processes, but changing temporal resolution of inflow has big impact on the sensitivity of model parameters. The PDFs of the most sensitive parameter shown in Figure 3.52 further support this conclusion.

Table 3.23. Medians (*Mdn*) and coefficient of variations (*CV*) of the most sensitive parameters for P_w under various temporal resolution analysis. Percent change indicates how a value has changed with respect to T_{new} values.

	BUB'		**T_{new}**		**T_{sub}**		**QT_{sub}**	
Parameter	***Mdn***	***CV***	***Mdn***	***CV***	***Mdn***	***CV***	***Mdn***	***CV***
Kw	34883	1.65	3276	2.66	3344	2.77	3255	2.74
% change					*2%*	*4%*	*-1%*	*3%*
fact	137	1.07	56.4	0.90	57.5	0.68	43.7	0.57
% change					*2%*	*-24%*	*-23%*	*-37%*
vels_s	232	1.49	66.8	2.08	57.9	2.07	179	1.53
% change					*-13%*	*-1%*	*168%*	*-27%*

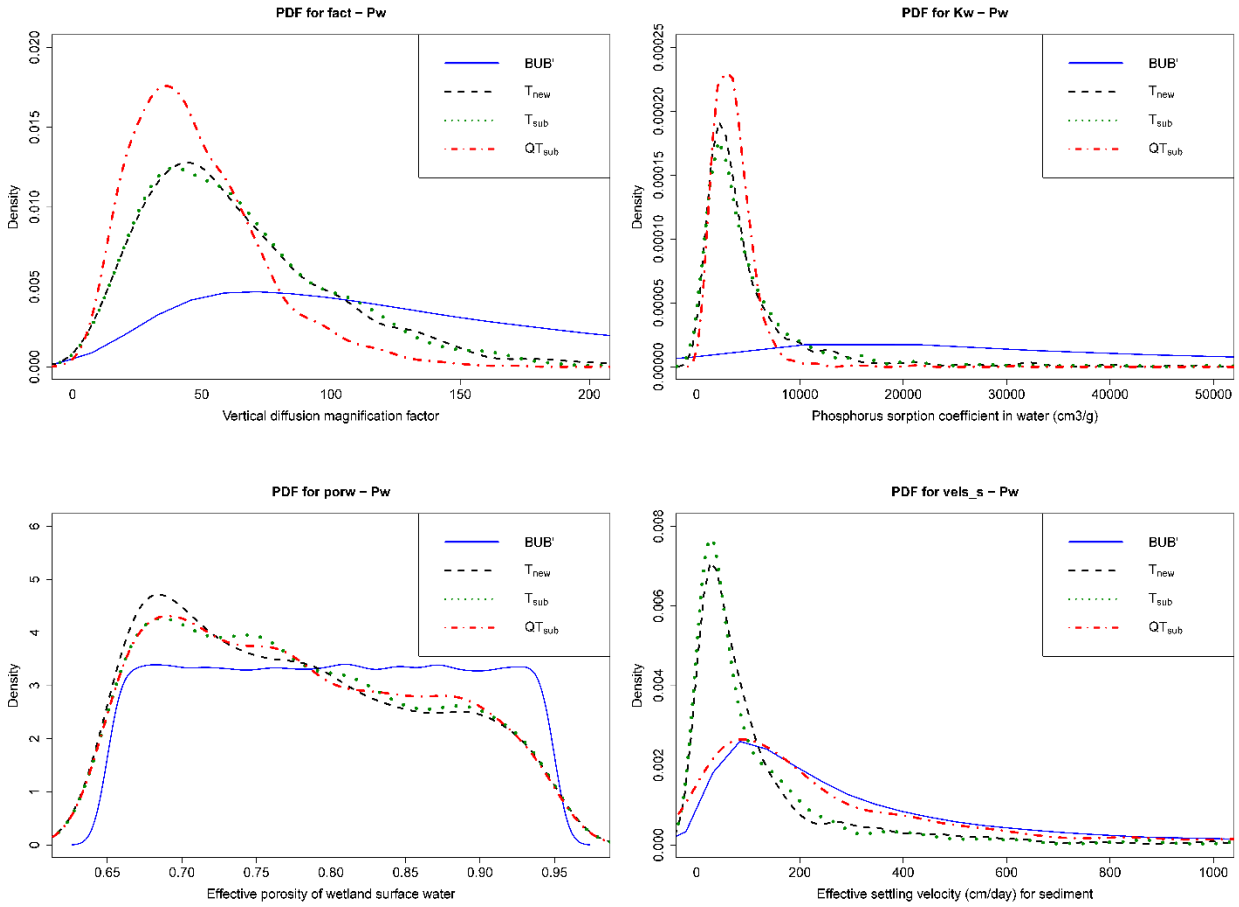

Figure 3.52. PDFs of the most sensitive parameters of Pw for temporal resolution analysis.

3.3.2.5 Sediment (m_w)

The top sensitive parameters for T_{new} are *a_vr_s*, *vels_s*, and *RanN1*, in order (Figure 3.53). There are no noticeable shifts among the sensitive parameters in all three applications.

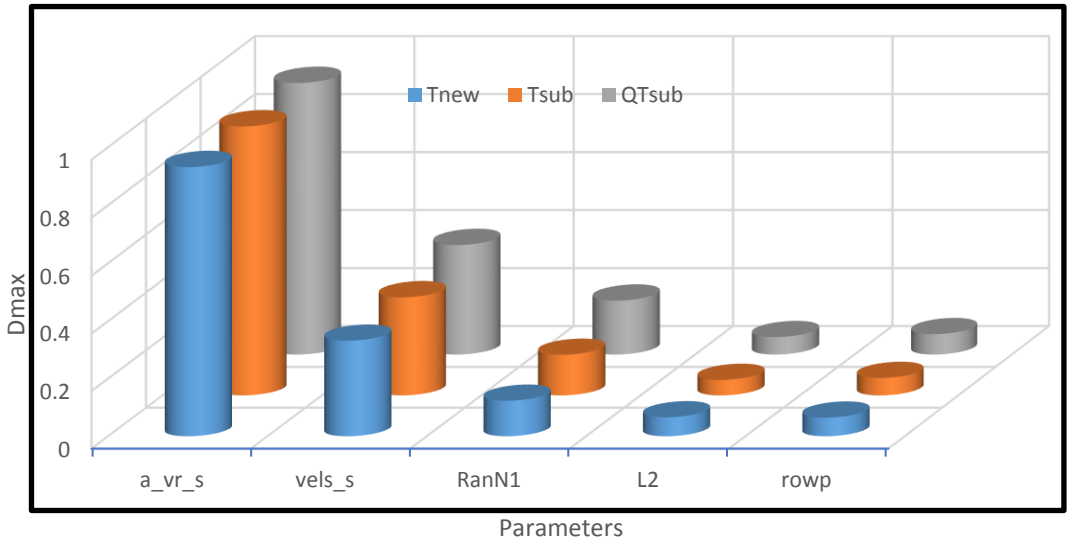

Figure 3.53. m_w K-S test results for temporal resolution analysis.

To do detailed analysis with the most sensitive parameters, *a_vr_s*, *vels_s*, and *RanN1*, median and CV values of these sensitive parameters were compared among all applications (Table 3.24). Between T_{new} and T_{sub}, median of the parameter values in the behavior set remains almost the same. There is some reduction in value of the resuspension parameter (9%). On the other hand, the median values of the resuspension and settling related parameters for QT_{sub} exhibit large deviations from the median values for T_{new} (48% increase and 13% reduction, respectively). The CV values do not vary much among the three models. To sum up, increasing the time resolution of temperature does not have much impact on m_w processes, but changing temporal resolution of inflow has small impact on the sensitivity of model parameters. The PDFs of the most sensitive parameter shown in Figure 3.54 further support this conclusion.

Table 3.24. Medians (*Mdn*) and coefficient of variations (*CV*) of the most sensitive parameters for m_w under various temporal resolution analysis. Percent change indicates how a value has changed with respect to T_{new} values.

	BUB'		**T_{new}**		**T_{sub}**		**QT_{sub}**	
Parameter	***Mdn***	***CV***	***Mdn***	***CV***	***Mdn***	***CV***	***Mdn***	***CV***
a_vr_s	0.002	5.18	0.09	0.87	0.08	0.97	0.13	0.90
% change					*-9%*	*11%*	*48%*	*3%*
vels_s	232	1.49	111	0.99	110	0.98	95.8	1.07
% change					*-1%*	*-1%*	*-13%*	*8%*
RanN1	0.50	0.58	0.39	0.65	0.38	0.66	0.32	0.72
% change					*-3%*	*1%*	*-17%*	*10%*

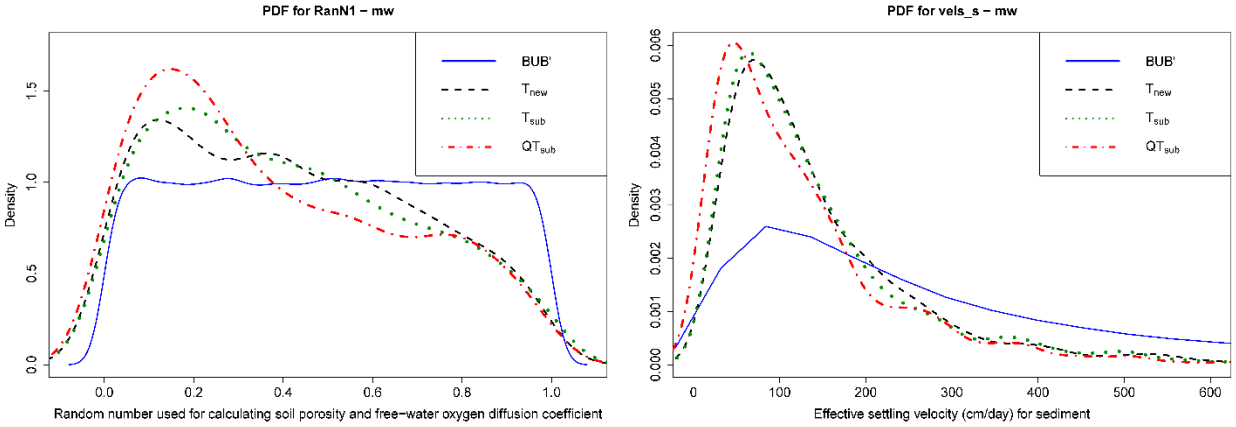

Figure 3.54. PDFs of the most sensitive parameters of m_w for temporal resolution analysis.

4 SUMMARY AND CONCLUSIONS

Wetlands are natural water purifiers treating nutrients and sediments from incoming runoff. However, their functioning can be influenced by many factors such as climate change and anthropogenic activities. Understanding their behavior under these stressors require a modeling approach because performing experiments by modifying real systems is not only expensive, but also time consuming and sometime an impossible task. The physically-based wetland water quality model WetQual is one such model in simulating nitrogen, phosphorus, carbon and sediment dynamics in real and constructed wetlands. WetQual requires input data at varying levels of complexities. In this study, the sensitivity of WetQual to three important inputs were explored in detail, which were bathymetry, temperature, and temporal resolution. Below, summary of those findings and the general conclusions that can be drawn from those findings are presented.

Bathymetry Analysis

Here we tested the implications of simplified wetland bathymetries on accuracy of model predictions and the associated uncertainties. Through sensitivity analysis, we also checked whether the use of simplified shapes leads to changes in dominant model processes. Results showed that even with a highly different profile one can achieve good model performances after calibration. On the other hand, calibration with a wrong bathymetry profile can lead to model parameters that are not representative of the real system. Results showed that the assumed profile based on fourth degree polynomial captured the actual wetland profile reasonably well, and thus had similar

loading and uncertainty estimates. Model predictive uncertainties based on the profile $W_{0.5}$ showed the largest difference compared to results from the actual profile. The overall order of similarity from highest to lowest with actual wetland was W_4, W_2, W_1 and $W_{0.5}$.

In Table 4.1, the similarities between actual wetland and synthetic wetlands are shown for each constituents based on the predictive uncertainties they resulted in (*r-factor* was used). Overall, W_4 wetland has the highest similarity to the actual wetland based on loads. This means that the profile of W_4 can be comfortably used if bathymetry information of the actual wetland is not available. For constituent concentrations, W_1 wetland can be the best option to use bathymetry instead of the actual wetland for ON_w and N_w concentrations. W_2 wetland can be the best option for P_w and m_w concentrations and W_4 wetland can be the best option for NO_{3w} concentration. Even though it produced good model performance, model predictive uncertainties based on $W_{0.5}$ are highly different than the ones based on the actual wetland.

Table 4.1. Summary of similarities based on uncertainty analysis. The level of similarities are graded as "+", "++", "+++", and "++++", where "+" means least similar, and "++++" means almost identical.

Wetland	**ON_w**		**N_w**		**NO_{3w}**		**P_w**		**m_w**	
	Conc	**Load**	**Conc**	**Load**	**Conc**	**Load**	**Conc**	**Load**	**Conc**	**Load**
$W_{0.5}$	+	+	+	+++	+	+	+	+	+	+
W_1	**++++**	++	**++++**	+	++	++	++	**++++**	++	++
W_2	+++	+++	+++	++	+++	+++	**++++**	++	**++++**	+++
W_4	++	**++++**	++	**++++**	**++++**	**++++**	+++	+++	+++	**++++**

Sensitivity analysis highlighted the important/dominant processes in the studied wetland. Resuspension and settling processes were the primary drivers and vegetation effects were the secondary drivers for organic nitrogen for all wetlands except $W_{0.5}$. Effect of vegetation became more prevalent with $W_{0.5}$. For organic nitrogen, W_2 wetland was more similar to the actual wetland.

Diffusion was the most important process for all wetlands for total ammonia. Temperature, adsorption and nitrification processes were also important drivers for total ammonia for all wetlands. However, the importance of adsorption increased for $W_{0.5}$, W_2, and W_1 wetlands. With $W_{0.5}$, nitrification became almost an insignificant process, and conversely mineralization became a dominant process. For total ammonia, W_4 wetland had the highest similarity to the actual wetland.

Plant effects, temperature and denitrification processes were the most important processes for nitrate for W_A, W_2, and W_4 wetlands, but diffusion was the main driver for $W_{0.5}$ and W_1 wetlands. The importance of temperature and denitrification decreased dramatically for $W_{0.5}$. For nitrate, W_4 wetland again had the highest level of similarity to the actual wetland.

Phosphorus sorption, diffusion and settling were the most sensitive processes for inorganic phosphorous. Settling became more important for $W_{0.5}$ and W_2 wetlands while sorption became less important for these wetlands. For inorganic phosphorus all profiles look acceptable based on sensitivity results.

Similar to organic nitrogen, sediment was sensitive to resuspension and settling processes. All the wetlands were by far most sensitive to the resuspension process and followed by the settling process. Resuspension was the most sensitive parameters because it can be affected by runoff forces. Based on sensitivity results, all profiles are acceptable.

Table 4.2 shows the similarities between the actual wetland and synthetic wetlands based on sensitivity analysis. The bathymetric profile of W_1 wetland can be used instead of actual wetland for P_w loadings when working on parameter sensitivity. For the dominant processes of the On_w and NO_{3w} loadings, W_2 wetland can be used instead of actual wetland. In addition, the bathymetric profile of W_4 wetland can be the best option for analyzing sensitive processes when

there is scant information about actual wetland bathymetry for N_w and m_w loadings. For sediment, all profiles look acceptable.

Table 4.2. Summary of similarities based on sensitivity analysis. The level of similarities are graded as "+", "++", "+++", and "++++", where "+" means least similar, and "++++" means almost identical.

Wetland	ON_w	N_w	NO_{3w}	P_w	m_w
$W_{0.5}$	+	+	+	+	**++++**
W_1	++	++	++	**++++**	**++++**
W_2	**++++**	+++	**++++**	+++	**++++**
W_4	+++	**++++**	+++	++	**++++**

In summary, after calibration one can achieve similar level of model performances with most assumed wetlands profiles. However, the calibrated model parameters and the associated processes can end up being highly different for profiles that deviate significantly from the actual profile.

Temperature analysis

Relaxing the temperature conversion equation's coefficients did not make any difference in model performances. It did not affect the predicted uncertainty of organic nitrogen, total ammonia and sediment loads, but led to reduction of the uncertainty of inorganic phosphorus loads and increased the uncertainty of nitrogen loading. As far as concentrations are concerned, there was a decrease in the uncertainty of total ammonia and an increase in uncertainty of nitrate.

The changes in temperature conversion equation's coefficients did not have impact on the sensitivity of the model processes for organic nitrogen, inorganic phosphorus, and sediment. Temperature played the most critical role on nitrate, where temperature conversion equation's coefficients were among the sensitive parameters. Denitrification and anaerobic soil layer thickness became less sensitive. For total ammonia, nitrification process became a less important

process after changes in coefficients of temperature conversion equation. However, the order of sensitive parameters did not change significantly.

Temperature conversion equation had bigger impact on individual years. The order of sensitive parameters changed by years. Resuspension process was more important than settling process in the year 2 while it was the opposite in year 1 for organic nitrogen. Vegetation effects represented by *porw* and *ana* parameters were more important for year 1. For total ammonia, the effect of temperature was more important for year 2. Adsorption, diffusion and nitrification processes were more important for year 1 while vegetation and temperature were more important for year 2. Similar to total ammonia, temperature became more important for year 2 for nitrate. Opposite to total ammonia, diffusion process was more important for year 2. Soil porosity and the thickness of anaerobic soil layer were more important for year 1. There were no remarkable changes in the sensitive parameter rankings of inorganic phosphorus and sediment when individual years were compared. This interannual analysis clearly shows that WetQual can benefit from relaxing the temperature equation coefficients.

Temporal resolution analysis

Changing the time resolution of temperature data did not change the model performance. When inflow data was provided in sub-daily form, model performance significantly improved for ONw, but surprisingly deteriorated for m_w although both are particulate matter. The sediment component of WetQual is simple, thus the result for sediment may indicate the need for improvement. Model performances were insensitive to these changes for total ammonia, nitrate and phosphorous. One can conclude that these changes in the model affect model performances in particulate forms (positively or not), but not the dissolved forms.

Results showed that increasing temporal resolution of temperature and inflow together caused higher uncertainties in predicted pollutant loadings. On the other hand, increasing temporal resolution of temperature resulted in reduced uncertainties of total ammonia and nitrate load predictions. This means that the two pollutants which were affected most by temperature responded well to the increase in temporal resolution of temperature.

Changing the temporal resolution of input forcings revealed different trends among the important processes. Sediment was not affected by temporal resolution of input forcings while others were affected significantly.

For organic nitrogen, increasing the temporal resolution of temperature and inflow together made resuspension and settling processes more important while soil porosity became less sensitive. The thickness of the anaerobic soil layer became more important when the temporal resolution of input forcings has increased.

For total ammonia, temperature conversion equation's coefficients, mineralization rate and anaerobic soil thickness became more important with increased temporal resolution. However, diffusion and adsorption processes became less sensitive. Although vegetation did not seem to play a critical role on ammonia cycling when temporal resolution of temperature was increased, increasing the temporal resolution of temperature and inflow together made vegetation an important player.

Changing the temporal resolution of temperature only made more differences than changing temporal resolution of temperature and inflow together for nitrate. There were big differences in rankings of sensitive parameters when higher temporal resolution was used in temperature. For instance, importance of vegetation almost disappeared, and the coefficients of the new temperature conversion equation became highly sensitive.

The importance of phosphorus sorption and diffusion processes rose when temporal resolution of temperature and inflow were both increased. On the contrary, importance of settling process dropped significantly with increased temporal resolution of temperature and inflow together.

In summary, increasing the temporal resolution of temperature and input forcings improves the model performances and helps in dominant processes represented better.

Study Limitations:

While this study contributes to better understanding of how wetland processes respond to changes in model inputs, it has limitations preventing the results to be generalized. First of all, the dominant processes can vary by wetlands. The results from this study can be much more meaningful in wetlands similar to the Barnstable wetland. Secondly, we used two years of data in all the analysis. Although there were differences in the hydrology of the two years, this is still a short-duration. On the other hand, we need to acknowledge that finding long-term water quality data from wetlands is not easy.

REFERENCES

Ahmadi-Nedushan, B., St-Hilaire, A., Ouarda, T., Bilodeau, L., Robichaud, É., Thiémonge, N., & Bobée, B. (2007). Predicting river water temperatures using stochastic models: case study of the Moisie River (Québec, Canada). *Hydrological Processes*, *21*(1), 21–34. https://doi.org/10.1002/hyp.6353

An, S., Li, H., Guan, B., Zhou, C., Wang, Z., Deng, Z., … Li, H. (2007). China's natural wetlands: past problems, current status, and future challenges. *Ambio. Vol. 36(4): 335-341*.

Beven, K. and Binley, A. (1992). The future of distributed models: Model calibration and uncertainty prediction. *Hydrol. Process*.

Beven, K., & Freer, J. (2001). Equifinality, data assimilation, and uncertainty estimation in mechanistic modelling of complex environmental systems using the GLUE methodology. *Journal of Hydrology*, *249*(1–4), 11–29. https://doi.org/10.1016/S0022-1694(01)00421-8

Caissie, D. (2006). The thermal regime of rivers: a review. *Freshwater Biology*, *51*(8), 1389–1406. https://doi.org/10.1111/j.1365-2427.2006.01597.x

Castaneda, C., & Garcia-Vera, M. A. (2008). *Water balance in the playa-lakes of an arid environment, Monegros, NE Spain*.

Dahl, T. E. (1990). *Wetland losses in the United States 1780's to 1980's*. Washington, DC.

Dankers, R., & Christensen, O. (2005). Climate Change Impact on Snow Coverage, Evaporation and River Discharge in the Sub-Arctic Tana Basin, Northern Fennoscandia. *Climatic Change*, *69*, 367–392. https://doi.org/10.1007/s10584-005-2533-y

Davidson, N. (2014). How much wetland has the world lost? Long-term and recent trends in global wetland area. In *Marine and Freshwater Research* (Vol. 65). https://doi.org/10.1071/MF14173

Dimova, N. T., & Burnett, W. C. (2011). Evaluation of groundwater discharge into small lakes based on the temporal distribution of radon-222. *Limnology and Oceanography*, *56*(2), 486–494. https://doi.org/10.4319/lo.2011.56.2.0486

El-Refaie, G. (2010). Temperature impact on operation and performance of Lake Manzala Engineered Wetland, Egypt. *Ain Shams Engineering Journal*, *1*(1), 1–9. https://doi.org/https://doi.org/10.1016/j.asej.2010.09.001

Erwin, K. L. (2009). Peatlands and global climate change: the role of peatland restoration in achanging world. *Wetlands Ecology and Management*, *17*, 71–84.

Fayer, M. J. (2000). *UNSAT-H Version 3.0: Unsaturated soil water and heat flow model theory, User manual, and examples*. Richland, Washington: PNNL-13249.

Finlayson, C. M. (2012). Forty years of wetland conservation and wise use. *Aquatic Conservation: Marine and Freshwater Ecosystems*, *22*(2), 139–143. https://doi.org/10.1002/aqc.2233

Gentine, P., Entekhabi, D., Chehbouni, A., Boulet, G., & Duchemin, B. (2007). Analysis of evaporative fraction diurnal behaviour. *Agricultural and Forest Meteorology*, *143*(1–2), 13–29. https://doi.org/10.1016/J.AGRFORMET.2006.11.002

Gurrieri, J. T., & Furniss, G. (2004). Estimation of groundwater exchange in alpine lakes using non-steady mass-balance methods. *Journal of Hydrology*, *297*(1), 187–208. https://doi.org/https://doi.org/10.1016/j.jhydrol.2004.04.021

Hantush, M. M., Kalin, L., Isik, S., & Yucekaya, A. (2013). Nutrient Dynamics in Flooded

Wetlands: I. Model Development. *Journal of Hydrologic Engineering*.

Hayashi, M., & van der Kamp, G. (2000). Simple equations to represent the volume–area–depth relations of shallow wetlands in small topographic depressions. *Journal of Hydrology*, *237*(1), 74–85. https://doi.org/https://doi.org/10.1016/S0022-1694(00)00300-0

Hebert, C., Caissie, D., Satish, M. G., & El-Jabi, N. (2011). Study of stream temperature dynamics and corresponding heat fluxes within Miramichi River catchments (New Brunswick, Canada). *Hydrological Processes*, *25*(15), 2439–2455. https://doi.org/10.1002/hyp.8021

Hua, Y., Peng, L., Zhang, S., V. Heal, K., Zhao, J., & Zhu, D. (2017). Effects of plants and temperature on nitrogen removal and microbiology in pilot-scale horizontal subsurface flow constructed wetlands treating domestic wastewater. *Ecological Engineering*, *108*, 70–77. https://doi.org/10.1016/j.ecoleng.2017.08.007

Jordan, T. E., Whigham, D. F., Hofmockel, K. H., & Pittek, M. A. (2003). Nutrient and Sediment Removal by a Restored Wetland Receiving Agricultural Runoff. *Journal of Environmental Quality*, *32*, 1534–1547. https://doi.org/10.2134/jeq2003.1534

Jourdonnais, J. H., Walsh, R. P., Pickett, F. J., & Goodman, D. (1992). *Structure and calibration strategy for a water temperature model of the lower Madison River, Montana*. *3*, 153–169.

Kadlec, R. H. (2006). Water temperature and evapotranspiration in surface flow wetlands in hot arid climate. *Ecological Engineering*, *26*(4), 328–340. https://doi.org/https://doi.org/10.1016/j.ecoleng.2005.12.010

Kadlec, R. H., & Wallace, S. D. (2009). *Treatment Wetlands*. Boca Raton: CRC Press.

Kalin, L., Hantush, M. M., Isik, S., Yucekaya, A., & Jordan, T. (2013). Nutrient Dynamics in Flooded Wetlands: II. Model Application. *Journal of Hydrologic Engineering*.

Kannan, N., White, S. M., Worrall, F., & Whelan, M. J. (2007). Sensitivity analysis and identification of the best evapotranspiration and runoff options for hydrological modelling in SWAT-2000. *Journal of Hydrology*, *332*(3–4), 456–466. https://doi.org/10.1016/J.JHYDROL.2006.08.001

Kazezyılmaz-Alhan, C. M., Medina Jr., M. A., & Richardson, C. J. (2007). A wetland hydrology and water quality model incorporating surface water/groundwater interactions. *Water Resources Research*, *43*(4). https://doi.org/10.1029/2006WR005003

Kothandaraman, V. (1971). Analysis of Water Temperature Variations in Large River. *Journal of the Sanitary Engineering Division*, *97*(1), 19–31.

Maharjan, G. R., Park, Y. S., Kim, N. W., Shin, D. S., Choi, J. W., Hyun, G. W., … Lim, K. J. (2013). Evaluation of SWAT sub-daily runoff estimation at small agricultural watershed in Korea. *Frontiers of Environmental Science & Engineering*, *7*(1), 109–119. https://doi.org/10.1007/s11783-012-0418-7

Meng, W., He, M., Hu, B., Mo, X., Li, H., Liu, B., & Wang, Z. (2017). Status of wetlands in China: A review of extent, degradation, issues and recommendations for improvement. *Ocean & Coastal Management*, *146*(Supplement C), 50–59. https://doi.org/https://doi.org/10.1016/j.ocecoaman.2017.06.003

Mitsch, W. J., & Gosselink, J. G. (1993). *Wetlands* (2nd Editio). Van Nostrand Reinhold Company.

Mitsch, W. J., & Gosselink, J. G. (2007). *Wetlands*.

Mohseni, O., Stefan, H. G., & Erickson, T. R. (1998). A nonlinear regression model for weekly stream temperatures. *Water Resources Research*, *34*(10), 2685–2692. https://doi.org/10.1029/98WR01877

Morrill, J., Bales, R., & Conklin, M. (2005). Estimating Stream Temperature from Air Temperature: Implications for Future Water Quality. *Journal of Environmental Engineering*, *131*(1), 139–146. https://doi.org/10.1061/(ASCE)0733-9372(2005)131:1(139)

Mote, P., Parson, E., F. Hamlet, A., Keeton, W., Lettenmaier, D., Mantua, N., … Snover, A. (2003). Preparing for Climate Change: The Water, Salmon, and Forests of the Pacific Northwest. *Climatic Change*, *61*, 45–88. https://doi.org/10.1023/A:1026302914358

Nash, J. E., & Sutcliffe, J. V. (1970). River flow forecasting through conceptual models part I — A discussion of principles. *Journal of Hydrology*, *10*(3), 282–290. https://doi.org/10.1016/0022-1694(70)90255-6

Padmanabhan, G., & Bengtson, M. L. (1999). *A Review of Models for Investigating the Influence of Wetlands on Flooding*.

Paschalis, A., Molnar, P., Fatichi, S., & Burlando, P. (2013). A stochastic model for high-resolution space-time precipitation simulation. *Water Resources Research*, *49*(12), 8400–8417. https://doi.org/10.1002/2013WR014437

Rashleigh, B. (2009). Modeling Options For Wetlands. *U.S Environmental Protection Agency Office of Research and Development*.

Saltelli, A., Ratto, M., Andres, T., Campolongo, F., Cariboni, J., Gatelli, D., … Tarantola, S. (2007). *Introduction to Sensitivity Analysis, in Global Sensitivity Analysis. The Primer*.

Saltelli, A., Tarantola, S., Campolongo, F., & Ratto, M. (2004). *Sensitivity analysis in practice. A guide to assessing scientific models*.

Schipper, L. A., Hobbs, J. K., Rutledge, S., & Arcus, V. L. (2014). Thermodynamic theory explains the temperature optima of soil microbial processes and high Q10 values at low temperatures. *Global Change Biology*, *20*(11), 3578–3586.

https://doi.org/10.1111/gcb.12596

Schnoor, J. L. (1996). *Environmental modeling: fate and transport of pollutants in water, air, and soil*. New York, USA: John Wiley and Sons.

Sharifi, A., Kalin, L., Hantush, M. M., Isik, S., & Jordan, T. E. (2013). Carbon dynamics and export from flooded wetlands: A modeling approach. *Ecological Modelling*, *263*, 196–210. https://doi.org/10.1016/j.ecolmodel.2013.04.023

Smith, K. (1981). The prediction of river water temperatures / Prédiction des températures des eaux de rivière. *Hydrological Sciences Bulletin*, *26*(1), 19–32. https://doi.org/10.1080/02626668109490859

Spear, R. C., & Hornberger, G. M. (1980). Eutrophication in peel inlet—II. Identification of critical uncertainties via generalized sensitivity analysis. *Water Research*, *14*(1), 43–49. https://doi.org/10.1016/0043-1354(80)90040-8

Stefan, H. G., & Preud'homme, E. B. (1993). *STREAM TEMPERATURE ESTIMATION FROM AIR TEMPERATURE*.

Trigg, M. A., Cook, P. G., & Brunner, P. (2014). Groundwater fluxes in a shallow seasonal wetland pond: The effect of bathymetric uncertainty on predicted water and solute balances. *Journal of Hydrology*, *517*(Supplement C), 901–912. https://doi.org/https://doi.org/10.1016/j.jhydrol.2014.06.020

Webb, B. W., & Nobilis, F. (1997). LONG-TERM PERSPECTIVE ON THE NATURE OF THE AIR–WATER TEMPERATURE RELATIONSHIP: A CASE STUDY. *Hydrological Processes*, *11*(2), 137–147. https://doi.org/10.1002/(SICI)1099-1085(199702)11:2<137::AID-HYP405>3.0.CO;2-2

Whigham, D., Pittek, M., Hofmockel, K. H., Jordan, T., & Pepin, A. L. (2002). BIOMASS AND

NUTRIENT DYNAMICS IN RESTORED WETLANDS ON THE OUTER COASTAL PLAIN OF MARYLAND, USA. *Wetlands*, *22*(3), 562–574. https://doi.org/10.1672/0277-5212(2002)022[0562:BANDIR]2.0.CO;2

White, W. N. (1932). A method of estimating ground-water supplies based on discharge by plants and evaporation from soil: Results of investigations in Escalante Valley, Utah. In *Water Supply Paper*. https://doi.org/10.3133/wsp659A

Woo, M., L. Young, K., & Brown, L. (2006). High Arctic Patchy Wetlands: Hydrologic Variability and Their Sustainability. *Physical Geography*, *27*, 297–307. https://doi.org/10.2747/0272-3646.27.4.297

Yang, X., Liu, Q., He, Y., Luo, X., & Zhang, X. (2015). Comparison of daily and sub-daily SWAT models for daily streamflow simulation in the Upper Huai River Basin of China. *Stochastic Environmental Research and Risk Assessment*, *166*, 120–128. https://doi.org/10.1007/s00477-015-1099-0

APPENDICES

APPENDIX 1: Derivation of A and V for an example profile ($W_{0.5}$)

For $W_{0.5}$ wetland:

$$h = a\sqrt{x}$$

$$x = \frac{h^2}{a^2}$$

$$h_{max} = a\sqrt{x_{max}}$$

$$x_{max} = \frac{h_{max}^2}{a^2}$$

$$A = \pi x^2$$

$$A = \frac{\pi h^4}{a^4}$$

$$A_{max} = \pi \frac{h_{max}^4}{a^4}$$

$$a^4 = \frac{h_{max}^4}{A_{max}}$$

$$A(h) = \frac{A_{max} * h^4}{h_{max}^4}$$

$$V_{max} = 2\pi \int_0^{\frac{h_{max}^2}{a^2}} x(h_{max} - a\sqrt{x})dx$$

$$V_{max} = 2\pi(\frac{h_{max}}{2}x^2 - a\frac{2}{5}x^{\frac{5}{2}}\Big|_0^{\frac{h_{max}^2}{a^2}}$$

$$V_{max} = 2\pi \frac{h_{max}}{2} \frac{h_{max}^4}{a^4} - 2\pi \frac{2a}{5} \frac{h_{max}^5}{a^5}$$

$$V_{max} = \pi \frac{h_{max}^5}{a^4} - 4\pi \frac{h_{max}^5}{5a^4}$$

$$V_{max} = \frac{\pi}{5} \frac{h_{max}^5}{a^4}$$

$$V = 2\pi \int_0^{\frac{h^2}{a^2}} x(h - a\sqrt{x})dx$$

$$V = 2\pi (\frac{h}{2}x^2 - a\frac{2}{5}x^{\frac{5}{2}}\Big|_0^{\frac{h^2}{a^2}}$$

$$V = 2\pi \frac{h}{2} \frac{h^4}{a^4} - 2\pi \frac{2a}{5} \frac{h^5}{a^5}$$

$$V = \frac{\pi}{5} \frac{h^5}{a^4}$$

$$V_{max} - V = \frac{\pi}{5} (\frac{h_{max}^5 - h^5}{a^4})$$

$$V_{max} - V = \frac{\pi}{5} (h_{max}^5 - h^5) \frac{A_{max}}{\pi h_{max}^4}$$

$$V = V_{max} - \frac{A_{max}}{5h_{max}^4} (h_{max}^5 - h^5)$$

APPENDIX 2: R codes for K-S test and PDF graphs for an example constituent (ON_w)

R codes for K-S Test:

```
## First I needed to identify my data.
## B represents behavioral (B) simulations (1,000)
## NB represents non-behavioral (B') simulations (99,000)
B<-read.csv("C:\\Users\\rzk0047\\Desktop\\New Bathymetry for R\\Actual Onw
B.csv",header=TRUE,sep=',')
NB<-read.csv("C:\\Users\\rzk0047\\Desktop\\New Bathymetry for R\\Actual Onw
NB.csv",header=TRUE,sep=',')

## "ks.test" code provide me to analyze Kolmogorov-Smirnov Test
## Each row represents one parameters K-S test
ks.test(B$L2,NB$L2)
ks.test(B$theta,NB$theta)
ks.test(B$Is,NB$Is)
ks.test(B$fNup,NB$fNup)
ks.test(B$kd,NB$kd)
ks.test(B$kep,NB$kep)
ks.test(B$kga0,NB$kga0)
ks.test(B$kgb0,NB$kgb0)
ks.test(B$kmin1s,NB$kmin1s)
ks.test(B$knw,NB$knw)
ks.test(B$kminw,NB$kminw)
ks.test(B$kns,NB$kns)
ks.test(B$kden,NB$kden)
ks.test(B$rowp,NB$rowp)
ks.test(B$vels_o,NB$vels_o)
ks.test(B$vels_s,NB$vels_s)
ks.test(B$velb,NB$velb)
ks.test(B$ana,NB$ana)
ks.test(B$rChl,NB$rChl)
ks.test(B$Ss,NB$Ss)
ks.test(B$Sw,NB$Sw)
ks.test(B$c_Uw,NB$c_Uw)
ks.test(B$frap,NB$frap)
ks.test(B$c1,NB$c1)
ks.test(B$c2,NB$c2)
ks.test(B$PH,NB$PH)
ks.test(B$S,NB$S)
ks.test(B$Kw,NB$Kw)
ks.test(B$apa,NB$apa)
ks.test(B$Dnp,NB$Dnp)
```

```
ks.test(B$Ksa,NB$Ksa)
ks.test(B$Ksb,NB$Ksb)
ks.test(B$RanN1,NB$RanN1)
ks.test(B$fW,NB$fW)
ks.test(B$fact,NB$fact)
ks.test(B$a_vr_o,NB$a_vr_o)
ks.test(B$a_vr_s,NB$a_vr_s)
ks.test(B$porw,NB$porw)
```

R codes for PDFs:

```
## Setting working directory
BUB<-read.csv("C:\\Users\\rzk0047\\Desktop\\New Bathymetry for R\\Actual
BUB'.csv",header=TRUE,sep=',')
WA<-read.csv("C:\\Users\\rzk0047\\Desktop\\New Bathymetry for R\\Actual ONw
B.csv",header=TRUE,sep=',')
W1<-read.csv("C:\\Users\\rzk0047\\Desktop\\New Bathymetry for R\\Conic ONw
B.csv",header=TRUE,sep=',')
W0.5<-read.csv("C:\\Users\\rzk0047\\Desktop\\New Bathymetry for R\\X0.5 ONw
B.csv",header=TRUE,sep=',')
W2<-read.csv("C:\\Users\\rzk0047\\Desktop\\New Bathymetry for R\\X2 ONw
B.csv",header=TRUE,sep=',')
W4<-read.csv("C:\\Users\\rzk0047\\Desktop\\New Bathymetry for R\\X4 ONw
B.csv",header=TRUE,sep=',')

## “density” code is providing me to plot PDF graphs
## “xlim” code is providing me to set x-axis limitations
## “ylim” code is providing me to set y-axis limitations
## “xlab” code is providing me to put a name for x-axis
## “ylab” code is providing me to put a name for y-axis
## “main” code is providing me to a name for whole graph
## “lines” code is providing me to add new line in the graph
## “legend” code is providing me to add legend in the graph


plot(density(BUB[,"a_vr_o"]),xlim=c(0,4),xlab="Coefficient for resuspension/recycling of
organic material",ylab="Density",main="PDF for a_vr_o - Onw",cex.main=1.5,
cex.lab=1.5,cex.axis=1.5,lty=1,lwd=2,col="blue")
```

```
lines(density(WA[,"a_vr_o"]),col="orange",lwd=3,lty=2)
lines(density(W0.5[,"a_vr_o"]),col="black",lwd=4,lty=3)
lines(density(W1[,"a_vr_o"]),col="green",lwd=3,lty=4)
lines(density(W2[,"a_vr_o"]),col="red",lwd=3,lty=5)
lines(density(W4[,"a_vr_o"]),col="cyan",lwd=3,lty=6)

mylegend= expression("BUB'",W[A],W[0.5],W[1],W[2],W[4])
legend('topright',legend=mylegend,col=c("blue","orange","black","green","red","cyan"),lwd=3,
cex=1.5,lty=1:2:3:4:5:6)


#porw

plot(density(BUB[,"porw"]),ylim=c(0,14),xlab="Effective porosity of wetland surface
water",ylab="Density",main="PDF for porw - Onw",cex.main=1.5,
cex.lab=1.5,cex.axis=1.5,lwd=2,col="blue")
lines(density(WA[,"porw"]),col="orange",lwd=2,lty=2)
lines(density(W0.5[,"porw"]),col="black",lwd=5,lty=3)
lines(density(W1[,"porw"]),col="green",lwd=3,lty=4)
lines(density(W2[,"porw"]),col="red",lwd=3,lty=5)
lines(density(W4[,"porw"]),col="cyan",lwd=3,lty=6)

mylegend= expression("BUB'",W[A],W[0.5],W[1],W[2],W[4])
legend('topleft',legend=mylegend,col=c("blue","orange","black","green","red","cyan"),lwd=3,
cex=1.5,lty=1:2:3:4:5:6)



#vels_o

plot(density(BUB[,"vels_o"]),ylim=c(0,0.8),xlim=c(0,10),xlab="Effective settling velocity
(cm/day) for organic material",ylab="Density",main="PDF for vels_o - Onw",cex.main=1.5,
cex.lab=1.5,cex.axis=1.5,lwd=2,col="blue")
lines(density(WA[,"vels_o"]),col="orange",lwd=2,lty=2)
lines(density(W0.5[,"vels_o"]),col="black",lwd=5,lty=3)
lines(density(W1[,"vels_o"]),col="green",lwd=3,lty=4)
lines(density(W2[,"vels_o"]),col="red",lwd=3,lty=5)
lines(density(W4[,"vels_o"]),col="cyan",lwd=3,lty=6)

mylegend= expression("BUB'",W[A],W[0.5],W[1],W[2],W[4])
legend('topright',legend=mylegend,col=c("blue","orange","black","green","red","cyan"),lwd=3,
cex=1.5,lty=1:2:3:4:5:6)
```

#L2

```
plot(density(BUB[,"L2"]),ylim=c(0,0.04),xlab="Thickness of anaerobic soil layer
(cm)",ylab="Density",main="PDF for L2 - Onw",cex.main=1.5,
cex.lab=1.5,cex.axis=1.5,lwd=2,col="blue")
lines(density(WA[,"L2"]),col="orange",lwd=2,lty=2)
lines(density(W0.5[,"L2"]),col="black",lwd=5,lty=3)
lines(density(W1[,"L2"]),col="green",lwd=3,lty=4)
lines(density(W2[,"L2"]),col="red",lwd=3,lty=5)
lines(density(W4[,"L2"]),col="cyan",lwd=3,lty=6)

mylegend= expression("BUB'",W[A],W[0.5],W[1],W[2],W[4])
legend('topright',legend=mylegend,col=c("blue","orange","black","green","red","cyan"),lwd=3,
cex=1.2,lty=1:2:3:4:5:6)
```

#ana

```
plot(density(BUB[,"ana"]),ylim=c(0,0.25),xlab="Gram of nitrogen per gram of chlorophyll-a in
plant/algae (gN/gChl)",ylab="Density",main="PDF for ana - Onw",cex.main=1.5,
cex.lab=1.5,cex.axis=1.5,lwd=2,col="blue")
lines(density(WA[,"ana"]),col="orange",lwd=2,lty=2)
lines(density(W0.5[,"ana"]),col="black",lwd=5,lty=3)
lines(density(W1[,"ana"]),col="green",lwd=3,lty=4)
lines(density(W2[,"ana"]),col="red",lwd=3,lty=5)
lines(density(W4[,"ana"]),col="cyan",lwd=3,lty=6)

mylegend= expression("BUB'",W[A],W[0.5],W[1],W[2],W[4])
legend('topleft',legend=mylegend,col=c("blue","orange","black","green","red","cyan"),lwd=3,
cex=1.5,lty=1:2:3:4:5:6)
```